Control of Electrical Machines

Commande des machines électriques — An Illustrated Graduate Handout

Dr. NOUR Mohamed

Centre Universitaire Nour El Bachir — El Bayadh, Algeria

Master 2 · Semester 3 · Course UEF 2.1.2 · 4 Credits · 45 h

Contents

Preface 4
Learning Objectives 5
Notation and Principal Symbols 5

Chapter 1 — Fundamentals of Electrical Motor Drives and Mechanical Dynamics 7
1.1 The Electrical Drive as a System 7
1.2 Dynamic Equation of the Motor–Load System 8
1.3 Torque–Speed Characteristics of Mechanical Loads 9
1.4 Four-Quadrant Operation 10
1.5 Steady-State Stability of an Operating Point 11
1.6 Constant-Torque and Constant-Power Regions 12
1.7 Worked Tutorials 13
1.8 Exercises 15
1.9 Advanced Topics in Drive Mechanics 15
1.10 Additional Solved Tutorials 17
1.11 Exercises (supplementary) 18

Chapter 2 — Variable-Speed Drives for Induction and Synchronous Machines (Scalar Control) 19
2.1 The Frequency-Control Principle 19
2.2 Constant-V/f Control of the Induction Motor 19
2.3 The Voltage-Source Inverter 22
2.4 Pulse-Width Modulation 23
2.5 Speed Control of Synchronous Machines 26
2.6 Limitations of Scalar Control 27
2.7 MATLAB/Simulink Implementation 27
2.8 Worked Tutorials 28
2.9 Exercises 28
2.10 Space-Vector Modulation in Depth 29
2.11 Additional Solved Tutorials 30
2.12 Exercises (supplementary) 31

Chapter 3 — Vector Control / Field-Oriented Control (FOC) of the PMSM 32
3.1 The Idea: Making an AC Machine Behave Like a DC Machine 32
3.2 Reference-Frame Transformations 32
3.3 Dynamic Model of the PMSM in the dq Frame 34
3.4 Torque-Producing Strategies 35

3.5 Current-Loop Design . . . 36
3.6 Speed-Loop Design by the Symmetrical Optimum . . . 38
3.7 The Complete FOC Structure . . . 39
3.8 Simulation Behaviour . . . 39
3.9 MATLAB/Simulink Implementation Guide . . . 40
3.10 Worked Tutorials . . . 41
3.11 Exercises . . . 42
3.12 Deeper Treatment of FOC . . . 42
3.13 Additional Solved Tutorials . . . 44
3.14 Exercises (supplementary) . . . 45

Chapter 4 — Direct Torque Control (DTC) of Induction Motors 46
4.1 Philosophy of Direct Torque Control . . . 46
4.2 The Governing Relations . . . 46
4.3 Sectors and Hysteresis Comparators . . . 48
4.4 The Switching Table and Control Structure . . . 49
4.5 Flux Trajectory and Torque Response . . . 50
4.6 Stator-Flux Estimation and the Drift Problem . . . 51
4.7 FOC versus DTC . . . 52
4.8 MATLAB/Simulink Layout . . . 53
4.9 Worked Tutorials . . . 53
4.10 Exercises . . . 54
4.11 Direct Torque Control in Depth . . . 54
4.12 Additional Solved Tutorials . . . 56
4.13 Exercises (supplementary) . . . 56

Chapter 5 — Control Strategies for Stepper Motors 57
5.1 Introduction . . . 57
5.2 Types of Stepper Motor . . . 57
5.3 Step Angle and Resolution . . . 58
5.4 Excitation Modes . . . 58
5.5 Static Torque and Holding Torque . . . 59
5.6 Open-Loop and Closed-Loop Control . . . 60
5.7 Torque–Speed Characteristics and Resonance . . . 61
5.8 MATLAB/Simulink Implementation . . . 62
5.9 Worked Tutorials . . . 62
5.10 Exercises . . . 63
5.11 Stepper Drives in Depth . . . 63
5.12 Additional Solved Tutorials . . . 64
5.13 Exercises (supplementary) . . . 65

6. Bibliography 66

Appendix A — Coordinate-Transformation Reference 68

Appendix B — The Per-Unit System 69

Appendix C — MATLAB Reference Code 70
C.1 Clarke and Park transformations (Chapter 3) . . . 70

C.2 FOC of a surface PMSM — speed-step simulation (Chapter 3) 70
C.3 Space-Vector Modulation dwell times (Chapter 2) 71
C.4 DTC flux/torque estimator and switching table (Chapter 4) 71
C.5 Microstepping current generation (Chapter 5) 72
C.6 V/f profile with boost and field weakening (Chapter 2) 72

Appendix D — Formula and Design Summary **73**
D.1 Mechanics of the drive 73
D.2 Scalar control, inverter and PWM 73
D.3 PMSM model and FOC design 74
D.4 Direct torque control 74
D.5 Stepper motors 75
D.6 Design rules of thumb 75

Appendix E — Digital Implementation of Controllers **76**
E.1 Why discretization is not optional 76
E.2 Discretization methods 76
E.3 The discrete PI controller 77
E.4 Integrator wind-up and its cure 77
E.5 Computational delay 78
E.6 Choosing the sample time 78

Appendix F — Sensorless Position and Speed Estimation **79**
F.1 Fundamental-excitation methods (medium and high speed) 79
F.2 Model-reference adaptive systems (MRAS) 80
F.3 Saliency-tracking (high-frequency injection) at low and zero speed 80
F.4 Angle tracking 80
F.5 Practical notes 81

Appendix G — Extended Worked Problems **82**
G.1 Thermal (RMS) sizing of a servo axis 82
G.2 Inertia-matching gear ratio 82
G.3 V/f set-point with slip 83
G.4 Full SVM dwell times with overmodulation check 83
G.5 Complete PMSM controller design 83
G.6 Field-weakening operating point 83
G.7 DTC vector choice and flux ripple 84
G.8 Stepper microstepping and resonance 84

Appendix H — Mechanical Resonance and Two-Mass Systems **85**
H.1 The two-mass model 85
H.2 Resonance and anti-resonance 85
H.3 Consequences for control and mitigation 86
G.9 Clarke and Park with numbers 86
G.10 Verifying the symmetrical-optimum margin 87
G.11 Flux-estimator drift 87
G.12 Stepper pull-in versus pull-out 87

Appendix I — Control-Strategy Selection Guide **88**

I.1 Method comparison matrix 88
I.2 Application-to-method mapping 88
I.3 Converter and modulator selection 89
I.4 Study questions 89

Appendix J — Typical Machine and Drive Parameters **90**
J.1 Induction motors (star-connected, 50 Hz) 90
J.2 Permanent-magnet synchronous motors 90
J.3 Hybrid stepper motors (NEMA sizes) 91
J.4 Typical control settings 91
J.5 Further reading 91

Preface

This handout addresses the modelling, simulation and control of modern electrical **drive systems** for Master 2 students specialising in Electrical Machines. Its guiding idea is that a machine is never controlled in isolation: what the engineer actually commissions is a *drive* — the closed cooperation of an **electrical machine**, a **static power converter**, a **mechanical load** and a **digital control algorithm**. Every chapter is written from that system viewpoint.

The book follows a deliberate arc of increasing performance and increasing sophistication. Chapter 1 builds the mechanical and energetic foundations shared by every drive. Chapter 2 introduces the simplest and still most widespread industrial philosophy, **scalar (V/f) control**, together with the inverter and pulse-width-modulation techniques on which all later chapters depend. Chapter 3 develops **Field-Oriented Control (FOC)** of the permanent-magnet synchronous motor — the reference method for high-performance servo drives — with complete controller-design procedures. Chapter 4 presents **Direct Torque Control (DTC)**, the fastest-responding torque controller, and contrasts it carefully with FOC. Chapter 5 closes with **stepper-motor drives**, the standard solution for open-loop incremental positioning.

Every chapter provides rigorous theory, complete mathematical modelling (state-space and transfer-function forms), controller-design procedures with numerical tuning, figures generated specifically for this text, MATLAB/Simulink implementation guidance, fully worked tutorial problems (TD), and a set of unsolved exercises. A consolidated IEEE-style bibliography and two appendices (transform reference and per-unit system) complete the volume.

Prerequisites. Electrical-machine theory (induction, synchronous and permanent-magnet machines), power electronics (rectifiers, choppers, inverters), linear control (Laplace transform, transfer functions, PI/PID design, root locus and Bode analysis) and basic MATLAB/Simulink.

How to read the figures. Block diagrams use a consistent colour code throughout: **orange** blocks are power-electronic converters, **blue** blocks are controllers or signal-processing operations, **green** blocks are machines or mechanical elements, red paths carry power and thin blue/grey paths carry information.

Learning Objectives

On completion of this course the student will be able to:

1. **Model** a complete electrical drive as a coupled electromechanical system and reduce it to state-space and transfer-function descriptions suitable for control design.
2. **Build and validate** MATLAB/Simulink models of drive systems and interpret their transient and steady-state behaviour.
3. **Analyse** stability, four-quadrant operation, and the constant-torque / constant-power operating regions of a drive.
4. **Design and tune** current, torque and speed controllers (PI/PID) by pole placement, internal-model control and the symmetrical optimum, and quantify the resulting bandwidth and damping.
5. **Compare** scalar control, field-oriented control and direct torque control, and select an appropriate strategy for a given application.
6. **Explain and dimension** stepper-motor drives, including microstepping and resonance mitigation.

Notation and Principal Symbols

Symbol	Quantity	Unit
v_s, i_s	stator voltage, current (vectors/components)	V, A
ψ_s, ψ_r, ψ_f	stator, rotor, magnet flux linkage	Wb
R_s, R_r	stator, rotor resistance	Ω
L_s, L_r, L_m	stator, rotor, magnetising inductance	H
L_d, L_q	direct- and quadrature-axis inductance	H
σ	total leakage coefficient $1 - L_m^2/(L_s L_r)$	–
T_{em}, T_L	electromagnetic, load torque	N·m
J, B	inertia, viscous-friction coefficient	kg·m², N·m·s
Ω, ω_r	mechanical, electrical rotor speed	rad/s
ω_s, ω_e	synchronous / electrical supply speed	rad/s
θ_e	electrical rotor angle	rad
p	number of pole pairs	–
s	slip (IM)	–
V_{dc}	inverter DC-bus voltage	V
T_s, f_{sw}	switching period, frequency	s, Hz
α_c	current-loop bandwidth	rad/s

Subscripts α, β denote the stationary two-phase frame; d, q the rotor-synchronous frame; a superscript * denotes a *reference* (commanded) value.

Chapter 1 — Fundamentals of Electrical Motor Drives and Mechanical Dynamics

(Duration: 2 weeks)

1.1 The Electrical Drive as a System

A modern **electrical drive** is the coordinated association of the sub-systems shown in Figure 1.1. Energy is drawn from an electrical supply, conditioned by a **static power converter**, and delivered to an **electrical machine** which produces the electromagnetic torque T_{em}. This torque acts through a **mechanical coupling** (a direct shaft, a gearbox, a belt) onto the **mechanical load**, which opposes motion with a load torque T_L. A **control unit** — today a microcontroller, DSP or FPGA — measures currents, voltages, speed and position, compares them with references, and commands the converter switches so that the machine develops exactly the torque the application requires.

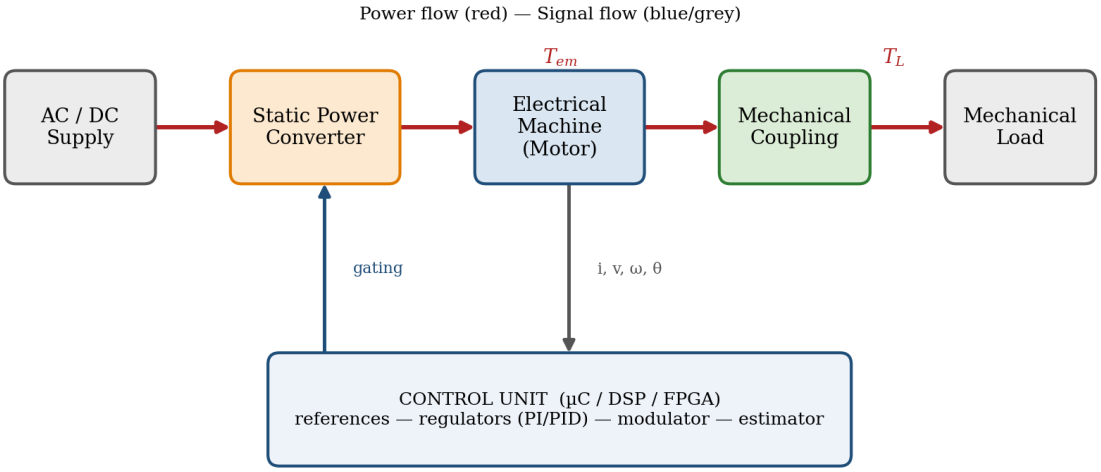


Figure 1: Figure 1.1 — The electrical drive as a system: power flow (red) from supply to load, information flow (blue/grey) through the digital control unit.

Two distinct flows coexist in every drive and it is essential never to confuse them. The

power flow (red path) is unidirectional in a simple drive but *bidirectional* in a regenerative one: during braking the mechanical energy of the load is converted back to electrical form. The **information flow** (blue/grey path) is always bidirectional — references descend from the operator while measurements ascend from sensors. The converter is the *actuator* of the loop: it is the only element that can impose the machine's terminal quantities, and therefore its torque. The control unit is the *intelligence*: its algorithms — the subject of this entire course — decide, thousands of times per second, which switches to close.

The performance the drive can achieve is bounded by four ratings that recur throughout the book: the **continuous torque** (set by thermal limits, i.e. RMS current), the **peak torque** (set by the converter's peak current and by magnetic saturation), the **maximum speed** (set by the available DC-bus voltage against the machine's back-EMF), and the **four-quadrant capability** (set by the converter topology). Chapter 1 establishes the mechanical and energetic relations that make these ratings quantitative.

1.2 Dynamic Equation of the Motor–Load System

1.2.1 Newton's law for the rotating shaft

Applying the rotational form of Newton's second law to the common shaft of motor and load gives the **fundamental equation of motion** of the drive:

$$T_{em} - T_L = J\,\frac{d\Omega}{dt} + B\,\Omega$$

The left-hand side is the *net* torque available to change the state of motion; the right-hand side distributes it between **acceleration** of the total inertia J and **viscous friction** $B\Omega$. Three regimes follow immediately:

- if $T_{em} > T_L + B\Omega$ the drive **accelerates**;
- if $T_{em} < T_L + B\Omega$ the drive **decelerates**;
- if $T_{em} = T_L + B\Omega$ the drive runs at **constant speed** (steady state).

In many machines the viscous term $B\Omega$ is small compared with the load torque and is either neglected or lumped into T_L. It is retained here because it provides the natural damping that stabilises the mechanical loop and sets the open-loop mechanical time constant.

1.2.2 Referring inertia and torque through a gearbox

Real loads are frequently coupled through a **gear reducer** of ratio $n = \Omega_m/\Omega_L$, where Ω_m is the motor speed and Ω_L the load speed. Power invariance of an ideal gearbox ($T_m\Omega_m = T'_L\Omega_L$) gives the quantities *referred to the motor shaft*:

$$J_{L,\mathrm{ref}} = \frac{J_L}{n^2}, \qquad T_{L,\mathrm{ref}} = \frac{T'_L}{n}, \qquad J = J_m + \frac{J_L}{n^2}$$

The inverse-square scaling of inertia is the single most important consequence of gearing: a large, slow load inertia is dramatically reduced when seen from a fast motor,

which is precisely why high-ratio reducers are used to drive high-inertia loads with small, agile motors. The gearbox does not change the *physics* — it changes the *reference frame* in which the designer works.

1.2.3 State-space and transfer-function forms

Taking speed Ω as the state, the electromagnetic torque T_{em} as the control input and the load torque T_L as a measurable disturbance,

$$\frac{d\Omega}{dt} = -\frac{B}{J}\,\Omega + \frac{1}{J}(T_{em} - T_L)$$

With $T_L = 0$ this is a **first-order lag** between torque and speed:

$$\frac{\Omega(s)}{T_{em}(s)} = \frac{1/B}{1 + s\,\tau_m}, \qquad \tau_m = \frac{J}{B}$$

where τ_m is the **mechanical time constant**. Its step response is plotted in Figure 1.2: the speed rises exponentially to its final value $\Omega_{ss} = T_{em}/B$, reaching 63.2 % of it after one time constant. Because τ_m is typically tens to hundreds of milliseconds — far slower than the electrical dynamics of the machine, which live on the millisecond scale — the drive designer can almost always treat the electrical and mechanical loops as operating on *separated time scales*. This separation is the foundation of the cascaded (inner current / outer speed) control structure used in Chapters 3 and 4.

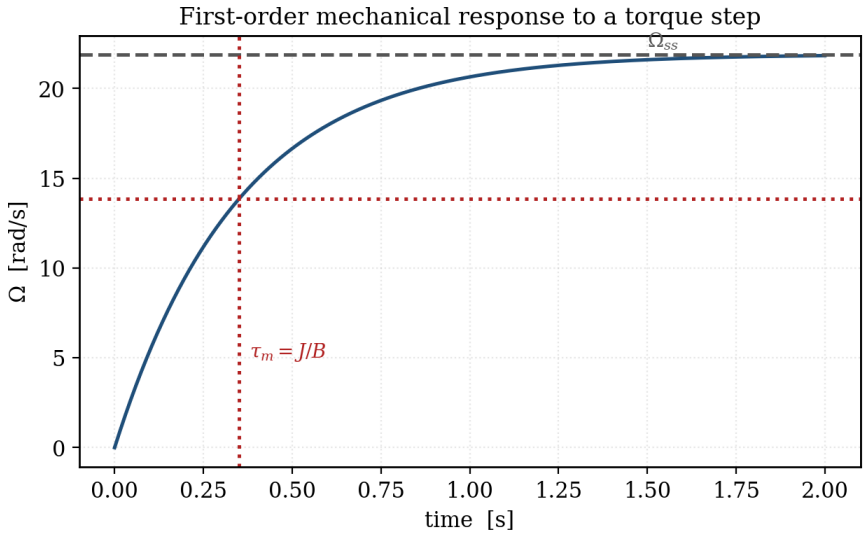


Figure 2: Figure 1.2 — First-order speed response to a torque step; the mechanical time constant $\tau_m = J/B$ locates the 63 % point.

1.3 Torque–Speed Characteristics of Mechanical Loads

The way the load torque varies with speed, $T_L(\Omega)$, decides the operating point, the converter rating and even the choice of control strategy. Four canonical characteristics cover the large majority of industrial loads; they are drawn together in Figure 1.3.

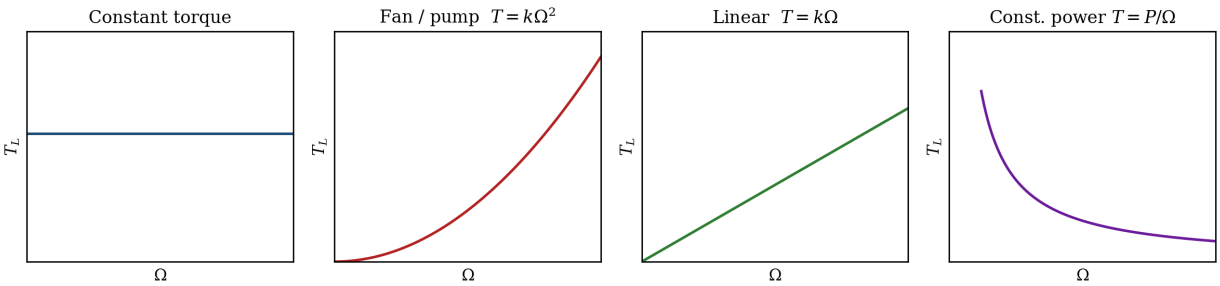


Figure 3: Figure 1.3 — The four canonical load torque–speed characteristics.

- **Constant-torque loads** (T_L = const). Hoists, cranes, conveyors, positive-displacement pumps and extruders. The torque demand is independent of speed, so the power demand rises linearly with speed. These loads dominate the *constant-torque region* below base speed.
- **Fan and centrifugal-pump loads** ($T_L = k\Omega^2$). Because torque falls steeply at low speed, a small reduction in speed produces a large reduction in power — the physical basis of the enormous energy savings achieved by variable-speed drives in HVAC and pumping. Power scales as Ω^3 (the *affinity law*).
- **Linear (viscous) loads** ($T_L = k\Omega$). Calendering, mixers with viscous fluids and eddy-current brakes approximate this law.
- **Constant-power loads** ($T_L = P/\Omega$). Winders, spindles and traction above base speed require constant power, so torque falls hyperbolically with speed. This is the *field-weakening region* (Section 1.6).

The steady-state operating point is the intersection $T_{em}(\Omega) = T_L(\Omega)$ of the motor and load characteristics. A variable-speed drive works by *moving the motor characteristic* (by changing voltage and frequency) so that this intersection slides to the desired speed.

1.4 Four-Quadrant Operation

The instantaneous operating state of any drive is fixed by the signs of **torque** and **speed**. Their product is the mechanical power $P_m = T_{em}\,\Omega$, whose sign tells us the *direction* of energy flow. Plotting torque on the horizontal axis and speed on the vertical axis divides the plane into the four quadrants of Figure 1.4.

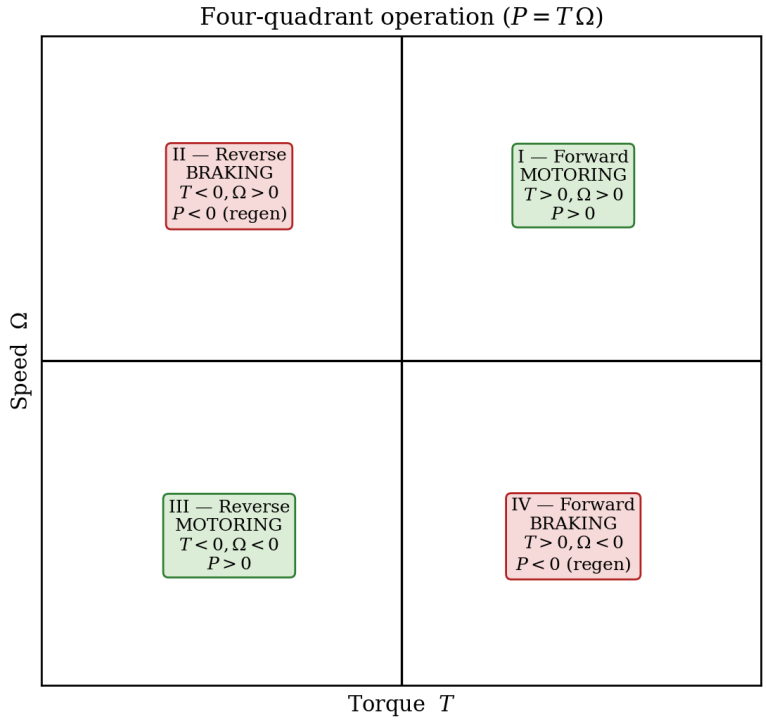


Figure 4: Figure 1.4 — The four quadrants of drive operation, coloured by the direction of mechanical power flow.

- **Quadrants I and III** ($P_m > 0$): **motoring**. Torque and speed have the same sign; electrical energy is converted to mechanical energy and delivered to the load. Quadrant I is forward motoring, Quadrant III is reverse motoring.
- **Quadrants II and IV** ($P_m < 0$): **braking / regeneration**. Torque opposes speed; mechanical energy is converted back to electrical form. If the converter can return this energy to the supply the drive is *regenerative*; otherwise the energy is burned in a braking resistor.

A load that must be raised and lowered, accelerated and decelerated, and run in both directions — a hoist or a traction drive — requires operation in **all four quadrants**. This in turn dictates a *four-quadrant converter*: a dual (antiparallel) controlled rectifier, or a voltage-source inverter equipped with a braking chopper (two-quadrant torque, dissipative braking) or an active front end (full regeneration). The control algorithms of later chapters are inherently four-quadrant because they command torque of either sign directly.

1.5 Steady-State Stability of an Operating Point

An intersection of the motor and load characteristics is an *equilibrium*, but not every equilibrium is **stable**. Consider an operating point Ω_0 where $T_{em}(\Omega_0) = T_L(\Omega_0)$ and impose a small speed perturbation $\Delta\Omega$. Linearising the equation of motion about Ω_0 (and absorbing the friction term into the characteristics) gives

$$J\,\frac{d\,\Delta\Omega}{dt} = \left(\frac{dT_{em}}{d\Omega} - \frac{dT_L}{d\Omega}\right)_{\Omega_0} \Delta\Omega$$

The perturbation decays — the point is **stable** — if and only if the bracketed coefficient is negative:

$$\boxed{\frac{dT_{em}}{d\Omega} < \frac{dT_L}{d\Omega}}$$

The interpretation is physical and worth stating carefully (Figure 1.5). At a stable point, a small increase in speed must create a *torque deficit* — the load torque must rise faster with speed than the motor torque does — so that the net torque becomes negative and drags the speed back down. Loads whose torque increases with speed (fans, pumps) are therefore inherently stabilising; a motor characteristic that rises with speed against a flat load torque is a recipe for instability. This criterion explains, for example, why the unstable (low-speed) branch of an induction motor's torque–speed curve cannot sustain operation against a constant-torque load.

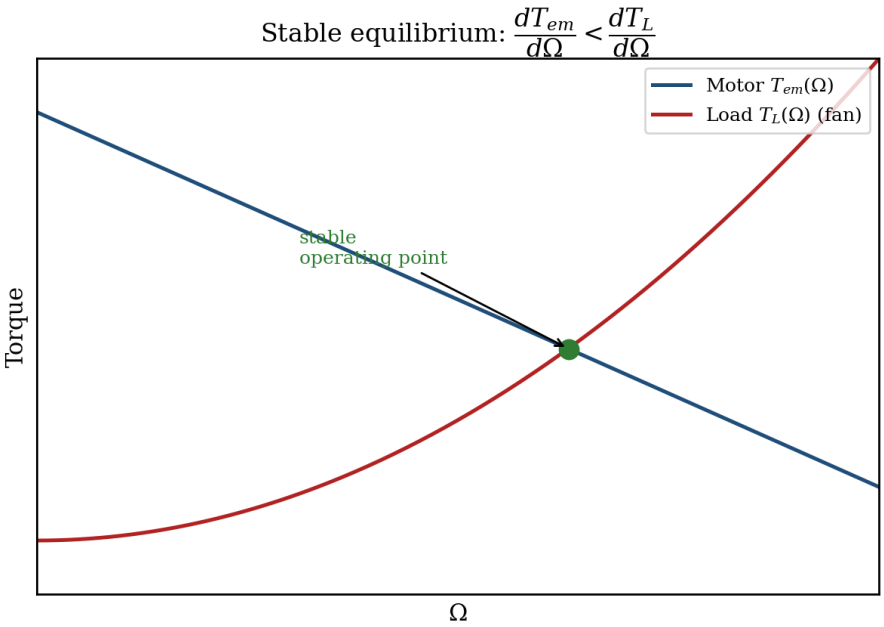


Figure 5: Figure 1.5 — A stable operating point: the fan load characteristic is steeper than the motor characteristic, so $dT_{em}/d\Omega < dT_L/d\Omega$.

1.6 Constant-Torque and Constant-Power Regions

The converter and machine together impose two natural operating regions, separated by the **base speed** Ω_{base} (Figure 1.6).

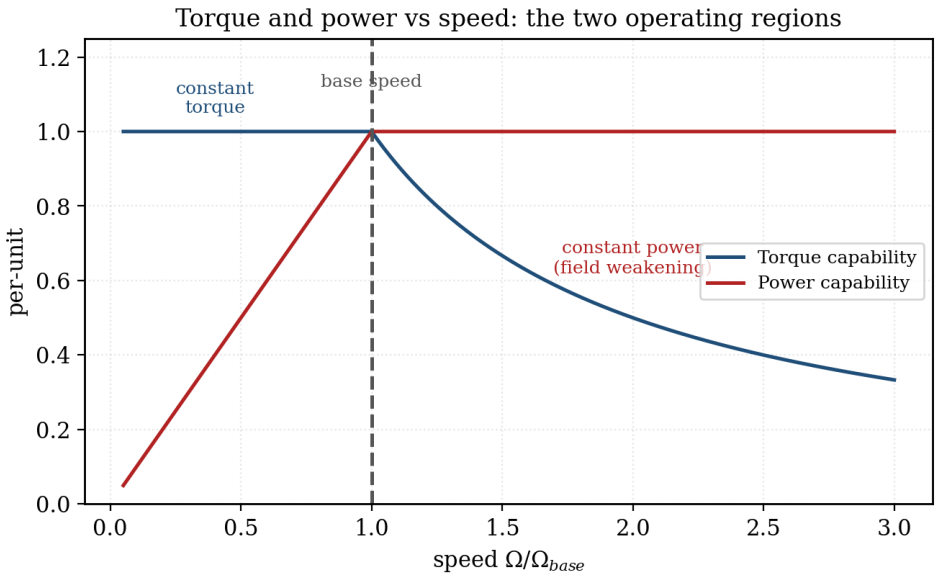


Figure 6: Figure 1.6 — Torque and power capability versus speed, showing the constant-torque and constant-power (field-weakening) regions.

- **Below base speed — constant-torque region.** The flux is held at its rated value; the machine can develop rated torque at any speed, limited only by current (heating). Power rises linearly with speed. This is the region of hoists and traction at low speed.
- **Above base speed — constant-power region.** The back-EMF has risen to the DC-bus ceiling, so the voltage can no longer increase. To go faster the flux must be *reduced* ("field weakening"), which lowers the available torque in inverse proportion to speed while holding power approximately constant. This is the region of spindles and traction at high speed.

The boundary between the regions — the corner point of Figure 1.6 — is where the machine simultaneously reaches rated voltage and rated current. Sizing a drive is largely the art of placing this corner correctly for the intended duty cycle.

1.7 Worked Tutorials

TD 1.1 — Referred inertia, operating point and acceleration time

A drive with motor inertia $J_m = 0.02$ kg·m^2 drives, through a gearbox of ratio $n = 4$, a fan of inertia $J_L = 0.5$ kg·m^2 whose load torque at the load shaft is $T'_L = 0.8\,\Omega_L^2$ (N·m). Friction is negligible. The motor develops a constant $T_{em} = 6$ N·m. Find (a) the equivalent inertia at the motor shaft, (b) the steady-state motor speed, and (c) the time to reach 90 % of that speed.

(a) Referring the load inertia through the gearbox,

$$J = J_m + \frac{J_L}{n^2} = 0.02 + \frac{0.5}{16} = 0.0513 \text{ kg·m}^2.$$

(b) The load torque referred to the motor shaft is $T_{L,\text{ref}} = T'_L/n = (0.8/4)(\Omega_m/4)^2 =$

$0.0125\,\Omega_m^2$. Setting $T_{em} = T_{L,\text{ref}}$,

$$6 = 0.0125\,\Omega_m^2 \;\Rightarrow\; \Omega_m = \sqrt{480} = 21.9 \text{ rad/s } (\approx 209 \text{ rpm}).$$

(c) With $J\,d\Omega/dt = T_{em} - k\Omega^2$, $k = 0.0125$, integration gives

$$t = \frac{J}{2\sqrt{kT_{em}}} \ln \frac{\Omega_{ss} + \Omega_1}{\Omega_{ss} - \Omega_1}, \quad \Omega_1 = 0.9\,\Omega_{ss} = 19.7 \text{ rad/s},$$

$$t = \frac{0.0513}{2\sqrt{0.0125 \cdot 6}} \ln \frac{41.6}{2.2} \approx 0.0936 \times 2.94 \approx 0.28 \text{ s}.$$

Figure 1.7 shows the full transient obtained by numerical integration; note how the approach to Ω_{ss} slows as the torque margin $T_{em} - k\Omega^2$ shrinks — the reason the 90 % figure, not the 100 % figure, is the meaningful one.

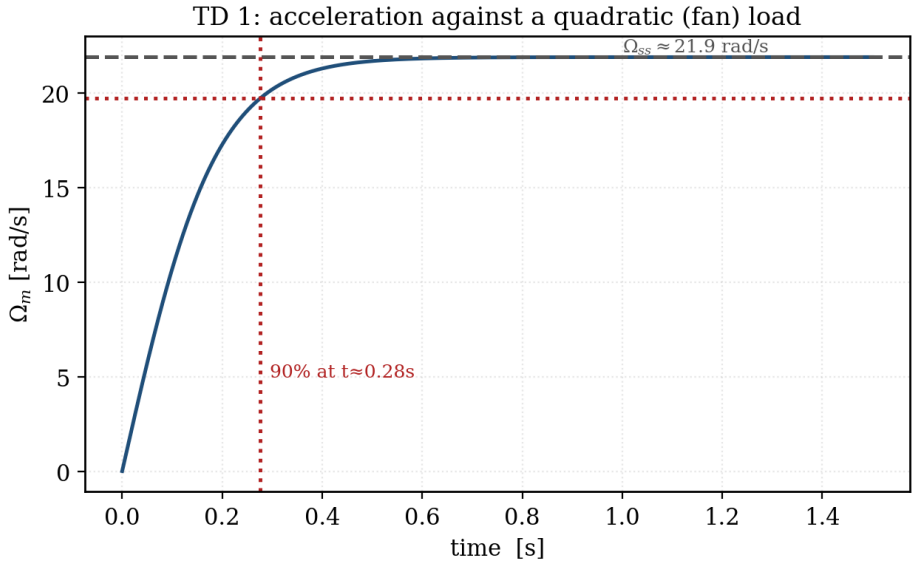


Figure 7: Figure 1.7 — Numerically integrated acceleration transient of TD 1.1 against the quadratic fan load.

TD 1.2 — Stability check

> A motor characteristic is $T_{em} = 40 - 2\Omega$ (N·m). It drives (i) a constant-torque load $T_L = 10$ N·m, and (ii) a load $T_L = 0.5\Omega^2$. Which operating points are stable?

For (i): $dT_{em}/d\Omega = -2$, $dT_L/d\Omega = 0$. Since $-2 < 0$ the criterion $dT_{em}/d\Omega < dT_L/d\Omega$ holds → **stable**. The operating point is $40 - 2\Omega = 10 \Rightarrow \Omega = 15$ rad/s.

For (ii): the equilibrium is $40 - 2\Omega = 0.5\Omega^2 \Rightarrow 0.5\Omega^2 + 2\Omega - 40 = 0 \Rightarrow \Omega = 7.4$ rad/s. There $dT_L/d\Omega = \Omega = 7.4$ and $dT_{em}/d\Omega = -2 < 7.4$ → **stable**, and even more strongly damped than case (i) because the load slope is large and positive.

TD 1.3 — Regenerative braking energy

> A 5 kg·m² flywheel spins at 1500 rpm. A regenerative drive brakes it to standstill. How much energy is returned to the supply, ignoring losses?

$\Omega = 1500 \cdot 2\pi/60 = 157.1$ rad/s. Kinetic energy $E = \tfrac{1}{2} J \Omega^2 = \tfrac{1}{2}(5)(157.1)^2 = 61.7$ kJ. All of it flows in Quadrant II/IV back toward the supply; a dissipative (resistor) drive would instead burn this 61.7 kJ as heat.

1.8 Exercises

1. A traction drive must climb a grade (constant-torque load) and coast downhill (overhauling load). In which quadrants does it operate in each case? Sketch the trajectory in the T–Ω plane.
2. Derive the mechanical time constant of a drive with $J = 0.1$ kg·m² and $B = 0.05$ N·m·s. What fraction of final speed is reached after 3 s under a torque step?
3. A load has $T_L = 5 + 0.02\Omega^2$. The motor characteristic is $T_{em} = 30 - 0.1\Omega$. Find all equilibria and classify their stability.
4. Explain why a high-ratio gearbox is favourable for driving a high-inertia load, and quantify the reflected inertia for $J_L = 20$ kg·m², $n = 10$.
5. A fan drive is slowed from 100 % to 80 % speed. By the affinity laws, estimate the new torque and power as percentages of rated.

1.9 Advanced Topics in Drive Mechanics

The single-inertia model of §1.2 is sufficient for most controller design, but three refinements matter in practice: **optimal gear matching**, **thermal (RMS) sizing**, and **elastic-shaft (two-mass) dynamics**. Each is developed below because each dictates a real design decision — respectively the choice of gearbox ratio, the choice of continuous motor rating, and the mechanical bandwidth beyond which a controller must not be pushed.

1.9.1 Optimal gear ratio for fastest acceleration

Consider a motor of inertia J_m driving, through a gearbox of ratio $n = \Omega_m / \Omega_L$, a load of inertia J_L that requires a torque T_L' at its own shaft. The torque the motor must supply is

$$T_{em} = J_m \, \dot{\Omega}_m + \frac{1}{n}\Big(J_L \, \dot{\Omega}_L + T_L' \Big) = \Big(J_m + \frac{J_L}{n^2} \Big) \dot{\Omega}_m + \frac{T_L'}{n}.$$

For a *pure inertial* load ($T_L' = 0$) accelerated as fast as possible for a given motor torque, the load acceleration is $\dot{\Omega}_L = \dot{\Omega}_m / n$, so

$$\dot{\Omega}_L = \frac{n \, T_{em}}{n^2 J_m + J_L}.$$

Maximising $\dot{\Omega}_L$ over n (set $\mathrm{d}\dot{\Omega}_L / \mathrm{d}n = 0$) gives the classic **inertia-matching** result:

$$\boxed{n_{opt} = \sqrt{\frac{J_L}{J_m}}} \qquad \Longrightarrow \qquad J_L / n_{opt}^2 = J_m .$$

At the optimum the load inertia *reflected to the motor* exactly equals the motor inertia; half of the motor torque accelerates its own rotor and half the load. Gearing well away from n_{opt} wastes available acceleration, which is why servo catalogues quote a **reflected-inertia ratio** and recommend keeping it below about 5–10:1.

1.9.2 RMS torque and thermal sizing

A motor's **continuous** torque is limited by heating, i.e. by the *root-mean-square* current, whereas its **peak** torque is limited by demagnetisation or converter current. Over a periodic motion profile of period T_{cyc} the thermally-equivalent torque is

$$T_{rms} = \sqrt{\frac{1}{T_{cyc}} \int_0^{T_{cyc}} T_{em}^2(t)\, \mathrm{d}t}.$$

For the common **trapezoidal velocity profile** (accelerate at T_a for t_a, run at constant speed with T_r for t_c, decelerate at $-T_d$ for t_d, dwell for t_0),

$$T_{rms} = \sqrt{\frac{T_a^2 t_a + T_r^2 t_c + T_d^2 t_d}{t_a + t_c + t_d + t_0}}.$$

A drive is correctly sized when $T_{rms} \le T_{cont}$ (motor continuous rating) **and** $\max(T_a, T_d) \le T_{peak}$. Ignoring the dwell time t_0 is the most common sizing error: a highly dynamic but low-duty profile can demand large peak torque yet a modest continuous rating.

1.9.3 The two-inertia (elastic-shaft) model

When motor and load are joined by a shaft, belt or long coupling of finite stiffness K_s (N·m/rad) and internal damping D_s, the drive is a **two-mass torsional system**:

$$\begin{aligned} J_m \,\dot{\omega}_m &= T_{em} - K_s(\theta_m - \theta_L) - D_s(\omega_m - \omega_L), \\ J_L \,\dot{\omega}_L &= K_s(\theta_m - \theta_L) + D_s(\omega_m - \omega_L) - T_L . \end{aligned}$$

Neglecting damping, the transfer function from motor torque to motor speed exhibits an **anti-resonance** (zero) and a **resonance** (pole) at

$$\omega_{ar} = \sqrt{\frac{K_s}{J_L}}, \qquad \omega_{res} = \sqrt{K_s\left(\frac{1}{J_m} + \frac{1}{J_L}\right)}.$$

The speed-loop bandwidth must be kept safely below ω_{res} (a common rule is $\le \tfrac{1}{3}\omega_{res}$) or the controller will excite torsional oscillation. This is the mechanical counterpart

of the electrical bandwidth limits derived in Chapter 3, and it explains why very stiff, low-inertia couplings are prized in servo applications.

1.10 Additional Solved Tutorials

TD 1.4 — Optimal gear ratio

A servo motor has $J_m = 0.4 \times 10^{-4}$ kg·m^2 and must accelerate a pure-inertia load $J_L = 9 \times 10^{-4}$ kg·m^2. Find the gear ratio giving maximum load acceleration and the resulting reflected-inertia ratio.

$$n_{opt} = \sqrt{J_L / J_m} = \sqrt{9 \times 10^{-4} / (0.4 \times 10^{-4})} = \sqrt{22.5} = 4.74.$$

Reflected load inertia $J_L / n_{opt}^2 = 9 \times 10^{-4} / 22.5 = 0.4 \times 10^{-4} = J_m$, so the ratio is exactly 1:1 — the motor "sees" its own inertia again, confirming the match.

TD 1.5 — RMS torque of a motion profile

A pick-and-place axis runs the cycle: accelerate at $T_a = 3.0$ N·m for 0.10 s, cruise at $T_r = 0.8$ N·m for 0.30 s, decelerate at $T_d = 3.0$ N·m for 0.10 s, then dwell $t_0 = 0.50$ s. Find T_{rms} and check a motor rated $T_{cont} = 1.2$ N·m, $T_{peak} = 4$ N·m.

$$\begin{aligned} T_{rms} &= \sqrt{\frac{3.0^2(0.10) + 0.8^2(0.30) + 3.0^2(0.10)}{0.10 + 0.30 + 0.10 + 0.50}} \\ &= \sqrt{\frac{0.90 + 0.192 + 0.90}{1.00}} = \sqrt{1.992} = 1.41 \text{ N·m}. \end{aligned}$$

Here $T_{rms} = 1.41 > T_{cont} = 1.2$ N·m, so although the peak ($3.0 < 4$ N·m) is fine, the motor would **overheat**: either a larger motor or a longer dwell is required. Lengthening t_0 to 0.9 s gives $T_{rms} = \sqrt{1.992/1.4} = 1.19$ N·m, just inside the continuous limit.

TD 1.6 — Torsional resonance

A motor ($J_m = 0.02$ kg·m²) drives a load ($J_L = 0.06$ kg·m²) through a coupling of stiffness $K_s = 1500$ N·m/rad. Find the anti-resonance and resonance frequencies and the maximum safe speed-loop bandwidth.

$$\omega_{ar} = \sqrt{K_s / J_L} = \sqrt{1500 / 0.06} = 158 \text{ rad/s } (25.2 \text{ Hz}),$$

$$\omega_{res} = \sqrt{1500 \left(\tfrac{1}{0.02} + \tfrac{1}{0.06} \right)} = \sqrt{1500 \times 66.7} = 316 \text{ rad/s } (50.3 \text{ Hz}).$$

A prudent speed-loop bandwidth is $\leq \tfrac{1}{3}\omega_{res} \approx 105$ rad/s (≈ 17 Hz); pushing beyond ω_{res} risks a lightly-damped 50 Hz torsional oscillation.

TD 1.7 — Regenerative energy on a downgrade

A 1200 kg electric vehicle descends a 6 % grade at a constant 15 m/s for 40 s with the drive in braking (Quadrant IV/II). Estimate the mechanical energy

returned toward the DC bus, ignoring losses. ($g = 9.81$ m/s².)

The gravitational power along the slope is $P = mg\sin\theta \cdot v$. For a 6 % grade, $\sin\theta \approx 0.06$:

$$P = 1200 \times 9.81 \times 0.06 \times 15 = 1.06 \times 10^4 \text{ W} = 10.6 \text{ kW}.$$

Over 40 s the returned energy is $E = P\,t = 10.6\times10^3\times40 = 4.24\times10^5$ J $= 0.118$ kWh. With a regenerative front end this energy recharges the battery; without one it must be burned in a braking resistor. This is precisely why traction drives are **four-quadrant** (§1.4).

1.11 Exercises (supplementary)

1. A hoist lifts a 500 kg mass at 1.2 m/s through a drum of radius 0.25 m. Find the load torque and motor speed, then the motor power. Which quadrant applies when lowering under control?
2. Derive the acceleration time from 0 to Ω_1 for a **constant-torque** load $T_L = T_0$ with constant motor torque T_{em}, and compare its form with the quadratic-load result of TD 1.1.
3. A fan load is $T_L = 0.02\,\Omega^2$. The motor characteristic is $T_{em} = 20 - 0.1\,\Omega$. Find the operating speed and verify stability using the criterion of §1.5.
4. For the two-inertia system of TD 1.6, recompute ω_{res} if the coupling stiffness is doubled. By what factor does the safe bandwidth change?
5. A motion profile must index 30° in 0.2 s with a triangular velocity profile (accelerate then immediately decelerate). If the reflected inertia is 2×10^{-4} kg·m², find the peak torque required.
6. Explain physically why a load whose torque *rises* with speed is inherently stabilising, whereas a series-DC-motor-like characteristic on a hoist can be unstable.

Chapter 2 — Variable-Speed Drives for Induction and Synchronous Machines (Scalar Control)

(Duration: 3 weeks)

2.1 The Frequency-Control Principle

The synchronous speed of any AC machine with p pole pairs supplied at frequency f is

$$n_s = \frac{60f}{p}\ [\text{rpm}], \qquad \Omega_s = \frac{2\pi f}{p}\ [\text{rad/s}].$$

The induction motor runs slightly below this at slip s: $\Omega_r = (1-s)\Omega_s$; the synchronous machine is locked exactly to Ω_s. In both cases **continuous speed control demands control of the supply frequency**. Because the utility grid offers only a fixed 50/60 Hz, the drive must interpose a **variable-frequency inverter** between supply and machine. Everything in this chapter — the V/f law, the inverter, and pulse-width modulation — exists to synthesise a balanced three-phase set of adjustable frequency *and* adjustable amplitude.

Scalar control is defined by what it regulates: only the **magnitudes** of voltage and frequency, in open loop (or with light speed feedback). It deliberately ignores the instantaneous phase relationship between current and flux. This makes it simple, cheap and robust — and, as Section 2.6 shows, dynamically limited.

2.2 Constant-V/f Control of the Induction Motor

2.2.1 Flux and the V/f law

The air-gap flux of an AC machine is fixed by the stator counter-EMF and the frequency. From the EMF equation,

$$E_s = 4.44\, N_s k_w f\, \phi_m \implies \phi_m = \frac{E_s}{4.44\, N_s k_w f} \propto \frac{E_s}{f}.$$

At medium and high speed the stator resistive and leakage drops are small, so $E_s \approx V_s$ and

$$\boxed{\phi_m \propto \frac{V_s}{f}}.$$

Holding the **voltage-to-frequency ratio constant** therefore holds the flux constant — the machine is neither driven into magnetic saturation (excess flux, overheating, distorted current) nor starved of flux (loss of torque capability). Constant flux, in turn, keeps the peak (breakdown) torque nearly constant across the speed range, which is the defining benefit of V/f control.

2.2.2 The three operating regions and voltage boost

The complete V/f profile has three parts, drawn in Figure 2.1.

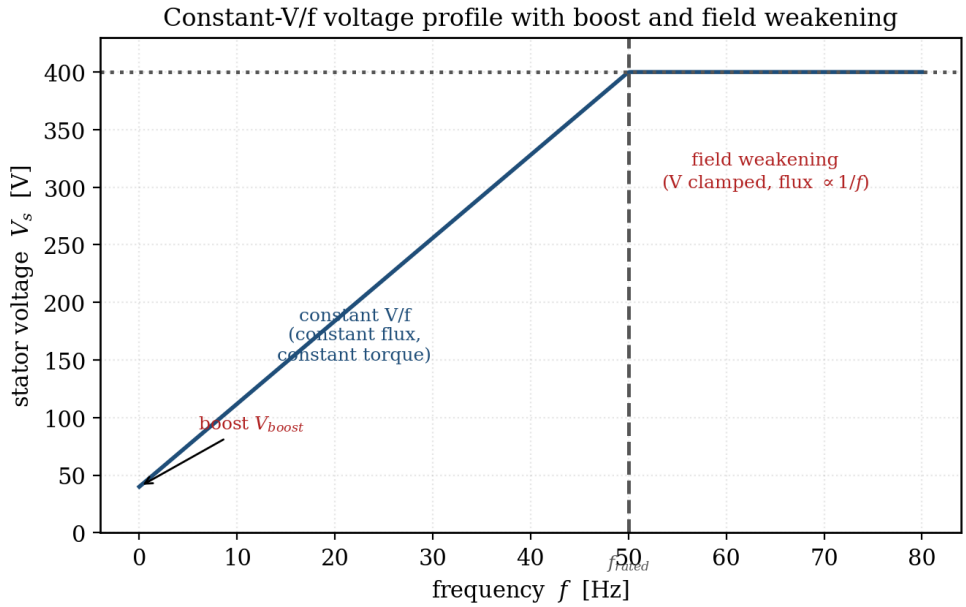


Figure 8: Figure 2.1 — The constant-V/f profile with low-speed voltage boost and the high-speed field-weakening region.

- **Low-frequency (boost) region.** As $f \to 0$ the neglected term $R_s I_s$ is no longer small compared with V_s; if V/f were kept strictly constant the flux would collapse and with it the starting torque. A fixed **voltage boost** V_{boost} is therefore added at low frequency to compensate the resistive drop and preserve flux.
- **Constant-flux region** ($0 < f < f_{rated}$). V_s/f is held constant, flux is constant, and the machine delivers constant maximum torque.
- **Field-weakening region** ($f > f_{rated}$). The voltage saturates at its rated value; flux falls as $1/f$; the machine enters constant-power operation with reduced torque.

2.2.3 Torque under constant V/f

From the steady-state equivalent circuit, the developed torque of the induction motor is

$$T_{em} = \frac{3p}{\Omega_s} \cdot \frac{V_s^2 \, (R_r/s)}{(R_s + R_r/s)^2 + (X_s + X_r)^2}.$$

The **breakdown (maximum) torque**, obtained by $dT_{em}/ds = 0$, is

$$T_{max} = \frac{3p}{2\Omega_s} \cdot \frac{V_s^2}{R_s + \sqrt{R_s^2 + (X_s + X_r)^2}}.$$

Since $X = 2\pi f L$ and $\Omega_s \propto f$, keeping V_s/f constant keeps $V_s^2/\Omega_s \propto V_s^2/f$ and the reactances scale with f, so T_{max} is very nearly constant with frequency (exactly so if R_s is neglected). Figure 2.2 shows the resulting family of torque–speed curves: each supply frequency simply **shifts the curve horizontally**, preserving its shape and peak. The drive selects a speed by selecting the frequency whose curve intersects the load at the desired point.

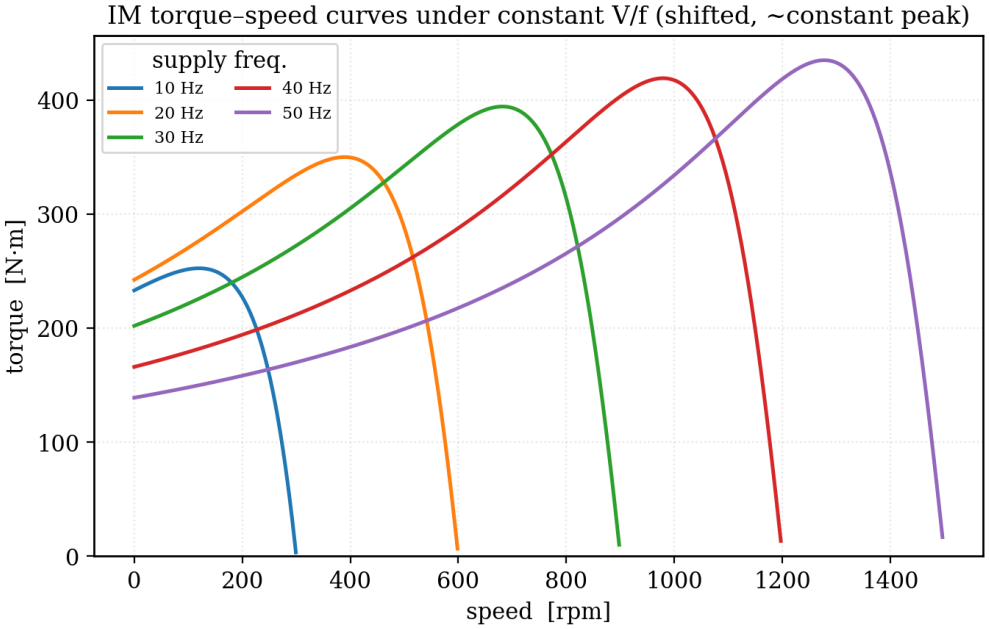


Figure 9: Figure 2.2 — Induction-motor torque–speed curves under constant V/f: changing frequency translates the curve while preserving breakdown torque.

2.2.4 Slip compensation

Open-loop V/f suffers a speed **droop**: under load the rotor slips, so the actual speed falls below the commanded synchronous speed. A simple and effective remedy is **slip compensation** (Figure 2.3): the slip frequency is estimated from the measured stator current (a proxy for torque) and *added* to the commanded frequency, $f^* = f_{cmd} + f_{slip}$, restoring the speed. This gives approximate speed regulation without a shaft sensor — a sensorless scalar drive.

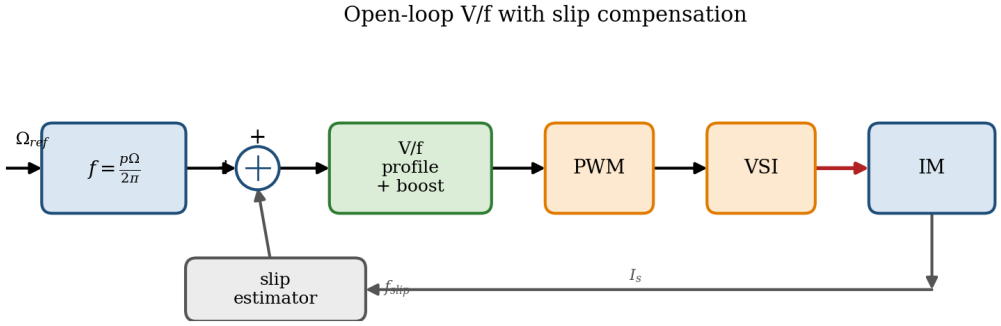


Figure 10: Figure 2.3 — Open-loop V/f with slip compensation: the estimated slip frequency is added to the command to cancel load-induced droop.

2.3 The Voltage-Source Inverter

The workhorse converter of AC drives is the **two-level three-phase voltage-source inverter (VSI)** of Figure 2.4. Three legs, each a pair of controlled switches with antiparallel diodes, connect the three motor terminals either to the positive rail ($+V_{dc}$) or to the negative rail. The two switches of a leg are operated in complementary fashion (with a small dead-time to prevent shoot-through).

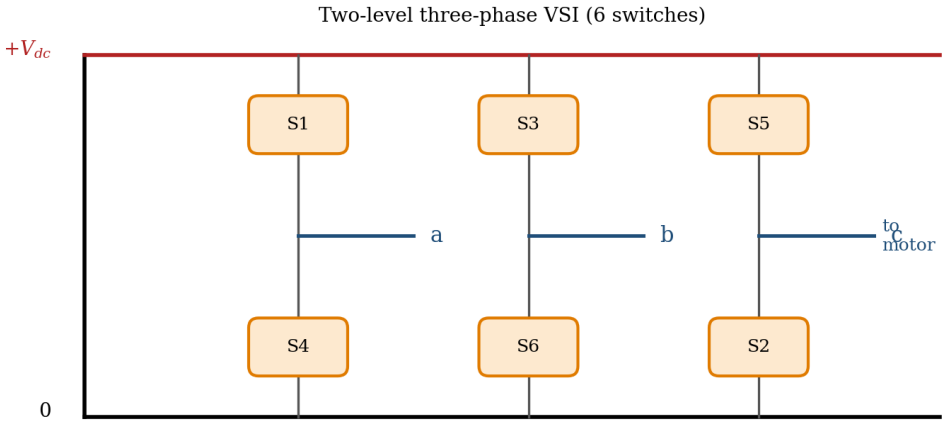


Figure 11: Figure 2.4 — Two-level three-phase voltage-source inverter feeding the motor.

Because each leg has two states, the inverter has $2^3 = 8$ switching combinations. Six of them apply a non-zero voltage to the machine — the **active vectors** $\mathbf{V}_1 \dots \mathbf{V}_6$, each of magnitude $\frac{2}{3}V_{dc}$ in the stationary $\alpha\beta$ plane — and two short the machine to a single rail, producing the **zero vectors** $\mathbf{V}_0$ (000) and $\mathbf{V}_7$ (111). The active vectors point to the vertices of a regular hexagon, 60° apart (Figure 2.5). Every modulation strategy in this book is, at bottom, a rule for choosing among these eight vectors and for how long to apply each.

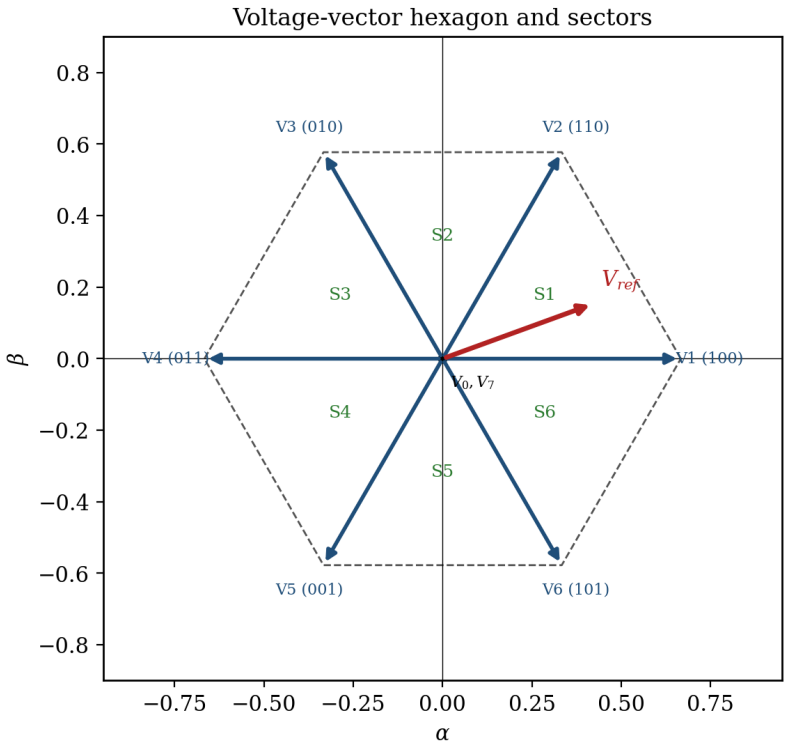


Figure 12: Figure 2.5 — The eight inverter states as space vectors: six active vectors on a hexagon, two zero vectors at the origin, and a reference vector in Sector I.

2.4 Pulse-Width Modulation

2.4.1 Sinusoidal PWM

The oldest and simplest modulator compares three sinusoidal **reference** (modulating) signals with a common high-frequency **triangular carrier** (Figure 2.6). Whenever a phase reference exceeds the carrier, that leg is switched to the positive rail; otherwise to the negative rail. The references are

$$v_a^* = M\cos\omega t, \quad v_b^* = M\cos(\omega t - \tfrac{2\pi}{3}), \quad v_c^* = M\cos(\omega t + \tfrac{2\pi}{3}),$$

and the **modulation index** is $M = \hat{V}^*/(V_{dc}/2)$. In the linear region $0 \le M \le 1$ the peak fundamental phase voltage reaches $V_{dc}/2$. The switching harmonics cluster around the carrier frequency and its multiples, far above the fundamental, and are filtered by the machine's own inductance.

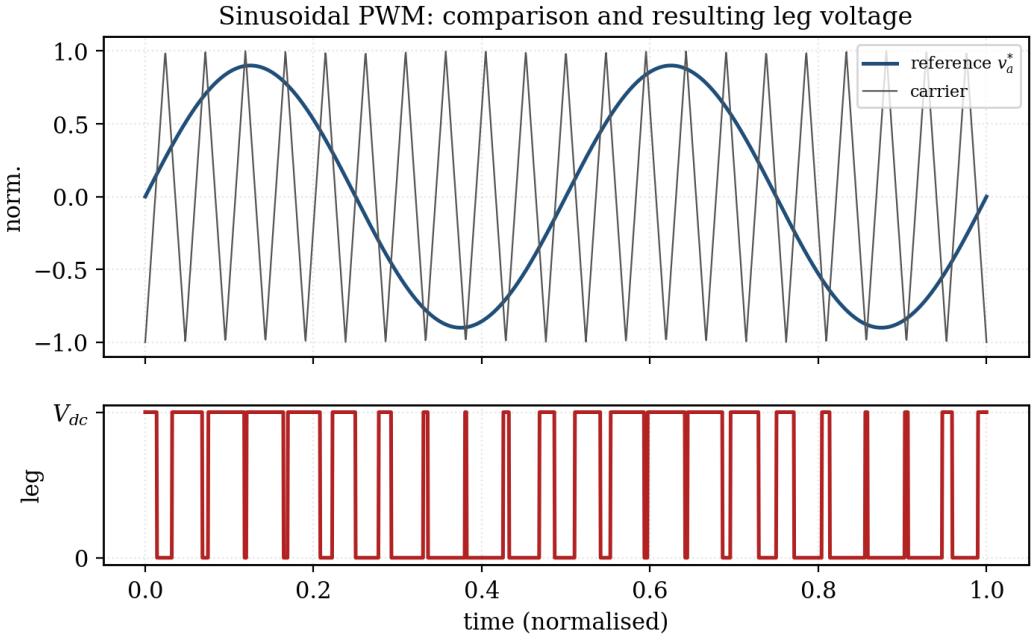


Figure 13: Figure 2.6 — Sinusoidal PWM: the intersections of the sinusoidal reference with the triangular carrier define the switched leg voltage.

2.4.2 Space-Vector Modulation

Space-vector modulation (SVM) treats the three reference voltages as a single rotating vector $\mathbf{V}_{ref}$ and synthesises it by time-averaging the two active vectors adjacent to it, plus the zero vectors, over each switching period T_s (Figure 2.7). For a reference in Sector I, lying at angle θ from $\mathbf{V}_1$,

$$T_1 = \frac{\sqrt{3}\,|\mathbf{V}_{ref}|\,T_s}{V_{dc}}\sin\!\left(\frac{\pi}{3}-\theta\right), \qquad T_2 = \frac{\sqrt{3}\,|\mathbf{V}_{ref}|\,T_s}{V_{dc}}\sin\theta,$$

$$T_0 = T_s - T_1 - T_2 \quad (\text{shared between } \mathbf{V}_0 \text{ and } \mathbf{V}_7).$$

The vector equation $\mathbf{V}_{ref}T_s = \mathbf{V}_1 T_1 + \mathbf{V}_2 T_2$ is exactly the parallelogram construction drawn in the figure.

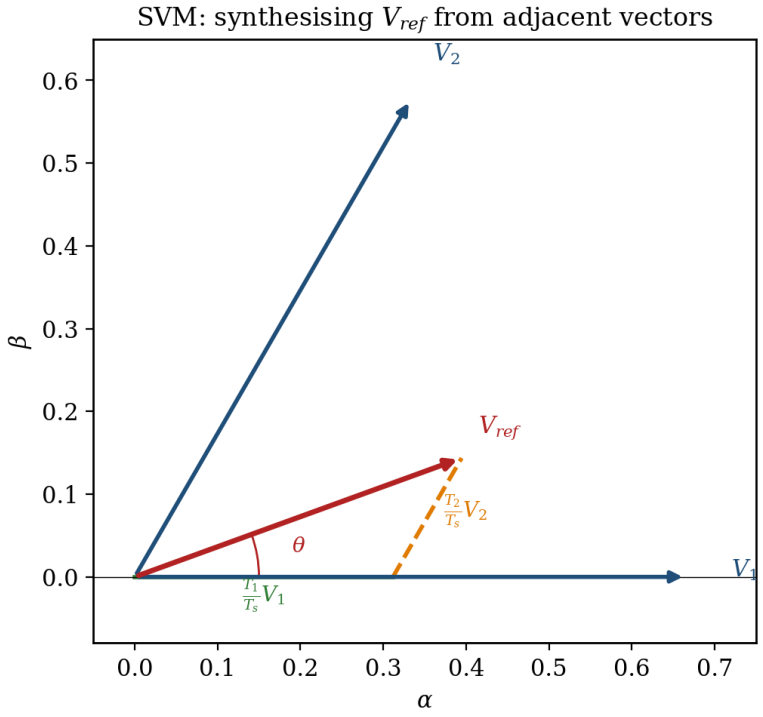


Figure 14: Figure 2.7 — SVM synthesises the reference as a time-weighted sum of the two adjacent active vectors.

Why SVM outperforms SPWM. The largest reference that still fits inside the hexagon lies on its *inscribed circle*, of radius $V_{dc}/\sqrt{3}$ (Figure 2.8). This gives a peak fundamental phase voltage of $V_{dc}/\sqrt{3} \approx 0.577\,V_{dc}$, about **15.5 % more** than SPWM's $V_{dc}/2$. SVM therefore extracts more voltage — and hence more speed — from the same DC bus, while also producing lower current harmonic distortion. For these reasons SVM is the standard modulator for the field-oriented drives of Chapter 3.

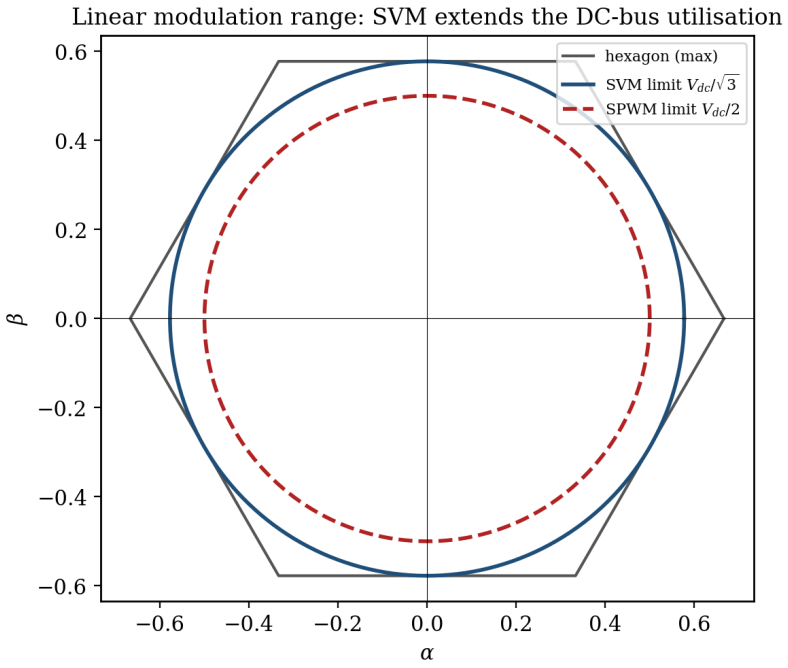


Figure 15: Figure 2.8 — Linear-modulation limits: SVM reaches the inscribed circle ($V_{dc}/\sqrt{3}$), SPWM only the smaller circle ($V_{dc}/2$).

2.5 Speed Control of Synchronous Machines

2.5.1 Open-loop V/f

A synchronous or permanent-magnet machine can also be run on an open-loop V/f profile. With no slip, the speed tracks the commanded frequency *exactly* — provided the machine remains synchronised. The danger is **loss of synchronism (pull-out)**: without rotor-position feedback, a load transient or an over-rapid frequency ramp can swing the load angle past 90°, and the rotor slips poles. Open-loop V/f is therefore confined to light, slowly varying loads such as some fans and pumps.

2.5.2 Self-controlled (autopilot) operation

To guarantee synchronism, the inverter frequency is **slaved to the measured rotor position** (Figure 2.9). The switching instants are commanded by the rotor angle itself, so the stator field is always held in the correct spatial relationship to the rotor — the machine can never lose synchronism, because it is the rotor that dictates the commutation.

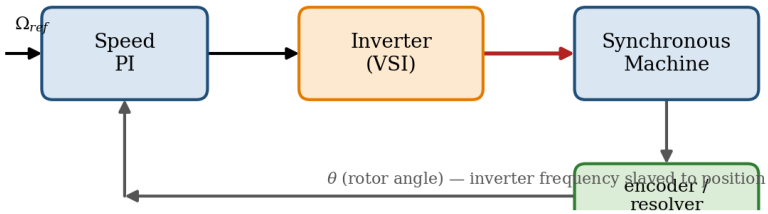


Figure 16: Figure 2.9 — Self-controlled (autopilot) synchronous drive: rotor position closes the commutation loop, making the machine behave like an electronically-commutated DC motor.

This **self-controlled synchronous machine** behaves electrically like a DC motor whose mechanical commutator has been replaced by the inverter plus position feedback — the essence of the *brushless DC* drive. It is the conceptual stepping-stone to the field-oriented control of Chapter 3, where the same idea is expressed through coordinate transformation rather than through direct commutation.

2.6 Limitations of Scalar Control

Scalar control regulates magnitudes only; it has no handle on the instantaneous *angle* between stator current and rotor flux. The consequences are fundamental:

- **No flux–torque decoupling.** A change in the torque-producing current inevitably disturbs the flux, so torque cannot be commanded cleanly.
- **Poor transient response.** Flux is controlled only in steady state; during fast transients the flux wanders, and the torque response is sluggish and oscillatory.
- **No direct torque command.** The drive commands frequency and voltage, not torque — unacceptable for servo, robotics and traction, where torque is the quantity of interest.

These limitations are not defects of tuning but of the *information* scalar control chooses to ignore. Overcoming them requires manipulating the current **vector** — its magnitude *and* its phase — which is precisely what vector control (Chapter 3) and direct torque control (Chapter 4) do.

2.7 MATLAB/Simulink Implementation

A minimal open-loop V/f drive is assembled from: a speed-to-frequency block ($f = p\Omega/2\pi$); a V/f look-up with boost; a three-phase reference-voltage generator; an SVM (or SPWM) modulator; a `Universal Bridge` inverter fed from a DC source; and an `Asynchronous Machine` block loaded by a mechanical torque. A representative reference-generation snippet is:

```
% ----- open-loop V/f reference (per sample) -----
f      = p*wref/(2*pi);            % command frequency [Hz]
V      = Vboost + (Vrated-Vboost)*min(f,frated)/frated;
if f > frated, V = Vrated; end     % field weakening
theta  = theta + 2*pi*f*Ts;        % integrate angle
```

```
Vabc   = V*[cos(theta); cos(theta-2*pi/3); cos(theta+2*pi/3)];
duty   = svm(Vabc, Vdc, Ts);       % space-vector modulator
```

Validate the model by (i) checking that flux stays near rated across the constant-V/f region, (ii) confirming the 15.5 % voltage advantage of SVM over SPWM at full modulation, and (iii) observing the speed droop under load *before* enabling slip compensation and its cancellation *after*.

2.8 Worked Tutorials

TD 2.1 — V/f ratio and SVM ceiling

> A 4-pole, 400 V (line, RMS), 50 Hz induction motor is fed from an SVM inverter with $V_{dc} = 600$ V. (a) Give the V/f constant and the voltage at 30 Hz. (b) What maximum line-RMS fundamental can the SVM inverter produce, and can it reach rated voltage?

(a) $V/f = 400/50 = 8$ V/Hz, so at 30 Hz, $V = 8 \times 30 = 240$ V (line, RMS).

(b) SVM's peak phase fundamental is $V_{dc}/\sqrt{3} = 346.4$ V, i.e. line-RMS $= 346.4 \times \sqrt{3}/\sqrt{2} = 424\,\text{V} > 400$ V. The inverter **reaches rated voltage** with ≈6 % margin. An SPWM inverter, capped at $V_{dc}/2 = 300$ V peak phase → 367 V line-RMS, could **not**.

TD 2.2 — SVM dwell times

> A reference of magnitude $|\mathbf{V}_{ref}| = 300$ V sits in Sector I at $\theta = 20°$, with $T_s = 100$ μs and $V_{dc} = 600$ V. Compute T_1, T_2, T_0.

$K = \sqrt{3}\,|\mathbf{V}_{ref}|T_s/V_{dc} = \sqrt{3}(300)(100\mu)/600 = 86.6$ μs. $T_1 = K\sin(40°) = 55.7$ μs, $T_2 = K\sin(20°) = 29.6$ μs, $T_0 = 100 - 55.7 - 29.6 = 14.7$ μs. The active vectors occupy 85 % of the period; the balance is zero-vector time.

TD 2.3 — Breakdown-torque invariance

> Show that, neglecting R_s, the breakdown torque of an induction motor is independent of supply frequency under constant V/f.

With $R_s \approx 0$, $T_{max} = \dfrac{3p}{2\Omega_s}\dfrac{V_s^2}{X_s + X_r}$. Now $\Omega_s \propto f$, $X_s + X_r \propto f$, and under constant V/f $V_s \propto f$ so $V_s^2 \propto f^2$. Hence $T_{max} \propto \dfrac{f^2}{f \cdot f} = \text{const}$. The breakdown torque is frequency-independent, confirming the horizontal translation seen in Figure 2.2.

2.9 Exercises

1. A 6-pole motor is to run at 900 rpm from a V/f drive. What supply frequency is required, and what is the slip if the measured speed is 870 rpm?
2. Compute the DC-bus voltage needed for an SVM drive to deliver 380 V line-RMS at the fundamental.
3. Sketch the V/f profile including boost for a motor rated 230 V, 50 Hz, and mark the field-weakening knee.
4. For a reference in Sector II at $\theta = 35°$ (measured from the sector's leading vector), write the dwell-time expressions and evaluate them for $|\mathbf{V}_{ref}| = 0.8\,V_{dc}/\sqrt{3}$.

5. Explain, with reference to the load angle, why an open-loop V/f synchronous drive can lose synchronism while a self-controlled one cannot.
6. A fan drive saves energy by reducing speed. Using the affinity laws, tabulate torque, power and (assuming constant efficiency) input current at 100 %, 80 % and 60 % speed.

2.10 Space-Vector Modulation in Depth

Section 2.4.2 introduced SVM for a reference in Sector I. Because SVM underlies every high-performance drive in Chapters 3–4, its full mechanics deserve a complete treatment.

2.10.1 The eight switching states

With the three leg-switching functions $(S_a, S_b, S_c) \in \{0,1\}^3$ the inverter produces eight states. The line-to-neutral voltages follow $v_a = \frac{V_{dc}}{3}(2S_a - S_b - S_c)$ and cyclic permutations, giving:

State	$(S_a S_b S_c)$	Vector	$\lvert\mathbf{V}\rvert$	Angle
$\mathbf{V}_0$	000	zero	0	—
$\mathbf{V}_1$	100	active	$\frac{2}{3}V_{dc}$	0°
$\mathbf{V}_2$	110	active	$\frac{2}{3}V_{dc}$	60°
$\mathbf{V}_3$	010	active	$\frac{2}{3}V_{dc}$	120°
$\mathbf{V}_4$	011	active	$\frac{2}{3}V_{dc}$	180°
$\mathbf{V}_5$	001	active	$\frac{2}{3}V_{dc}$	240°
$\mathbf{V}_6$	101	active	$\frac{2}{3}V_{dc}$	300°
$\mathbf{V}_7$	111	zero	0	—

The six active vectors form the vertices of the hexagon; the two zero vectors sit at the origin and are used to "park" the average while the reference is synthesised.

2.10.2 General dwell-time equations

For a reference $\mathbf{V}_{ref} = |\mathbf{V}_{ref}|e^{j\theta}$ falling in sector k ($k = 1 \dots 6$), let $\theta' = \theta - (k-1)\frac{\pi}{3}$ be the angle measured from the sector's leading active vector. The two active dwell times over a switching period T_s are

$$T_a = \frac{\sqrt{3}\,|\mathbf{V}_{ref}|\,T_s}{V_{dc}}\sin\!\Big(\frac{\pi}{3} - \theta'\Big), \qquad T_b = \frac{\sqrt{3}\,|\mathbf{V}_{ref}|\,T_s}{V_{dc}}\sin\theta',$$

$$T_0 = T_s - T_a - T_b.$$

Defining the **modulation index** $m = |\mathbf{V}_{ref}|/(V_{dc}/\sqrt{3})$, the linear range is $0 \le m \le 1$. The zero-vector time T_0 is split equally between $\mathbf{V}_0$ and $\mathbf{V}_7$ in **symmetric seven-**

segment SVM, which centres the pulses and minimises current ripple and harmonic distortion.

2.10.3 Voltage ceiling and overmodulation

The largest circle inscribed in the hexagon has radius $V_{dc}/\sqrt{3}$ (peak phase), i.e. $m = 1$. Compared with SPWM's ceiling of $V_{dc}/2$, SVM delivers

$$\frac{V_{dc}/\sqrt{3}}{V_{dc}/2} = \frac{2}{\sqrt{3}} = 1.1547,$$

a **15.5 % higher fundamental** from the same DC bus — one reason SVM is preferred. Pushing $m > 1$ enters **overmodulation**, where the reference leaves the inscribed circle: the trajectory is clipped to the hexagon boundary, low-order harmonics appear, and at the limit ($m \approx 1.103$, the hexagon-inscribed operation) the modulator degenerates into **six-step** operation with peak fundamental $\frac{2}{\pi}V_{dc}$.

2.10.4 Dead-time and its voltage error

Real switches need a **dead time** t_d between turning one leg-switch off and the complementary one on, to avoid shoot-through. During t_d the leg voltage is set by the current direction, not the command, producing a per-phase fundamental voltage error

$$\Delta V \approx t_d\, f_{sw}\, V_{dc} \cdot \text{sgn}(i_{phase}) = t_d f_{sw} V_{dc}\ \text{sgn}(i_{phase}).$$

This error is a square wave in phase with the current, so it injects 5^{th}, 7^{th}, 11^{th}... harmonics and causes current-zero-crossing distortion ("clamping"). High-performance drives add **dead-time compensation**, feeding $+\Delta V$ forward according to the measured current sign.

2.10.5 Harmonic quality

For symmetric SVM the dominant voltage harmonics cluster around the switching frequency and its multiples ($f_{sw} \pm 2f_1$, $2f_{sw} \pm f_1$, ...). The **total harmonic distortion** of the current falls with f_{sw} and with load inductance L; a useful estimate for the ripple current amplitude is

$$\Delta i_{pp} \approx \frac{V_{dc}\, T_s}{8L} \quad \text{(worst case, mid-modulation)}.$$

This links the modulator directly to the current-loop design of Chapter 3: raising f_{sw} shrinks ripple and permits a wider current-loop bandwidth α_c.

2.11 Additional Solved Tutorials

TD 2.4 — SVM in Sector III

For $V_{dc} = 540$ V, $T_s = 125$ μs, a reference of $|\mathbf{V}_{ref}| = 280$ V lies at $\theta = 140^\circ$. Identify the sector, the two active vectors, and the dwell times.

140° lies in $[120^\circ, 180^\circ) \rightarrow$ **Sector III**, bounded by $\mathbf{V}_3$ (120°) and $\mathbf{V}_4$ (180°). The in-sector angle is $\theta' = 140 - 120 = 20^\circ$.

$$K = \frac{\sqrt{3}\,|\mathbf{V}_{ref}|\,T_s}{V_{dc}} = \frac{\sqrt{3} \times 280 \times 125 \times 10^{-6}}{540} = 1.122 \times 10^{-4}\ \text{s} = 112.2\ \mu\text{s},$$

$$T_a = K \sin(60^\circ - 20^\circ) = 112.2 \sin 40^\circ = 72.1\ \mu\text{s}\ (\text{on}\ \mathbf{V}_3),$$

$$T_b = K \sin 20^\circ = 38.4\ \mu\text{s}\ (\text{on}\ \mathbf{V}_4), \qquad T_0 = 125 - 72.1 - 38.4 = 14.5\ \mu\text{s}.$$

TD 2.5 — Modulation index and headroom

A motor needs 230 V (line RMS) fundamental. With $V_{dc} = 650$ V, find the SVM modulation index and the remaining voltage headroom.

Peak phase required: $\hat{V}_{ph} = \sqrt{2} \cdot 230/\sqrt{3} = 187.8$ V. SVM ceiling $V_{dc}/\sqrt{3} = 375.3$ V.

$$m = \frac{187.8}{375.3} = 0.500.$$

Only half the linear range is used, leaving generous headroom for the transient voltage the current controllers demand during fast torque steps — exactly the margin field weakening later consumes.

TD 2.6 — Dead-time voltage error

With $t_d = 2\ \mu$s, $f_{sw} = 10$ kHz, $V_{dc} = 540$ V, estimate the per-phase fundamental voltage error introduced by dead time.

$$\Delta V \approx t_d f_{sw} V_{dc} = 2 \times 10^{-6} \times 10^4 \times 540 = 10.8\ \text{V}.$$

Nearly 11 V of square-wave error per phase — about 6 % of a 187 V peak fundamental — which is why dead-time compensation is standard below a few hundred volts of command.

2.12 Exercises (supplementary)

1. Derive $v_a = \frac{V_{dc}}{3}(2S_a - S_b - S_c)$ from the leg definitions, and verify the magnitude $\frac{2}{3}V_{dc}$ of an active vector.
2. Compute the SVM dwell times for $m = 0.9$, $\theta' = 45^\circ$, $T_s = 100\ \mu$s.
3. A drive runs at $m = 1.05$. Explain qualitatively what happens to the reference trajectory and which harmonics appear.
4. Show that six-step operation gives a peak fundamental phase voltage of $\frac{2}{\pi}V_{dc}$ and compute the ratio to the SVM linear limit.
5. For $V_{dc} = 600$ V, $L = 3$ mH, $f_{sw} = 8$ kHz, estimate the worst-case peak-to-peak ripple current.
6. A 4-pole IM runs V/f at 35 Hz from an SVM inverter with $V_{dc} = 560$ V and a 400 V/50 Hz nameplate. Find the commanded voltage and the modulation index.

Chapter 3 — Vector Control / Field-Oriented Control (FOC) of the PMSM

(Duration: 4 weeks)

3.1 The Idea: Making an AC Machine Behave Like a DC Machine

In a separately-excited DC machine, torque control is trivial because nature has already decoupled the variables: the field winding sets the flux, the armature winding sets the torque, and the mechanical commutator holds the two magnetic axes permanently orthogonal, so that

$$T_{em} = k\,\phi_f\,i_a.$$

Flux and torque are controlled by two independent currents. This is why, for a century, the DC drive was the benchmark for high-performance motion control.

Field-Oriented Control (FOC), introduced by Hasse and Blaschke around 1970, recreates exactly this decoupling inside an AC machine — without a commutator — by transforming the machine's variables into a reference frame that rotates *with the rotor flux*. In that frame the d-axis is aligned with the flux and the q-axis is 90° ahead of it. The d-axis current i_d then plays the role of the DC field current (it controls flux), and the q-axis current i_q plays the role of the DC armature current (it controls torque). The whole apparatus of FOC — the transforms, the position measurement, the current regulators — exists to hold the frame correctly oriented and to command i_d and i_q independently.

3.2 Reference-Frame Transformations

Two successive transformations carry the three physical phase quantities into the two orthogonal, rotor-synchronous dq components.

3.2.1 The Clarke transformation (abc → αβ)

The three phase quantities, being balanced, carry only two independent degrees of freedom; the Clarke transformation projects them onto a fixed two-axis (stationary)

frame. In its amplitude-invariant form,

$$\begin{bmatrix} x_\alpha \\ x_\beta \end{bmatrix} = \frac{2}{3} \begin{bmatrix} 1 & -\frac{1}{2} & -\frac{1}{2} \\ 0 & \frac{\sqrt{3}}{2} & -\frac{\sqrt{3}}{2} \end{bmatrix} \begin{bmatrix} x_a \\ x_b \\ x_c \end{bmatrix}.$$

Geometrically (Figure 3.1) the three phase axes, 120° apart, are resolved onto the orthogonal α (aligned with phase a) and β axes. A balanced sinusoidal set maps to a vector of constant length rotating at the supply frequency.

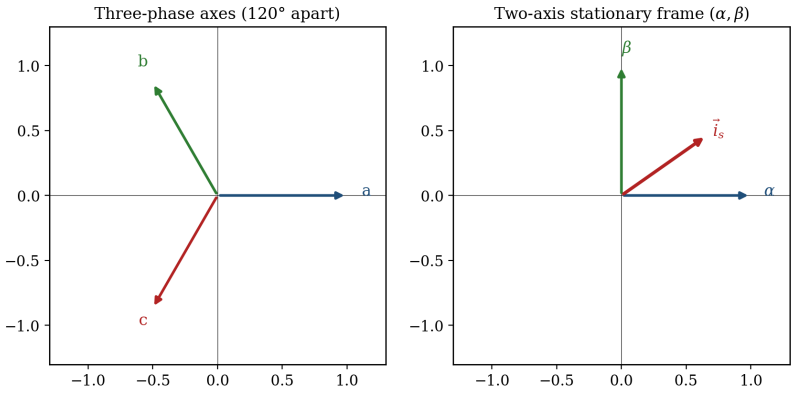


Figure 17: Figure 3.1 — The Clarke transformation resolves the three phase axes (120° apart) onto the orthogonal stationary αβ frame.

3.2.2 The Park transformation (αβ → dq)

The Park transformation rotates the stationary $\alpha\beta$ vector by the electrical rotor angle θ_e into the rotor-synchronous frame (Figure 3.2):

$$\begin{bmatrix} x_d \\ x_q \end{bmatrix} = \begin{bmatrix} \cos\theta_e & \sin\theta_e \\ -\sin\theta_e & \cos\theta_e \end{bmatrix} \begin{bmatrix} x_\alpha \\ x_\beta \end{bmatrix}, \qquad \theta_e = p\,\theta_m.$$

In steady state the $\alpha\beta$ vector rotates at ω_e and the frame rotates with it, so the dq components become **DC quantities** — the single fact that makes PI regulators (which give zero steady-state error only on DC) the natural choice for current control. The inverse Park transformation returns to the stationary frame:

$$\begin{bmatrix} x_\alpha \\ x_\beta \end{bmatrix} = \begin{bmatrix} \cos\theta_e & -\sin\theta_e \\ \sin\theta_e & \cos\theta_e \end{bmatrix} \begin{bmatrix} x_d \\ x_q \end{bmatrix}.$$

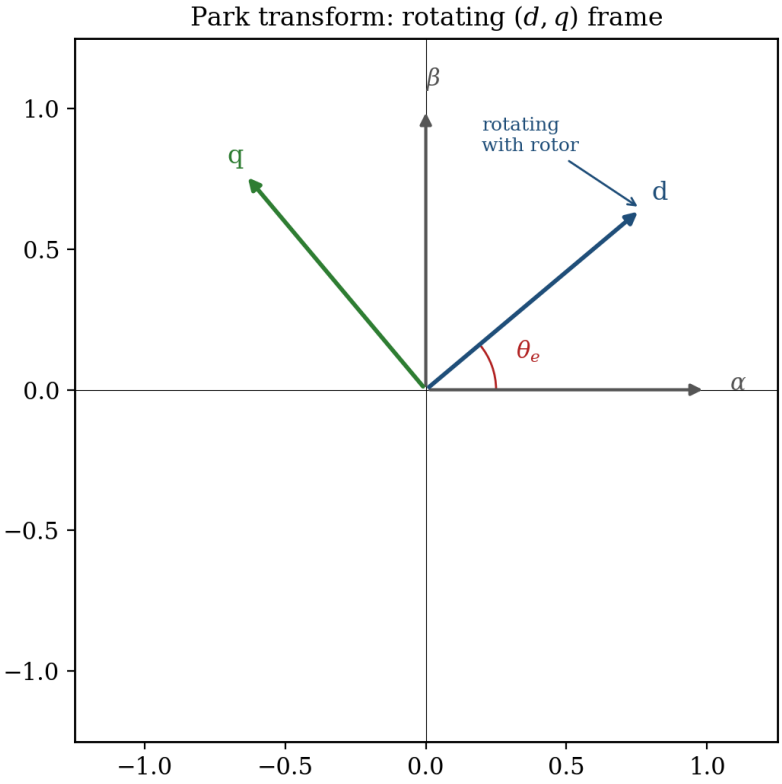


Figure 18: Figure 3.2 — The Park transformation rotates the stationary vector into the rotor frame, where balanced AC quantities become constant (DC).

3.3 Dynamic Model of the PMSM in the dq Frame

Applying the Park transformation to the stator voltage equations yields the standard PMSM model in the rotor frame (motor convention):

$$\boxed{\begin{aligned} v_d &= R_s i_d + L_d \frac{di_d}{dt} - \omega_e L_q i_q, \\ v_q &= R_s i_q + L_q \frac{di_q}{dt} + \omega_e (L_d i_d + \psi_f), \end{aligned}}$$

with flux linkages $\psi_d = L_d i_d + \psi_f$ and $\psi_q = L_q i_q$. The corresponding dq equivalent circuits are drawn in Figure 3.3: each axis is an R–L branch driven by the applied voltage and by a *speed-dependent coupling source* that injects the other axis's flux.

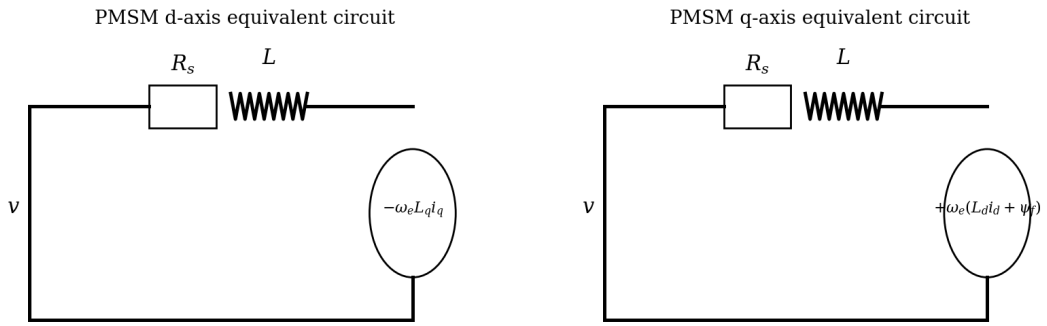


Figure 19: Figure 3.3 — The d- and q-axis equivalent circuits of the PMSM; the rotational-EMF sources couple the two axes.

3.3.1 Electromagnetic torque

The torque follows from the cross-product of flux and current:

$$\boxed{T_{em} = \frac{3}{2} p[\psi_f \, i_q + (L_d - L_q) \, i_d i_q].}$$

The first term is the **magnet (alignment) torque**, present in every PMSM. The second is the **reluctance torque**, non-zero only in *salient* (interior-magnet) machines where $L_d \neq L_q$. For a **surface-mounted PMSM**, $L_d = L_q$ and the law collapses to the DC-machine-like form

$$T_{em} = \frac{3}{2} p \, \psi_f \, i_q \quad \Longrightarrow \quad T_{em} \propto i_q,$$

the cornerstone of FOC: with the frame correctly oriented, torque is simply proportional to the q-axis current.

3.3.2 The coupling terms and feed-forward decoupling

The terms $-\omega_e L_q i_q$ and $+\omega_e L_d i_d$ cross-couple the two axes: a change in i_q perturbs the d-axis voltage and vice-versa, and both grow with speed. FOC removes them by **feed-forward decoupling** — the controller computes the coupling terms from the measured currents and speed and adds equal-and-opposite compensation voltages, so that each current axis is left facing the simple R–L plant

$$v'_d = R_s i_d + L_d \frac{di_d}{dt}, \qquad v'_q = R_s i_q + L_q \frac{di_q}{dt}.$$

3.4 Torque-Producing Strategies

3.4.1 The $i_d = 0$ strategy (maximum torque per ampere)

Setting $i_d^* = 0$ places the whole stator current on the q-axis. For a surface PMSM this is **maximum torque per ampere (MTPA)** — it minimises copper loss for a given torque — and is the default strategy below base speed. The current-limit circle $i_d^2 + i_q^2 \leq I_{max}^2$ then fixes the maximum torque as $T_{max} = \frac{3}{2} p \psi_f I_{max}$.

3.4.2 Field weakening

As speed rises, the back-EMF $\omega_e \psi_f$ grows until the required stator voltage reaches the inverter ceiling $V_{max} = V_{dc}/\sqrt{3}$. To go faster, the drive injects a **negative** i_d, which reduces the net d-axis flux $\psi_d = L_d i_d + \psi_f$ and holds the voltage within the limit:

$$\sqrt{v_d^2 + v_q^2} \le V_{max}.$$

The operating point must now respect two constraints simultaneously — the current-limit circle and the *voltage-limit ellipse* $ (L_d i_d+□f)^2 + (L_q i_q)^2 ≤(V{max}/□_e)^2$, which shrinks as speed increases. Their intersection (Figure 3.4) traces the field-weakening trajectory, trading torque for speed at constant power.

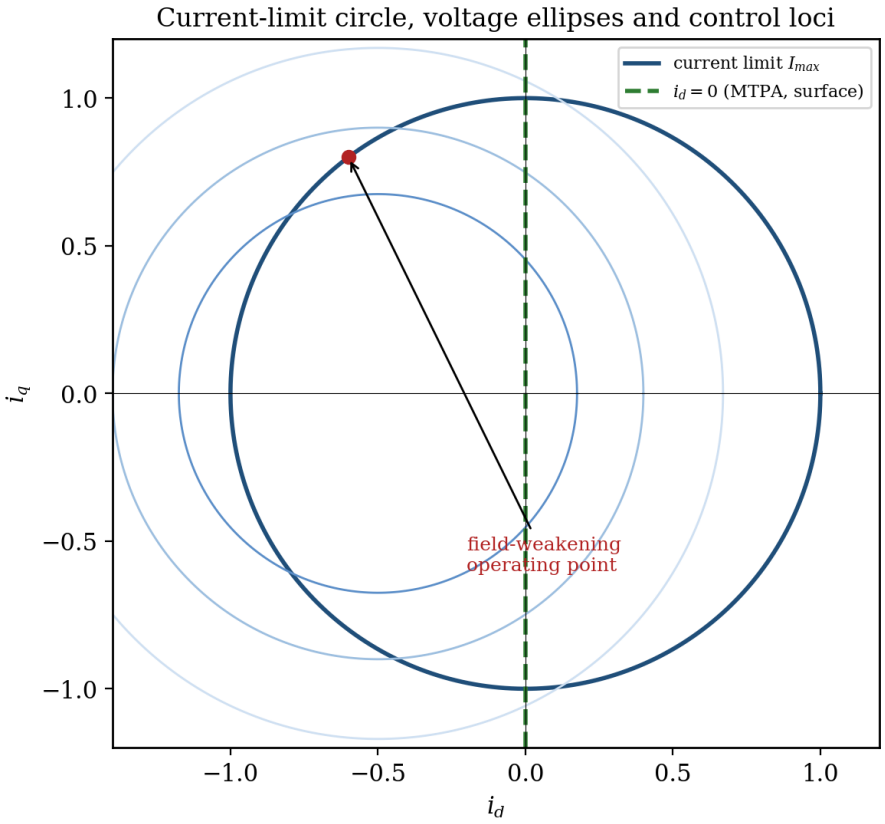


Figure 20: Figure 3.4 — Current-limit circle and speed-dependent voltage-limit ellipses in the i_d–i_q plane; the feasible operating region is their intersection.

3.5 Current-Loop Design

3.5.1 The decoupled plant

After feed-forward decoupling, each axis is the first-order plant

$$G_i(s) = \frac{i(s)}{v'(s)} = \frac{1}{R_s + sL} = \frac{1/R_s}{1 + s\tau}, \qquad \tau = \frac{L}{R_s}.$$

A PI regulator wrapped around it (Figure 3.5) must give a fast, well-damped, zero-steady-state-error current response — the inner loop on which the whole cascade

depends.

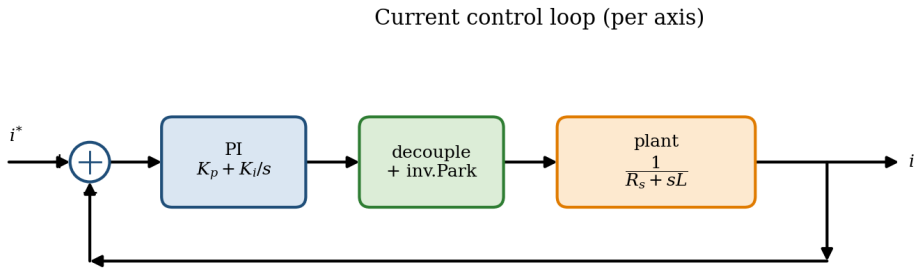


Figure 21: Figure 3.5 — The current control loop: PI regulator, decoupling feed-forward, inverter (unity gain over the loop bandwidth) and the R–L plant.

3.5.2 Tuning by pole–zero cancellation (Internal Model Control)

Write the PI as $C_i(s) = K_p + \dfrac{K_i}{s} = K_p \dfrac{s + K_i/K_p}{s}$. Choose its zero to **cancel the plant pole**,

$$\frac{K_i}{K_p} = \frac{R_s}{L},$$

so that the open-loop transfer function becomes a pure integrator $K_p/(Ls)$ and the closed loop is the first-order system

$$\frac{i(s)}{i^*(s)} = \frac{\alpha_c}{s + \alpha_c},$$

with a single design parameter, the **closed-loop bandwidth** α_c (rad/s). Equating coefficients gives the elegant **IMC tuning rule**

$$\boxed{K_p = \alpha_c L, \qquad K_i = \alpha_c R_s.}$$

The bandwidth is chosen roughly a decade below the switching frequency, $\alpha_c \approx 2\pi f_{sw}/10$, to keep the loop well within the modulator's capability. The resulting closed-loop step response is a clean exponential with no overshoot, and its rise time $t_r \approx 2.2/\alpha_c$ (Figure 3.6). Because the same rule applies with L_d and L_q, the two axes are tuned identically (surface PMSM) or with the two inductances (salient PMSM).

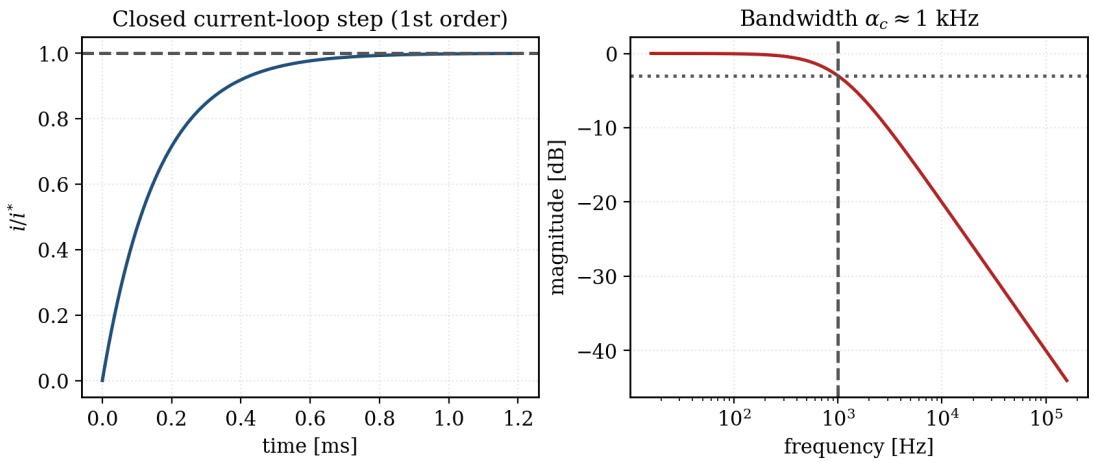


Figure 22: Figure 3.6 — Closed-loop current step response (first-order) and open-loop Bode plot for the IMC-tuned PI regulator.

3.5.3 Anti-windup and voltage saturation

The PI output is a voltage reference, physically limited to V_{max}. When the reference saturates during large transients, the integrator would otherwise "wind up", causing large overshoot on recovery. A **back-calculation anti-windup** (feeding the difference between the unsaturated and saturated output back to the integrator) keeps the integral state consistent with the achievable voltage and is mandatory in any practical implementation.

3.6 Speed-Loop Design by the Symmetrical Optimum

The speed loop is cascaded *outside* the current loop (Figure 3.7). Because the current loop is roughly ten times faster, it can be approximated, for speed-loop design, by a first-order lag of small time constant $T_{eq} \approx 1/\alpha_c$ (or simply by unity). The torque command i_q^* then drives the mechanical plant

$$G_\Omega(s) = \underbrace{\tfrac{3}{2} p \psi_f}_{K_T} \cdot \frac{1}{Js + B}.$$

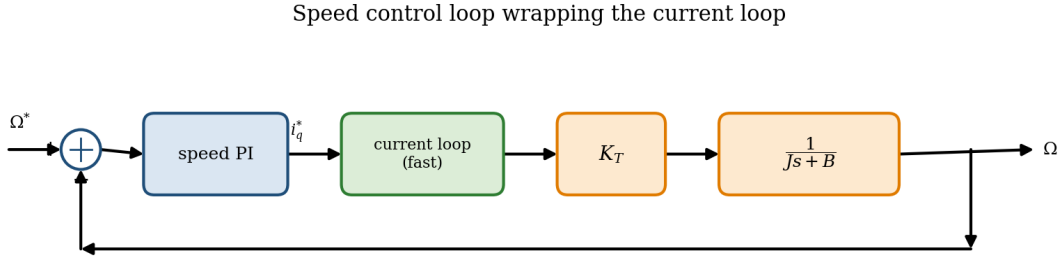


Figure 23: Figure 3.7 — The speed loop wraps the fast current loop; the plant is torque-constant × mechanical lag.

Since the mechanical plant is nearly a pure integrator (small B) preceded by the

current-loop lag, the open loop has the double-integrator character for which the **symmetrical optimum** is designed. With symmetry factor a (typically 2–4) the PI gains are

$$K_{p,\Omega} = \frac{J}{a\,K_T\,T_{eq}}, \qquad K_{i,\Omega} = \frac{J}{a^3 K_T T_{eq}^2},$$

giving a phase margin of about 37° at $a = 2$ rising to 53° at $a = 4$. The symmetrical optimum inherently produces some overshoot on a step command; a **reference pre-filter** $1/(1 + aT_{eq}s)$ is added to cancel the controller zero and restore a smooth response.

3.7 The Complete FOC Structure

Figure 3.8 assembles every element into the full field-oriented controller. Each sampling instant executes the following chain: the three phase currents are measured and passed through Clarke and Park transforms (using the measured rotor angle θ_e) to yield i_d, i_q; these are compared with $i_d^* = 0$ and the torque command i_q^* from the speed loop; the two PI regulators produce voltage references; decoupling feedforward is added; the inverse Park transform returns to $\alpha\beta$; and the space-vector modulator gates the inverter. The rotor angle threads through the entire structure — a wrong angle rotates the frame away from the flux and destroys the decoupling, which is why accurate position sensing (or estimation) is the make-or-break element of an FOC drive.

Complete Field-Oriented Control (FOC) structure

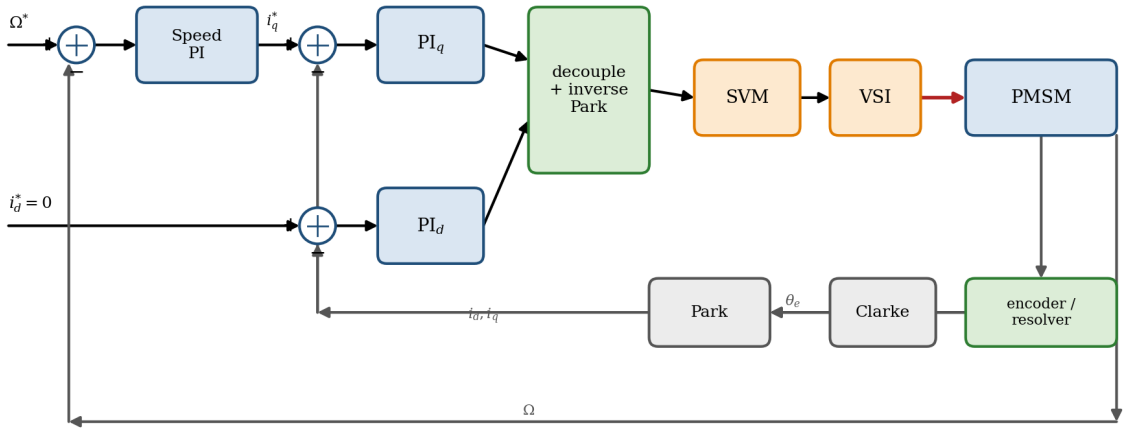


Figure 24: Figure 3.8 — Complete field-oriented control of the PMSM: cascaded speed and current loops, decoupling, coordinate transforms, SVM and inverter, closed by rotor-position feedback.

3.8 Simulation Behaviour

Figure 3.9 shows a representative closed-loop simulation: a speed reference step followed by a load-torque step. The q-axis current (and hence torque) rises rapidly to

accelerate the machine, then settles to the value that balances the load; the d-axis current is held at zero throughout, confirming correct decoupling; the speed tracks its reference with the small, well-damped overshoot set by the symmetrical optimum, and rejects the load disturbance with a brief, bounded dip. This clean, decoupled behaviour — fast torque, invariant flux, accurate speed — is exactly what scalar control cannot deliver and is the reason FOC dominates high-performance drives.

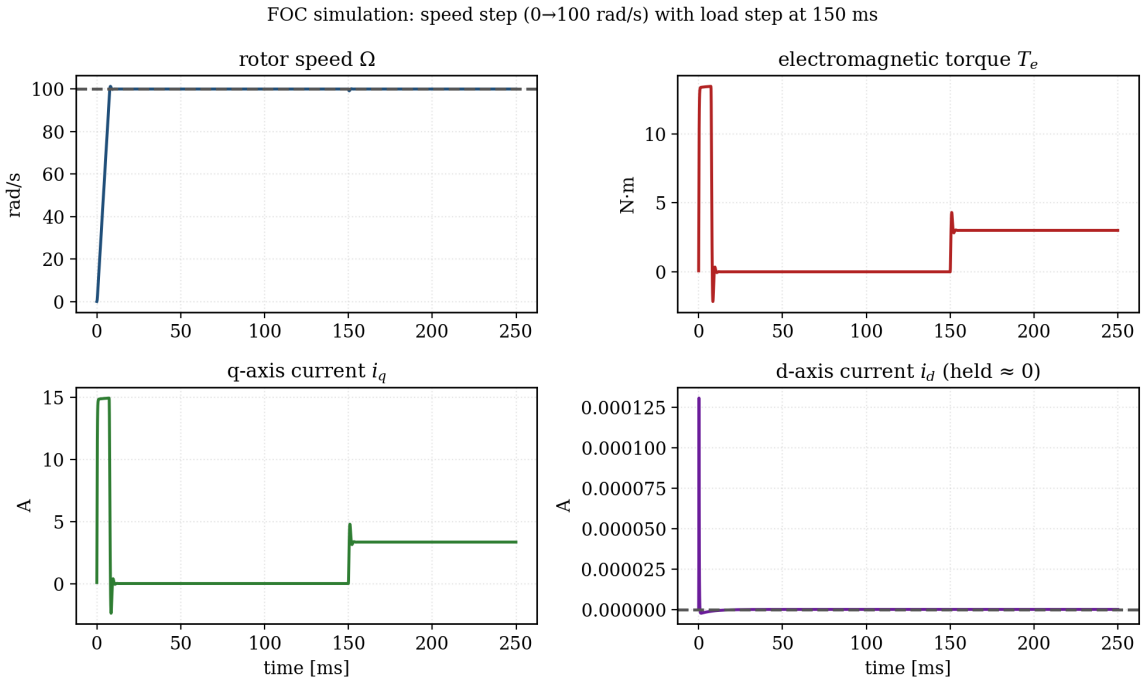


Figure 25: Figure 3.9 — FOC simulation: response to a speed step and a subsequent load-torque step, showing decoupled i_d/i_q, torque and speed.

3.9 MATLAB/Simulink Implementation Guide

A discrete-time FOC model is built from the following blocks and executed every $T_s = 1/f_{sw}$:

```
% ===== Field-Oriented Control – per-sample algorithm =====
theta_e = p*theta_m;                    % electrical angle
% --- Clarke + Park on measured phase currents ---
ialpha = (2*ia - ib - ic)/3;
ibeta  = (ib - ic)/sqrt(3);
id =  cos(theta_e)*ialpha + sin(theta_e)*ibeta;
iq = -sin(theta_e)*ialpha + cos(theta_e)*ibeta;
% --- outer speed PI -> torque (iq) reference ---
ew   = wref - wm;
iqref = pi_speed(ew);                   % with anti-windup + prefilter
idref = 0;                              % MTPA below base speed
% --- inner current PIs ---
vd_p = pi_d(idref - id);
vq_p = pi_q(iqref - iq);
% --- feed-forward decoupling ---
vd = vd_p - we*Lq*iq;
vq = vq_p + we*(Ld*id + psi_f);
% --- inverse Park -> SVM -> inverter ---
valpha = cos(theta_e)*vd - sin(theta_e)*vq;
```

```
vbeta  = sin(theta_e)*vd + cos(theta_e)*vq;
duty   = svm(valpha, vbeta, Vdc, Ts);
```

Recommended block structure. (1) PMSM plant — the Simscape `PMSM` block or a custom dq model with two current integrators and one speed integrator. (2) Clarke/Park and their inverses from the library or the code above. (3) Two discrete PI current regulators with output saturation at $V_{max} = V_{dc}/\sqrt{3}$ and back-calculation anti-windup. (4) Decoupling gains. (5) `SVPWM Generator` and `Universal Bridge`. (6) Outer speed PI with reference pre-filter.

Commissioning checklist. Choose $\alpha_c = 2\pi(f_{sw}/10)$ and speed bandwidth $\approx \alpha_c/10$; verify the current step response is first-order with no overshoot; step i_q^* and confirm i_d stays near zero (decoupling); run the PWM at a fixed-step solver interval $\leq T_s/10$.

3.10 Worked Tutorials

TD 3.1 — Current-loop tuning

> A surface PMSM has $R_s = 0.5\ \Omega$, $L_d = L_q = 4$ mH, $\psi_f = 0.15$ Wb, $p = 4$, $f_{sw} = 10$ kHz. Tune the current PI for a bandwidth of one-tenth the switching frequency.

$\alpha_c = 2\pi(10\text{k}/10) = 6283$ rad/s. Then $K_p = \alpha_c L = 6283 \times 0.004 = 25.1$ V/A and $K_i = \alpha_c R_s = 6283 \times 0.5 = 3142$ V/(A·s). Check: $K_i/K_p = 125 = R_s/L$. □

TD 3.2 — Torque current and speed-loop tuning

> For the machine of TD 3.1 with $J = 0.001$ kg·m², $B \approx 0$: (a) find i_q for 5 N·m; (b) tune the speed PI by the symmetrical optimum with $a = 2$.

(a) $i_q = \dfrac{2T_{em}}{3p\psi_f} = \dfrac{2 \times 5}{3 \times 4 \times 0.15} = 5.56$ A.

(b) $K_T = \frac{3}{2}p\psi_f = 0.9$ N·m/A, $T_{eq} = 1/\alpha_c = 1.59 \times 10^{-4}$ s. $K_{p,\Omega} = \dfrac{J}{aK_T T_{eq}} = \dfrac{0.001}{2(0.9)(1.59\text{e-}4)} = 3.49$ A·s/rad; $K_{i,\Omega} = \dfrac{J}{a^3 K_T T_{eq}^2} = \dfrac{0.001}{8(0.9)(1.59\text{e-}4)^2} = 5493$ A/rad.

TD 3.3 — Field-weakening onset

> The machine of TD 3.1 runs with $i_d = 0$. At what electrical speed does the required voltage reach $V_{max} = V_{dc}/\sqrt{3}$ with $V_{dc} = 300$ V, when delivering $i_q = 5.56$ A? (Neglect the resistive drop.)

$V_{max} = 300/\sqrt{3} = 173.2$ V. Neglecting R_s, $v_d = -\omega_e L_q i_q$, $v_q = \omega_e \psi_f$, so $|v| = \omega_e\sqrt{(L_q i_q)^2 + \psi_f^2}$. With $L_q i_q = 0.004 \times 5.56 = 0.0222$ Wb, $\sqrt{0.0222^2 + 0.15^2} = 0.1516$. Thus $\omega_e = 173.2/0.1516 = 1142$ rad/s (electrical), i.e. mechanical $\Omega = \omega_e/p = 285.5$ rad/s ≈ 2726 rpm. Above this speed, negative i_d (field weakening) is required.

3.11 Exercises

1. Derive the inverse Park transformation from the forward one and verify that the product of the two matrices is the identity.
2. For an interior PMSM with $L_d = 3$ mH, $L_q = 7$ mH, $\psi_f = 0.1$ Wb, $p = 3$, write the torque as a function of the current angle and find, numerically, the MTPA angle for $|i| = 10$ A.
3. Show that IMC tuning makes the closed current loop exactly first-order and derive the 10–90 % rise time.
4. A current loop is tuned for $\alpha_c = 4000$ rad/s on a machine with $L = 6$ mH, $R_s = 0.8\ \Omega$. Give K_p, K_i and the open-loop crossover frequency.
5. Explain the role of the reference pre-filter in the symmetrical-optimum speed loop and sketch the step response with and without it.
6. Discuss how a $\pm 5^\circ$ error in the measured rotor angle affects the decoupling and the torque per ampere.

3.12 Deeper Treatment of FOC

3.12.1 From abc to dq: where the model comes from

The dq model of §3.3 is obtained by applying the **power-invariant Park transform** to the natural three-phase stator equation $\mathbf{v}_{abc} = R_s \mathbf{i}_{abc} + \frac{\mathrm{d}}{\mathrm{d}t}\psi_{abc}$. Writing the transform $\mathbf{x}_{dq} = \mathbf{P}(\theta_e)\mathbf{x}_{abc}$ and using $\dot{\mathbf{P}} = \mathbf{P}\,\mathbf{J}\,\omega_e$ with $\mathbf{J} = \begin{bmatrix} 0 & -1 \\ 1 & 0 \end{bmatrix}$, the time derivative of any transformed flux becomes

$$\frac{\mathrm{d}}{\mathrm{d}t}\psi_{abc} \;\xrightarrow{\;\mathbf{P}\;}\; \frac{\mathrm{d}\psi_{dq}}{\mathrm{d}t} + \omega_e \mathbf{J}\,\psi_{dq},$$

which is exactly the origin of the **speed-voltage (motional-EMF) terms** $\pm\omega_e\psi$ in the dq voltage equations. The term $\omega_e \mathbf{J}\psi_{dq}$ rotates the flux vector; it is a *coupling*, not a loss, and it is what feed-forward decoupling cancels. Recognising this structure is the key insight of vector control: in the rotating frame the machine looks like two coupled RL circuits, and cancelling the coupling leaves two independent DC-like loops.

3.12.2 Salient (interior) PMSM and MTPA

For the interior PMSM (IPMSM) $L_d \neq L_q$, and the torque

$$T_{em} = \tfrac{3}{2} p \big[\psi_f i_q + (L_d - L_q) i_d i_q\big]$$

contains a **reluctance term**. Setting $i_d = 0$ is then *no longer optimal*: because $L_q > L_d$, a **negative** i_d adds positive reluctance torque. Minimising the stator-current magnitude $|\mathbf{i}_s| = \sqrt{i_d^2 + i_q^2}$ for a required torque yields the **Maximum-Torque-Per-Ampere** locus

$$\boxed{i_d = \frac{\psi_f - \sqrt{\psi_f^2 + 8(L_q - L_d)^2 i_q^2}}{4(L_q - L_d)}}.$$

Following this curve instead of $i_d = 0$ can cut copper loss by 10–20 % in a strongly-salient machine. For the surface PMSM ($L_d = L_q$) the reluctance term vanishes and MTPA collapses to $i_d = 0$, recovering §3.4.1.

3.12.3 The symmetrical optimum, derived

The speed loop wraps the current loop (equivalent lag $T_{eq} \approx 1/\alpha_c$) around the mechanical integrator $1/(Js)$. The open loop with a PI $K_p(1 + 1/(T_i s))$ is a **type-2** system:

$$L(s) = \frac{K_p K_T}{J} \frac{1 + T_i s}{T_i\, s^2\, (1 + T_{eq} s)}.$$

The **symmetrical optimum** places the PI zero and the gain so that the Bode magnitude is *geometrically symmetric* about the crossover on a log scale, maximising phase margin for the given T_{eq}. Choosing a symmetry factor a (ratio of the two corner frequencies),

$$T_i = a^2 T_{eq}, \qquad K_p = \frac{J}{a\, K_T\, T_{eq}}, \qquad K_i = \frac{K_p}{T_i} = \frac{J}{a^3 K_T T_{eq}^2}.$$

The phase margin is $\varphi_m = \arctan\frac{a^2-1}{2a}$: $a = 2 \Rightarrow 37^\circ$, $a = 3 \Rightarrow 53^\circ$, $a = 4 \Rightarrow 62^\circ$. Larger a is more damped but slower. A **reference pre-filter** $1/(1 + aT_{eq}s)$ cancels the closed-loop zero and removes the otherwise large step overshoot.

3.12.4 Discrete-time implementation

On a DSP the PI is discretised. The **backward-Euler** form (stable, minimal phase loss) is

$$u_k = u_{k-1} + K_p(e_k - e_{k-1}) + K_i T_s\, e_k,$$

with **anti-windup by back-calculation**: when the voltage command saturates at $V_{max} = V_{dc}/\sqrt{3}$, the excess $(u_k - u_{sat})$ is fed back to the integrator through a gain $1/T_t$ (tracking time constant $T_t \approx \sqrt{T_i T_{eq}}$). Sampling is synchronised to the PWM (once or twice per period) so that current is measured at the pulse centre, where the ripple momentarily crosses its average — a subtlety that removes the need for heavy analog filtering.

3.12.5 A note on sensorless operation

The rotor angle θ_e that FOC needs can be *estimated* rather than measured. Two families exist: **model-based** observers (back-EMF / flux observers, sliding-mode or Luenberger) that work from medium to high speed where the back-EMF $\omega_e \psi_f$ is observ-

able; and **saliency-tracking** methods (high-frequency injection) that exploit $L_d \neq L_q$ to find the angle down to zero speed. Sensorless FOC removes the encoder cost but reintroduces a low-speed observability problem analogous to the DTC flux-drift issue of Chapter 4.

3.13 Additional Solved Tutorials

TD 3.4 — MTPA operating point

> An IPMSM has $\psi_f = 0.12$ Wb, $L_d = 3$ mH, $L_q = 6$ mH, $p = 3$. For $i_q = 8$ A, find the MTPA i_d and compare the torque with the $i_d = 0$ case.

MTPA current:

$$i_d = \frac{0.12 - \sqrt{0.12^2 + 8(6-3)^2 \times 10^{-6} \cdot 8^2}}{4(6-3) \times 10^{-3}} = \frac{0.12 - \sqrt{0.0144 + 0.00461}}{0.012}.$$

$\sqrt{0.01901} = 0.1379$, so $i_d = (0.12 - 0.1379)/0.012 = -1.49$ A.

Torque at MTPA:

$$T = \tfrac{3}{2} \cdot 3\big[0.12 \cdot 8 + (3-6) \times 10^{-3}(-1.49)(8)\big] = 4.5\big[0.96 + 0.0358\big] = 4.48 \text{ N·m}.$$

At $i_d = 0$: $T = \frac{3}{2} \cdot 3 \cdot 0.12 \cdot 8 = 4.32$ N·m. The reluctance term adds ≈3.7 % torque **for the same** i_q — and MTPA achieves a target torque with less total current.

TD 3.5 — Speed-loop pre-filter overshoot

> Using the FOC of TD 3.2 ($K_T = 0.9$, $J = 10^{-3}$, $T_{eq} = 1.59 \times 10^{-4}$ s), take $a = 3$. Find $K_p,\ K_i,\ T_i$ and the phase margin, and state the pre-filter.

$$T_i = a^2 T_{eq} = 9 \times 1.59 \times 10^{-4} = 1.43 \times 10^{-3} \text{ s},$$

$$K_p = \frac{J}{a K_T T_{eq}} = \frac{10^{-3}}{3 \cdot 0.9 \cdot 1.59 \times 10^{-4}} = 2.33, \qquad K_i = K_p / T_i = 1630.$$

Phase margin $\arctan \frac{9-1}{6} = 53^\circ$. Pre-filter: $1/(1 + aT_{eq}s) = 1/(1 + 4.77 \times 10^{-4} s)$.

TD 3.6 — Field-weakening base speed

> A surface PMSM has $\psi_f = 0.15$ Wb, $p = 4$, $R_s \approx 0$, $L = 4$ mH, and is fed from $V_{dc} = 300$ V. Estimate the base electrical speed (onset of field weakening) at rated $i_q = 6$ A, $i_d = 0$.

Voltage limit $V_{max} = V_{dc}/\sqrt{3} = 173.2$ V. At $i_d = 0$, $v_q \approx \omega_e \psi_f$ and $v_d \approx -\omega_e L i_q$:

$$V_{max}^2 = (\omega_e \psi_f)^2 + (\omega_e L i_q)^2 \Rightarrow \omega_e = \frac{V_{max}}{\sqrt{\psi_f^2 + (L i_q)^2}} = \frac{173.2}{\sqrt{0.15^2 + (0.004 \cdot 6)^2}}.$$

$\sqrt{0.0225 + 0.000576} = 0.1519$, so $\omega_e = 1140$ rad/s → mechanical $\Omega = \omega_e / p = 285$ rad/s (≈ 2721 rpm). Above this, negative i_d (field weakening) is required.

3.14 Exercises (supplementary)

1. Starting from $\dot{\mathbf{P}} = \mathbf{P}\mathbf{J}\omega_e$, show that the derivative of a dq flux acquires the term $\omega_e \mathbf{J}\psi_{dq}$, and identify the two scalar speed-voltage terms.
2. For an IPMSM with $L_d = 2.5$ mH, $L_q = 7$ mH, $\psi_f = 0.1$ Wb, sketch the MTPA locus in the (i_d, i_q) plane for $i_q = 0 \dots 10$ A.
3. Tune a current PI for $R_s = 0.8\ \Omega$, $L = 6$ mH, $f_{sw} = 12$ kHz using the IMC rule; give K_p, K_i and the closed-loop bandwidth.
4. Derive the back-calculation anti-windup update and explain why $T_t \approx \sqrt{T_i T_{eq}}$ is a reasonable choice.
5. Explain why saliency-tracking sensorless methods succeed at zero speed while back-EMF observers fail there.
6. A speed loop designed with $a = 2$ shows too much overshoot despite the pre-filter. Give two design changes that reduce it and their trade-offs.

Chapter 4 — Direct Torque Control (DTC) of Induction Motors

(Duration: 3 weeks)

4.1 Philosophy of Direct Torque Control

Direct Torque Control, proposed by Takahashi and Noguchi in 1986 (and, in the Direct Self-Control variant, by Depenbrock in 1988), takes a radically different route from FOC. It **discards** the current regulators, the coordinate transforms and the modulator. In their place it puts two hysteresis comparators and a look-up table that, at every control instant, selects the one inverter voltage vector best able to push the **stator-flux magnitude** and the **electromagnetic torque** toward their references. The entire calculation lives in the stationary $\alpha\beta$ frame and needs **no rotor-position sensor** — only the DC-bus voltage, the switching states and two measured phase currents.

The result is the fastest torque response of any AC drive — a torque step is answered within one or two switching actions — obtained with a strikingly simple structure. The price, examined in Section 4.7, is higher torque and flux ripple and a switching frequency that varies with operating point.

4.2 The Governing Relations

4.2.1 Stator flux from the voltage model

Integrating the stator voltage equation in the stationary frame gives the stator flux directly:

$$\psi_s = \int (\mathbf{v}_s - R_s \mathbf{i}_s)\, dt \;\Longrightarrow\; \begin{cases} \psi_{s\alpha} = \int (v_{s\alpha} - R_s i_{s\alpha})\, dt, \\ \psi_{s\beta} = \int (v_{s\beta} - R_s i_{s\beta})\, dt, \end{cases}$$

$$|\psi_s| = \sqrt{\psi_{s\alpha}^2 + \psi_{s\beta}^2}, \qquad \theta_s = \tan^{-1}\frac{\psi_{s\beta}}{\psi_{s\alpha}}.$$

The voltages need not even be measured — they are reconstructed from the known switching state and the DC-bus voltage. Only the stator resistance R_s enters, which is why DTC is comparatively insensitive to parameter variation.

4.2.2 Torque from flux and current

The electromagnetic torque is the cross product of stator flux and stator current:

$$\boxed{T_{em} = \frac{3}{2} p \left(\psi_{s\alpha} i_{s\beta} - \psi_{s\beta} i_{s\alpha} \right).}$$

Equivalently $T_{em} = \frac{3}{2} p \frac{|\psi_s||\psi_r|}{\sigma L_s L_r} \sin \delta$, where δ is the **load angle** between stator and rotor flux. Since the rotor flux has a long time constant and moves slowly, the torque is controlled by rapidly **advancing or retarding the stator flux** — changing δ — which the inverter can do within a single switching period.

4.2.3 How a voltage vector moves the flux

Over a short interval, neglecting the resistive drop, the flux increment follows the applied voltage:

$$\Delta \psi_s \approx \mathbf{v}_s \, \Delta t.$$

The stator flux therefore moves *in the direction of the chosen voltage vector* (Figure 4.1). A vector with an **outward radial** component increases $|\psi_s|$; an inward one decreases it. A vector with a **forward tangential** component advances the flux, increasing δ and hence the torque; a backward or zero vector reduces the torque. Selecting a vector is thus simultaneously selecting how flux and torque will change.

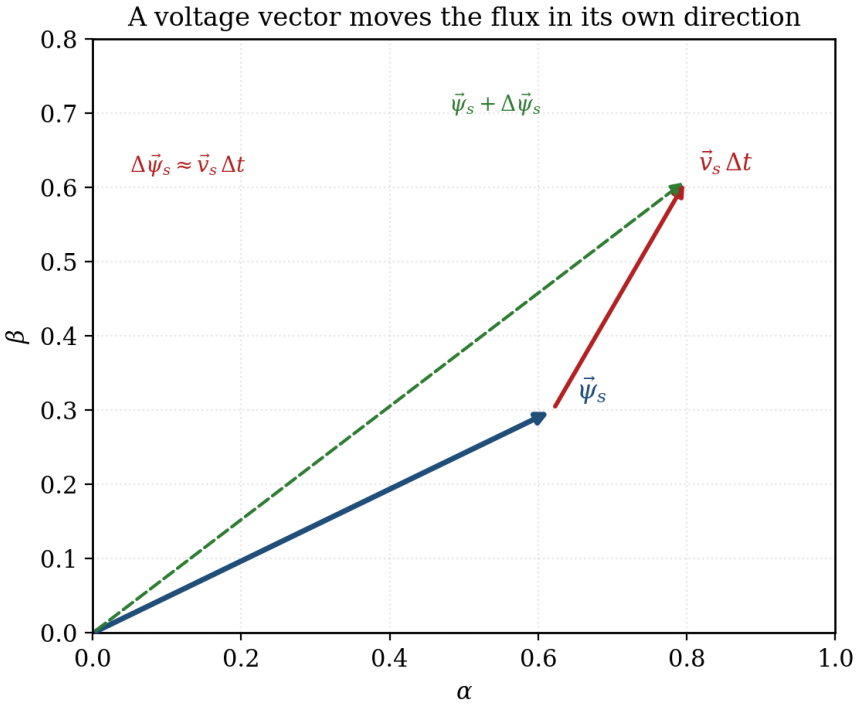


Figure 26: Figure 4.1 — Effect of the inverter voltage vectors on the stator-flux tip: radial components change $|\psi_s|$, tangential components change the torque via the load angle.

4.3 Sectors and Hysteresis Comparators

The $\alpha\beta$ plane is divided into six 60° **sectors** $S_1 \dots S_6$, each centred on an active vector (Figure 4.2). The controller first identifies which sector the flux vector currently occupies.

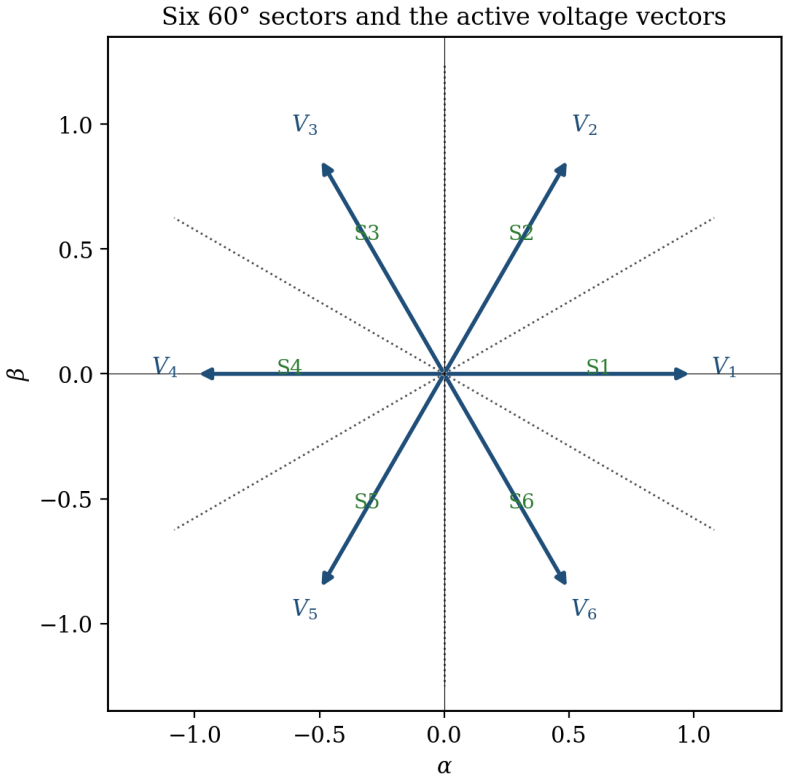


Figure 27: Figure 4.2 — The six 60° flux sectors and the six active voltage vectors used by the DTC switching table.

Two hysteresis comparators then quantise the control demands (Figure 4.3):

- a **two-level flux comparator** outputs $d\psi = 1$ to raise the flux or $d\psi = 0$ to lower it, within a band $\pm\Delta\psi$;
- a **three-level torque comparator** outputs $dT = +1$ (raise), $dT = 0$ (hold — apply a zero vector) or $dT = -1$ (lower), within a band $\pm\Delta T$.

The band widths trade ripple against switching frequency: narrow bands give low ripple but switch often; wide bands do the opposite.

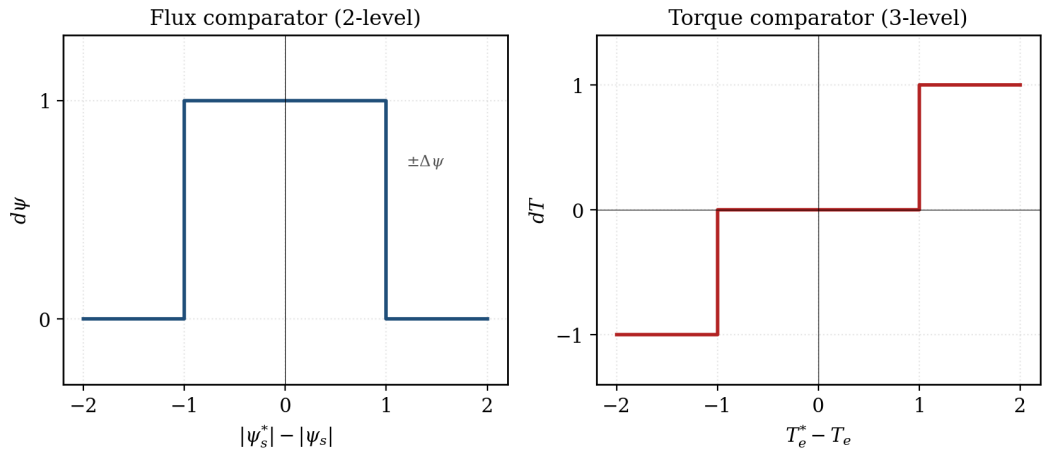


Figure 28: Figure 4.3 — The two-level flux and three-level torque hysteresis comparators that quantise the DTC demands.

4.4 The Switching Table and Control Structure

Given the flux sector S_k and the comparator outputs $(d\psi, dT)$, the optimal vector is read from the **Takahashi switching table**:

$d\psi$	dT	S_1	S_2	S_3	S_4	S_5	S_6
1	+1	V_2	V_3	V_4	V_5	V_6	V_1
1	0	V_7	V_0	V_7	V_0	V_7	V_0
1	−1	V_6	V_1	V_2	V_3	V_4	V_5
0	+1	V_3	V_4	V_5	V_6	V_1	V_2
0	0	V_0	V_7	V_0	V_7	V_0	V_7
0	−1	V_5	V_6	V_1	V_2	V_3	V_4

The mnemonic, for flux in sector S_k: raise-flux/raise-torque selects V_{k+1}; raise-flux/lower-torque selects V_{k-1}; lower-flux/raise-torque selects V_{k+2}; lower-flux/lower-torque selects V_{k+3}; and hold-torque selects a zero vector. The complete control structure (Figure 4.4) contains no transforms, no current PIs and no PWM modulator — the table *is* the modulator, switching at a variable rate set by the hysteresis bands.

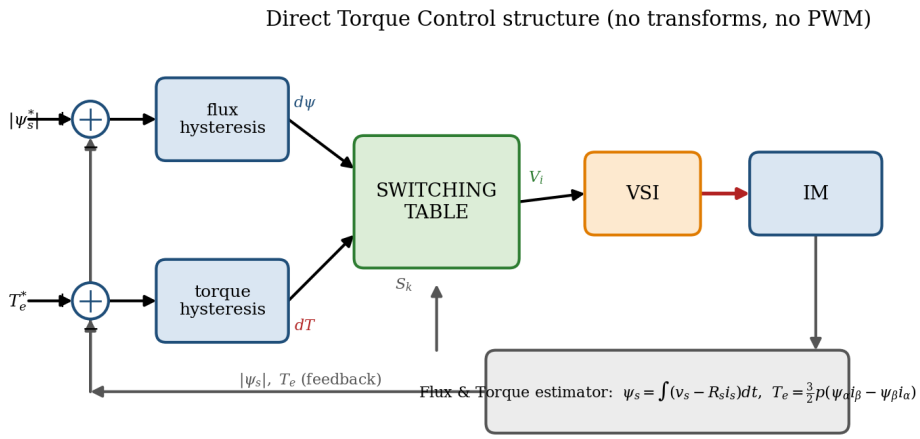


Figure 29: Figure 4.4 — The complete DTC scheme: flux/torque estimator, two hysteresis comparators, sector detection and the switching table driving the inverter.

4.5 Flux Trajectory and Torque Response

Because DTC keeps $|\psi_s|$ within its band while the flux angle advances, the flux tip traces an almost **circular locus** built from short straight segments — one per applied vector (Figure 4.5). The near-circular trajectory corresponds to near-sinusoidal flux and therefore smooth average torque, while the hysteresis bands appear as the characteristic ripple. Figure 4.6 shows the torque and flux responses to a torque-reference step: the torque snaps to its new level within a switching action or two — the hallmark fast response of DTC — while the flux magnitude stays locked in its band.

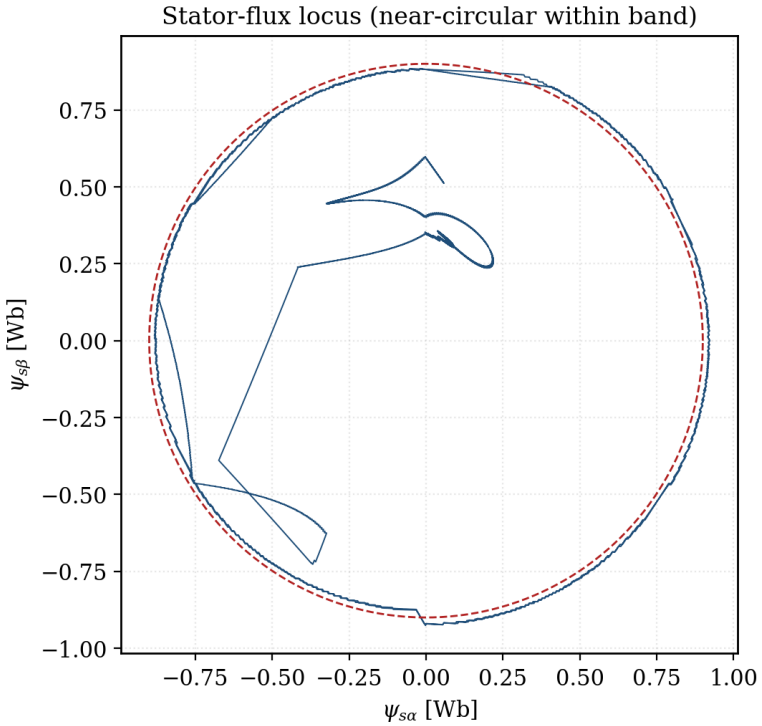


Figure 30: Figure 4.5 — Stator-flux trajectory under DTC: a near-circular locus made of straight voltage-vector segments, bounded by the flux hysteresis band.

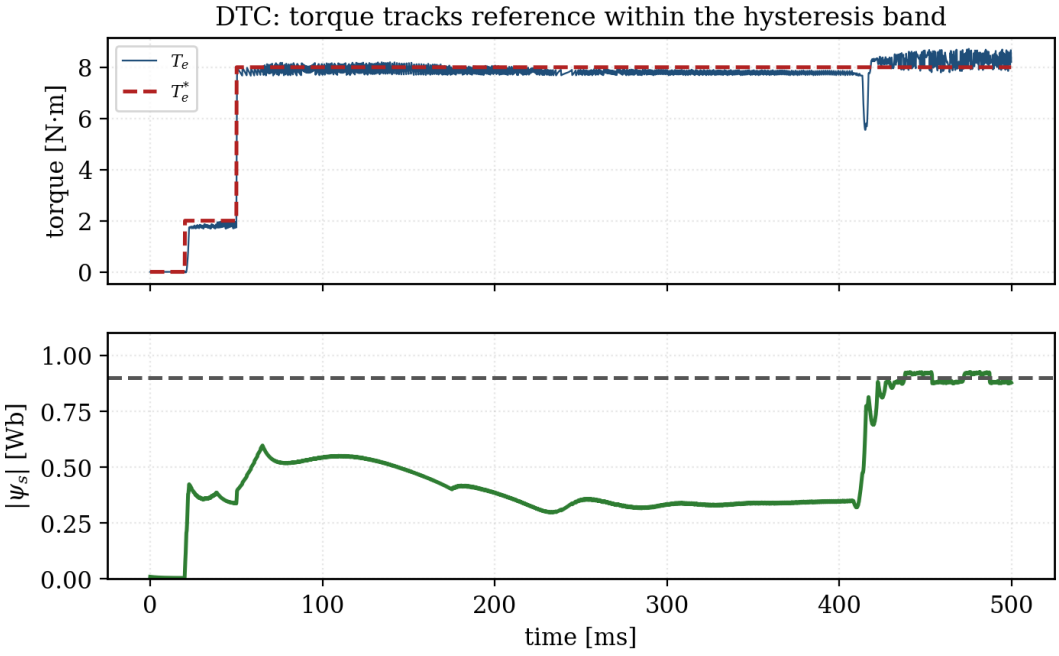


Figure 31: Figure 4.6 — DTC response to a torque-reference step: near-instant torque change with the flux magnitude held constant.

4.6 Stator-Flux Estimation and the Drift Problem

The estimator is the Achilles' heel of DTC. The **voltage model** used above requires only R_s and is accurate at medium and high speed, but it relies on a **pure open-loop integration**. Any DC offset or measurement bias — inevitable in real acquisition chains — is integrated without bound, so the estimated flux **drifts** and the trajectory spirals off-centre (Figure 4.7). At **low speed** the problem compounds: the terminal voltage becomes small, the $R_s i_s$ term dominates, and any error in R_s corrupts the estimate.

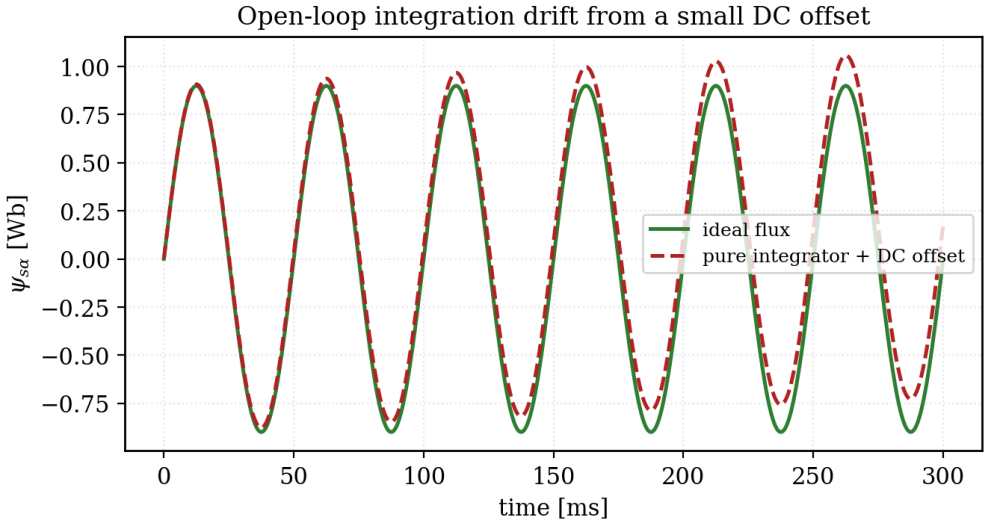


Figure 32: Figure 4.7 — The pure integrator amplifies any DC offset into an unbounded drift of the estimated flux; a low-pass replacement bounds it.

Practical remedies replace the pure integrator $1/s$ with a **low-pass filter** $1/(s+\omega_c)$ (with magnitude and phase compensation), or use a **current model** (which relies on rotor equations and a speed measurement, valid down to zero speed but sensitive to rotor resistance), or blend the two in a **hybrid / observer-based** estimator (Luenberger or sliding-mode) that uses the voltage model at high speed and the current model at low speed.

4.7 FOC versus DTC

The two high-performance strategies are complementary; their trade-offs are summarised below and illustrated in Figure 4.8.

Feature	**FOC**	**DTC**
Controlled variables	i_d, i_q	$\lvert\psi_s\rvert$, T_{em}
Frame	rotating dq (needs θ_e)	stationary $\alpha\beta$
Position sensor	usually required	not required
Modulator	PWM/SVM (fixed f_{sw})	switching table (variable f_{sw})
Regulators	linear PI	hysteresis comparators
Torque response	fast (~ms)	fastest (~µs)
Torque/flux ripple	low	higher
Parameter sensitivity	R_s, L_d, L_q, ψ_r	mainly R_s
Structure	complex	simple

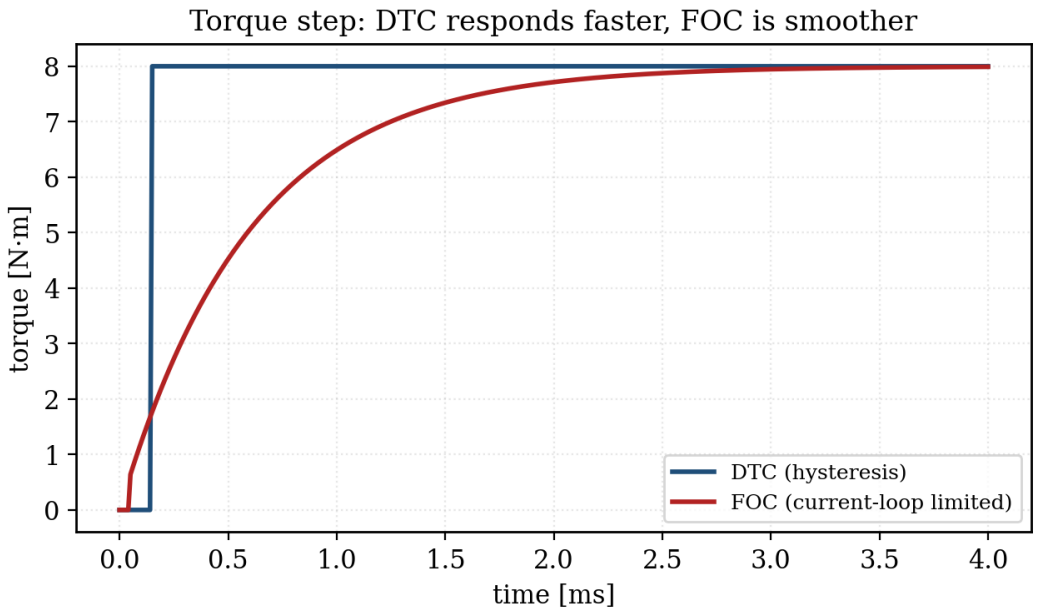


Figure 33: Figure 4.8 — Comparative torque response of FOC and DTC to a step demand: DTC reacts faster but with more ripple.

FOC delivers smooth, low-ripple torque at a constant, predictable switching frequency, at the cost of transforms and position feedback. DTC delivers the fastest possible torque response from the simplest structure, at the cost of ripple and a variable switching frequency. Modern hybrids — **DTC-SVM** and **model-predictive torque control** — combine DTC's fast dynamics with a fixed switching frequency and reduced ripple, and are an active research area.

4.8 MATLAB/Simulink Layout

```
% ===== DTC — per-sample algorithm (stationary frame) =====
[valpha, vbeta] = inverter_voltage(state, Vdc);      % from switching state
ialpha = (2*ia - ib - ic)/3;  ibeta = (ib - ic)/sqrt(3);
psia = psia + Ts*(valpha - Rs*ialpha);               % integrator (use LPF!)
psib = psib + Ts*(vbeta  - Rs*ibeta);
psi  = hypot(psia, psib);
Te   = 1.5*p*(psia*ibeta - psib*ialpha);
sector = flux_sector(atan2(psib, psia));             % 1..6
dpsi = (psiref - psi)  > 0;                           % 2-level
dT   = torque_hyst(Teref - Te);                       % 3-level {-1,0,+1}
state = switching_table(dpsi, dT, sector);           % V0..V7
```

Run the loop fast ($T_s = 20$–$50\ \mu$s) so the hysteresis bands are respected, and replace the naive integrator with a compensated low-pass filter to avoid drift.

4.9 Worked Tutorials

TD 4.1 — Flux magnitude, sector and torque

> Estimated flux $\psi_{s\alpha} = 0.62$ Wb, $\psi_{s\beta} = 0.30$ Wb; measured $i_{s\alpha} = 12$ A, $i_{s\beta} = -4$ A; $p = 2$. Find $|\psi_s|$, the sector, and the torque.

$|\psi_s| = \sqrt{0.62^2 + 0.30^2} = 0.689$ Wb. $\theta_s = \text{atan2}(0.30, 0.62) = 25.8^\circ \Rightarrow$ **Sector 1**. $T_{em} = 1.5 \times 2 \times (0.62(-4) - 0.30(12)) = 3 \times (-2.48 - 3.60) = -18.2$ N·m (braking sample).

TD 4.2 — Vector selection

> With flux in S_1 and demands $(d\psi = 1,\ dT = +1)$, which vector does the table select, and why is it correct?

The table gives $\mathbf{V}_2$ (110). In Sector 1, $\mathbf{V}_2$ has an **outward radial** component (raising $|\psi_s|$) and a **forward tangential** component (advancing the flux, increasing δ and the torque). It satisfies both demands at once.

TD 4.3 — Effect of a zero vector

> The torque is within its band ($dT = 0$) while the flux is high ($d\psi = 0$) in Sector 3. What is applied, and what happens?

From the table, $(d\psi = 0, dT = 0, S_3) \rightarrow V_0$. A zero vector freezes the stator flux (no voltage, so $\Delta\psi_s \approx -R_s i_s\,\Delta t$, very small); the rotor flux continues to rotate, so the load angle δ slowly *decreases*, gently reducing torque — the intended "coast" action that keeps torque in band without switching an active vector.

4.10 Exercises

1. Construct the switching table entry for flux in Sector 4 with $(d\psi = 1, dT = -1)$ from first principles (radial/tangential reasoning) and check it against the table.
2. Explain quantitatively why narrowing the torque hysteresis band raises the switching frequency.
3. Derive the load-angle form of the torque and identify the pull-out angle.
4. A DC offset of 10 mV is present on the α voltage channel. Estimate the flux drift after 1 s with a pure integrator, and show how a 5 Hz low-pass filter bounds it.
5. Compare the number of look-up/arithmetic operations per sample in DTC and FOC and comment on the implications for a low-cost microcontroller.

4.11 Direct Torque Control in Depth

4.11.1 The torque–load-angle relation, derived

DTC controls torque by controlling the angle between stator and rotor flux. Starting from $T_{em} = \frac{3}{2} p \, (\psi_s \times \mathbf{i}_s)$ and expressing the stator current through the two flux linkages of the induction machine, $\mathbf{i}_s = \dfrac{1}{\sigma L_s}\left(\psi_s - \dfrac{L_m}{L_r}\psi_r\right)$, the cross product leaves only the term between the two fluxes:

$$\boxed{T_{em} = \frac{3}{2}\, p \, \frac{L_m}{\sigma L_s L_r} \, |\psi_s| \, |\psi_r| \, \sin\delta}$$

where δ is the **load angle** between ψ_s and ψ_r and $\sigma = 1 - L_m^2/(L_s L_r)$ is the total leakage factor. Two facts follow immediately and justify the whole method:

- The **rotor flux is slow**: its time constant $\tau_r = L_r/R_r$ is large (tens of ms), so $|\psi_r|$ and its angle barely move within one switching period.
- Therefore **torque is changed by moving** ψ_s: advancing the stator flux (increasing δ) raises torque almost instantly, retarding it lowers torque. Since $\Delta\psi_s \approx \mathbf{v}_s \, \Delta t$, the inverter voltage vector is the direct torque actuator — hence *direct* torque control.

4.11.2 Effect of every voltage vector, by region

With ψ_s in Sector I, the six active vectors have both a **radial** component (changing $|\psi_s|$) and a **tangential** component (changing δ, i.e. torque):

Vector	Radial (flux)	Tangential (torque)
$\mathbf{V}_2$ (110)	+ (increase)	+ (increase)
$\mathbf{V}_3$ (010)	− (decrease)	+ (increase)
$\mathbf{V}_1$ (100)	+ (increase)	− (decrease)
$\mathbf{V}_6$ (101)	− (decrease)	− (decrease)

$\mathbf{V}_0, \mathbf{V}_7$	≈ 0	freeze (slight decrease)

Rotating this pattern by 60° per sector yields the full Takahashi table of §4.4. The zero vectors briefly *freeze* the stator flux; because the rotor flux keeps advancing, the load angle — and thus torque — slowly falls, which is why the three-level torque comparator uses a zero vector for its "hold" state.

4.11.3 Switching frequency and ripple

Classical DTC has a **variable switching frequency** set by the hysteresis band widths and the operating point. Narrow bands give low torque ripple but high switching loss; wide bands do the opposite. Approximately, the torque loop switches when the torque error traverses the band $2\Delta T$, so

$$f_{sw} \;\propto\; \frac{1}{2\Delta T}\left|\frac{\mathrm{d}T_{em}}{\mathrm{d}t}\right|.$$

Because $\mathrm{d}T_{em}/\mathrm{d}t$ itself depends on speed and DC-bus voltage, the frequency wanders — a drawback for filter and thermal design that motivates the fixed-frequency variants below.

4.11.4 DTC-SVM and predictive torque control

Two modern refinements keep DTC's fast response while fixing its ripple/frequency problems:

- **DTC-SVM.** The hysteresis controllers and table are replaced by PI (or deadbeat) regulators of torque and flux that output a *reference voltage vector*, which a space-vector modulator (§2.10) then realises at a **constant** switching frequency. Ripple drops markedly.
- **Finite-Control-Set Model Predictive Control (FCS-MPC).** At each sampling instant the drive *predicts* torque and flux for each of the eight inverter states one step ahead and applies the state minimising a cost $g = |T^* - \hat{T}| + \lambda\,|\,|\psi_s^*| - |\hat{\psi}_s|\,|$. It needs an accurate model and is computationally heavy, but handles constraints naturally and unifies current-, torque- and flux-control.

4.11.5 Curing the integrator drift

The pure integrator $\psi_s = \int (\mathbf{v}_s - R_s\mathbf{i}_s)\,\mathrm{d}t$ accumulates any DC offset without bound (§4.6). Practical fixes:

- Replace $1/s$ by a **first-order low-pass** $1/(s+\omega_c)$ with magnitude/phase compensation, sacrificing accuracy only well below ω_c.
- Use a **programmable-cutoff** integrator whose ω_c scales with speed.
- Blend the **voltage model** (accurate at high speed) with the **current model** (valid at zero speed) in a closed-loop observer — the standard industrial solution for wide-range DTC.

4.12 Additional Solved Tutorials

TD 4.4 — Load angle and torque

An IM has $L_m = 0.11$ H, $L_s = L_r = 0.12$ H, $p = 2$, $|\psi_s| = 0.9$ Wb, $|\psi_r| = 0.85$ Wb, load angle $\delta = 18^\circ$. Find the torque.

$\sigma = 1 - L_m^2/(L_s L_r) = 1 - 0.0121/0.0144 = 0.1597.$

$$T = \tfrac{3}{2} \cdot 2 \cdot \frac{0.11}{0.1597 \cdot 0.12 \cdot 0.12} \cdot 0.9 \cdot 0.85 \cdot \sin 18^\circ.$$

The coefficient $\frac{0.11}{0.1597 \times 0.0144} = 47.8$; then $T = 3 \times 47.8 \times 0.765 \times 0.309 = 33.9$ N·m. Doubling δ to 36° (still $< 90^\circ$) would raise $\sin\delta$ from 0.309 to 0.588, nearly doubling torque — the fast lever DTC pulls.

TD 4.5 — Switching frequency estimate

A torque hysteresis band $2\Delta T = 0.4$ N·m sees a torque slew of $|\mathrm{d}T/\mathrm{d}t| = 1600$ N·m/s at a given point. Estimate the local torque-loop switching rate.

$$f_{sw} \approx \frac{|\mathrm{d}T/\mathrm{d}t|}{2\Delta T} = \frac{1600}{0.4} = 4000 \text{ Hz}.$$

Halving the band to 0.2 N·m doubles the rate to 8 kHz and halves the ripple — the direct ripple/loss trade of classical DTC.

TD 4.6 — Cost function of FCS-MPC

With $T^* = 20$ N·m, $|\psi_s^*| = 0.9$ Wb, $\lambda = 30$, two candidate vectors predict $(\hat{T}, |\hat{\psi}_s|) = (19.2, 0.905)$ and $(21.0, 0.880)$. Which is applied?

$g_1 = |20 - 19.2| + 30|0.9 - 0.905| = 0.8 + 0.15 = 0.95$. $g_2 = |20 - 21.0| + 30|0.9 - 0.880| = 1.0 + 0.60 = 1.60$. $g_1 < g_2 \rightarrow$ the **first** vector is applied. Note how the weighting factor λ trades torque accuracy against flux accuracy; choosing λ is the central design decision in FCS-MPC.

4.13 Exercises (supplementary)

1. Derive $\mathbf{i}_s = \frac{1}{\sigma L_s}(\psi_s - \frac{L_m}{L_r}\psi_r)$ from the IM flux equations and hence the $\sin\delta$ torque law.
2. For ψ_s in Sector IV, write the four-way vector choice for the comparator outputs $(d\psi, dT)$ and check it against the Takahashi table.
3. Explain, using $\Delta\psi_s \approx \mathbf{v}_s \Delta t$, why a zero vector reduces torque even though it does not move the stator flux.
4. Compare the memory/compute cost of classical DTC, DTC-SVM and FCS-MPC for a one-step horizon.
5. Design a programmable low-pass flux estimator whose cutoff is $\omega_c = 0.05\,\omega_e$; discuss its behaviour at 1 Hz and at 50 Hz.
6. A DTC drive shows growing flux-estimate offset at low speed. Identify the cause and two remedies.

Chapter 5 — Control Strategies for Stepper Motors

(Duration: 3 weeks)

5.1 Introduction

A **stepper motor** converts a train of digital pulses into discrete, precise angular increments. Each pulse advances the shaft by one fixed **step angle**, so shaft position is the running count of pulses — inherently quantised, repeatable, and controllable *without feedback*, provided the motor never loses synchronism. This makes steppers the standard actuator for open-loop incremental positioning: 3-D printers, CNC axes, printers, camera platforms, valves and instrument drives. This chapter treats their types, drive modes, control strategies and the two phenomena — resonance and step loss — that dominate their practical behaviour.

5.2 Types of Stepper Motor

Three constructions are in use (Figure 5.1):

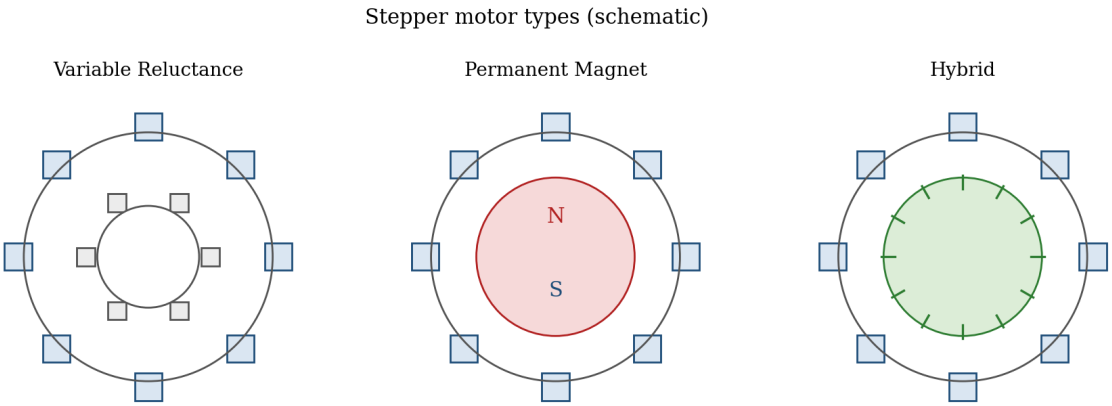


Figure 34: Figure 5.1 — The three stepper-motor constructions: variable-reluctance, permanent-magnet and hybrid.

- **Variable-Reluctance (VR).** A soft-iron toothed rotor with no magnet; torque arises solely from the rotor's tendency to move to the minimum-reluctance (aligned) position. VR motors give small step angles and low rotor inertia (fast response) but have **no detent torque** when unpowered.

- **Permanent-Magnet (PM).** A cylindrical magnetised rotor; the magnet adds an alignment torque and a **detent torque** felt even de-energised. PM motors are low-cost with larger step angles (7.5°–15°).
- **Hybrid (HB).** An axially-magnetised magnet with finely toothed end-caps combines PM torque with VR fine teeth, giving a small step (typically **1.8° = 200 steps/rev**), high torque and high accuracy — the industrial standard.

5.3 Step Angle and Resolution

For a hybrid or PM motor with N_r rotor teeth and m phases, the **full-step angle** and the steps per revolution are

$$\boxed{\beta = \frac{360^\circ}{2\,m\,N_r}, \qquad S = \frac{360^\circ}{\beta} = 2\,m\,N_r.}$$

The canonical industrial motor — 2-phase, $N_r = 50$ — gives $\beta = 360/(2 \cdot 2 \cdot 50) = 1.8^\circ$, i.e. **200 full steps per revolution**. (For a multi-stack VR motor the equivalent relation is $\beta = 360^\circ/(mN_r)$; conventions vary, so the manufacturer's steps/rev figure is the safe anchor.)

5.4 Excitation Modes

The way the phases are energised sets the resolution and the torque smoothness (Figure 5.2).

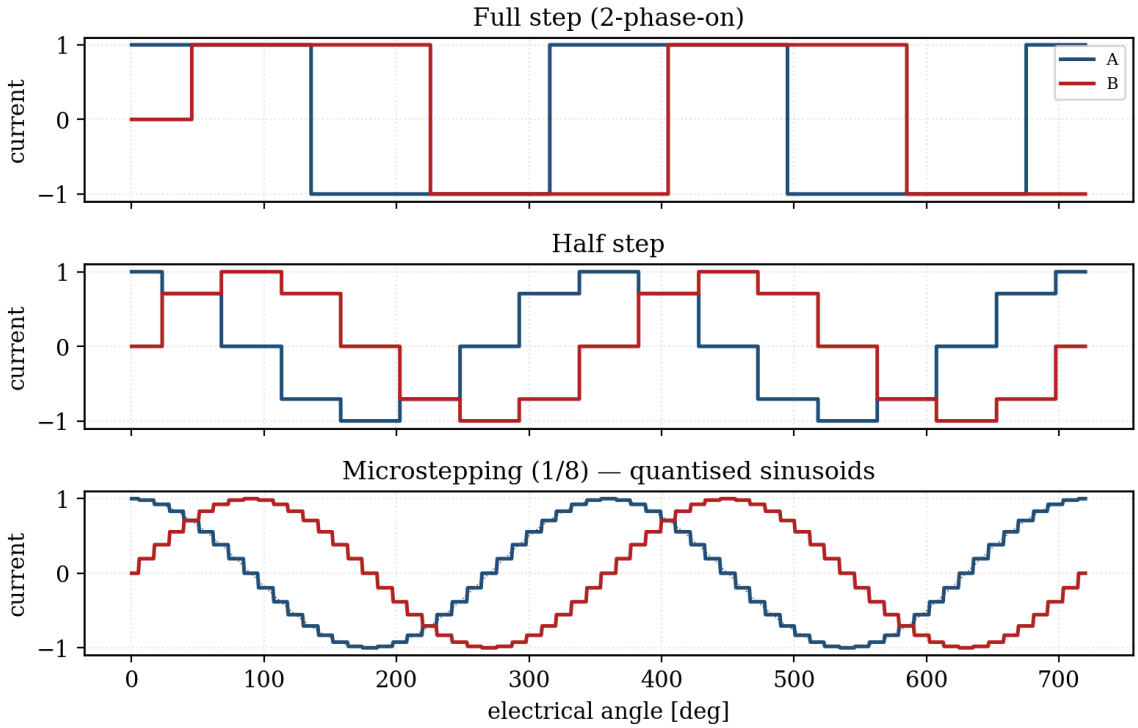


Figure 35: Figure 5.2 — Full-step, half-step and microstep phase-current waveforms and the corresponding MMF-vector positions.

- **Full-step, one-phase-on (wave drive).** One phase energised at a time: A+, B+, A−, B−. Simplest, but only ~70 % of rated torque.

- **Full-step, two-phase-on.** Both phases energised each step, giving ~1.41× the wave-drive torque; the usual full-step mode.
- **Half-step.** Alternating one-phase-on and two-phase-on states **doubles the resolution** (1.8° → 0.9°, 400 steps/rev), at the cost of a slight torque ripple between the stronger and weaker states.
- **Microstepping.** The phase currents are driven as quantised sinusoids in quadrature,

$$i_A = I_{max}\cos\theta_e, \qquad i_B = I_{max}\sin\theta_e,$$

positioning the resultant MMF vector at intermediate angles (Figure 5.3). Advancing θ_e in small increments (1/16, 1/32, 1/256 of a full step) yields very fine resolution and much **smoother motion** with reduced resonance and audible noise. Micro-step *accuracy*, however, is limited by detent torque and current-regulation precision — resolution improves faster than absolute accuracy.

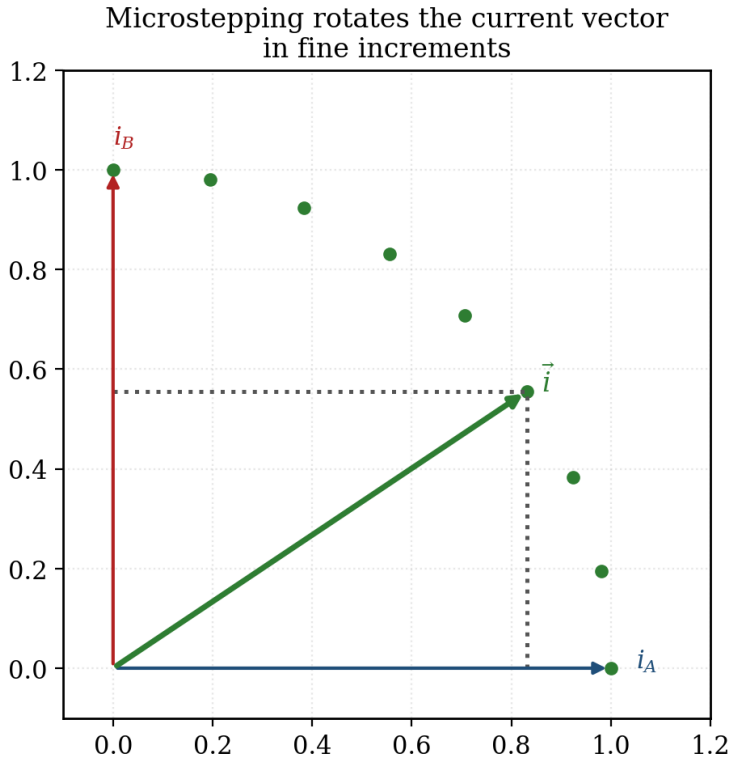


Figure 36: Figure 5.3 — Microstepping positions the current (MMF) vector at intermediate angles by controlling the ratio of the two phase currents.

5.5 Static Torque and Holding Torque

With a phase energised and the rotor displaced by an electrical angle θ_e from alignment, the motor develops a restoring **static torque** that is approximately sinusoidal (Figure 5.4):

$$T(\theta_e) = -T_h \sin\theta_e,$$

where T_h is the **holding torque** — the peak static torque, and the key catalogue rating. The rotor rests at the stable zero-crossing; a load torque displaces it along the curve until the load and static torques balance, which is the source of the static

position error under load.

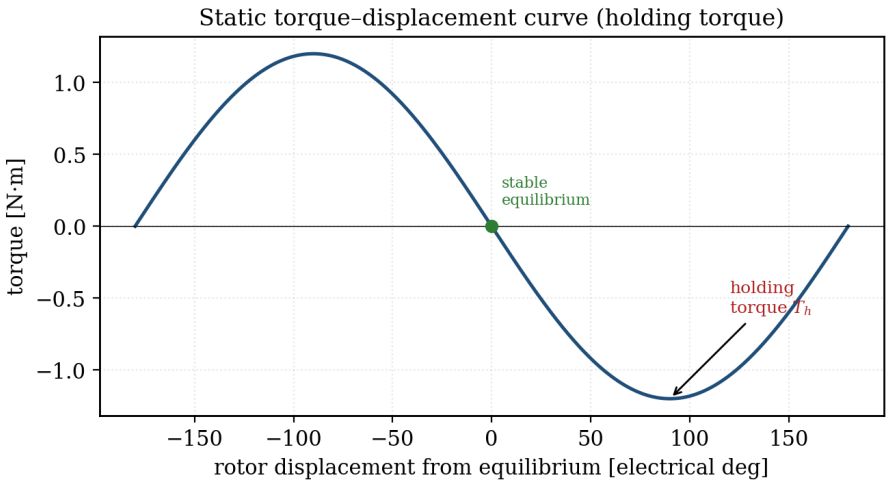


Figure 37: Figure 5.4 — Static (restoring) torque versus rotor displacement; the peak is the holding torque T_h.

5.6 Open-Loop and Closed-Loop Control

Open-loop is the classic mode: a step-and-direction controller emits pulses and the motor is *assumed* to follow. It is simple and cheap, but it has no confirmation that each step was taken — if the load torque exceeds the available torque the motor **loses steps** silently and the position count is corrupted. Open-loop drives must therefore be oversized (full current even at standstill, wasting energy) and are prone to resonance.

Closed-loop ("smart" or servo steppers) add an encoder. Strategies range from simple **stall detection / step-loss recovery** to full **field-oriented control of the stepper as a two-phase PMSM**, commutating the current from the measured position. Benefits: no lost steps, current scaled to the actual load (cooler, more efficient), higher usable speed and active resonance damping — at the cost of an encoder and servo-grade electronics. The drive block diagram is shown in Figure 5.5.

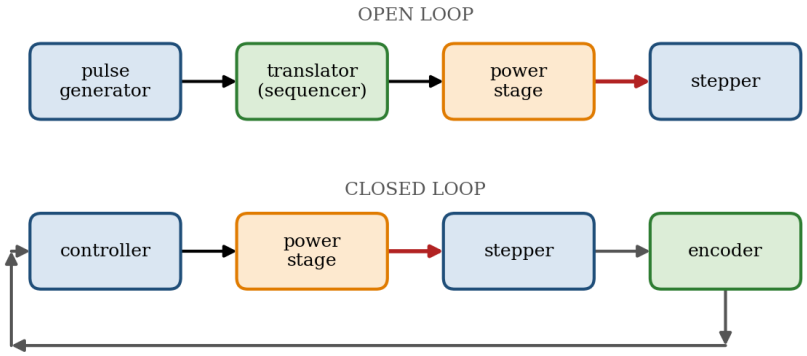


Figure 38: Figure 5.5 — Open-loop (step/direction) versus closed-loop (encoder feedback) stepper drive structures.

5.7 Torque–Speed Characteristics and Resonance

Two curves bound the safe operating envelope (Figure 5.6):

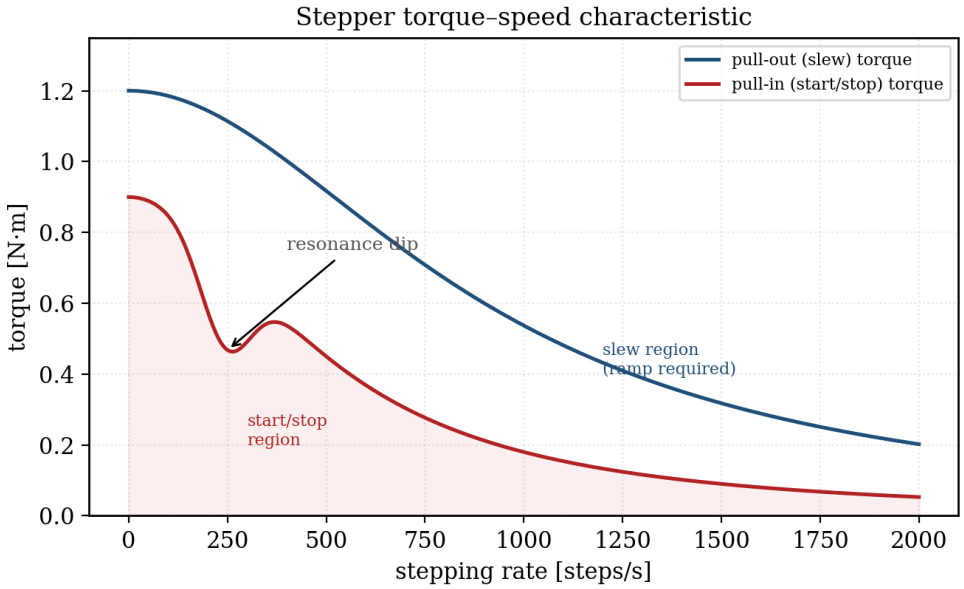


Figure 39: Figure 5.6 — Stepper torque–speed characteristic: pull-in (start/stop) and pull-out (slew) curves, with the low-speed resonance dip.

- The **pull-in (start/stop) torque** is the load torque against which the motor can start, stop or reverse *without ramping and without losing steps*; it is bounded by rotor-plus-load inertia.
- The **pull-out (slew) torque** is the maximum torque the motor can sustain while running, *after* being ramped up to speed. It always exceeds the pull-in torque, so high speeds are reached only with an acceleration ramp.

Resonance. A stepper is a lightly-damped second-order system: each step excites a decaying oscillation of the rotor about its new equilibrium (Figure 5.7). If the stepping rate coincides with the natural frequency — usually a **low-speed** region around 100–300 steps/s — the oscillations build up and the motor may stall or lose steps, producing the characteristic mid-band dip in the pull-in curve. The single-step natural frequency is approximately

$$f_n \approx \frac{1}{2\pi}\sqrt{\frac{p\,N_r\,T_h}{J}}.$$

Mitigation: microstepping (smaller torque impulses per step), mechanical or electronic damping, avoiding sustained operation at resonant rates, and acceleration profiles that pass quickly through the resonant band.

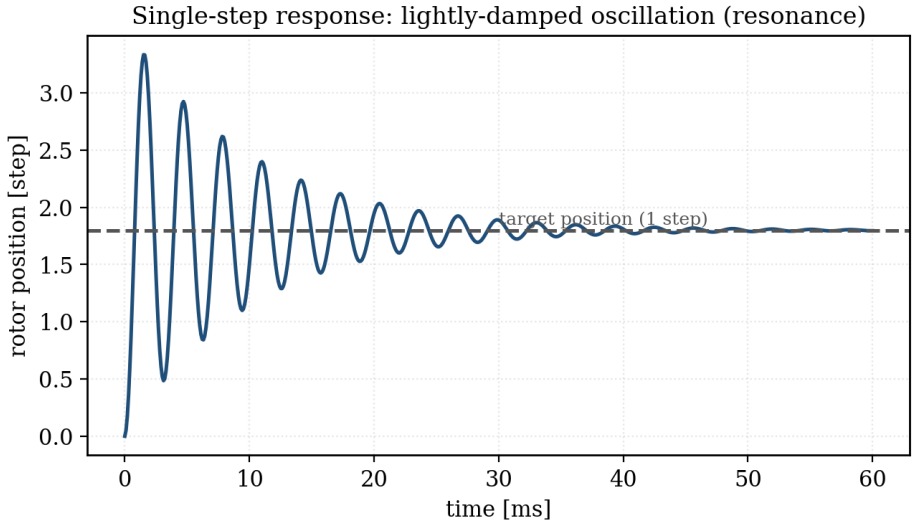


Figure 40: Figure 5.7 — Single-step response showing the lightly-damped oscillation responsible for low-speed resonance.

5.8 MATLAB/Simulink Implementation

```
% ===== Microstepping current reference (per micro-step) =====
theta_e = theta_e + dtheta;              % advance electrical angle
iA_ref  = Imax*cos(theta_e);             % phase-A current command
iB_ref  = Imax*sin(theta_e);             % phase-B current command
% current-controlled H-bridges (PI or hysteresis) drive iA, iB to refs
```

Model the two phases as R–L windings with position-dependent back-EMF, drive each from a current-controlled H-bridge, and load the rotor with inertia plus detent torque. Study step loss by ramping the load past the pull-out torque, and resonance by stepping at rates near f_n.

5.9 Worked Tutorials

TD 5.1 — Resolution and microstep currents

> A 2-phase hybrid stepper has $N_r = 50$, $T_h = 1.2$ N·m, $J = 1.5 \times 10^{-5}$ kg·m². (a) Full-step angle and steps/rev. (b) Resolution in half-step and 1/16 microstep. (c) Phase currents at micro-step 3 of a 1/16 scheme with $I_{max} = 2$ A. (d) Resonant frequency.

(a) $\beta = 360/(2 \cdot 2 \cdot 50) = 1.8°$, $S = 200$ steps/rev. **(b)** Half-step: $0.9°$, 400 steps/rev; 1/16: $0.1125°$, 3200 steps/rev. **(c)** One full step $= 90°$ electrical, so a 1/16 microstep $= 5.625°$; micro-step 3 $\Rightarrow \theta_e = 16.875°$. $i_A = 2\cos 16.875° = 1.914$ A, $i_B = 2\sin 16.875° = 0.581$ A (resultant $= 2$ A, as required). **(d)** Taking $p = 1$: $f_n = \dfrac{1}{2\pi}\sqrt{\dfrac{1 \cdot 50 \cdot 1.2}{1.5 \times 10^{-5}}} = \dfrac{1}{2\pi}\sqrt{4 \times 10^6} = 318$ Hz — the drive should ramp quickly through ≈318 steps/s.

TD 5.2 — Static error under load

> The motor above holds position with one phase energised. A load torque of 0.6 N·m is applied. What is the static angular error?

$T = T_h \sin\theta_e = 0.6 \Rightarrow \sin\theta_e = 0.5 \Rightarrow \theta_e = 30^\circ$ electrical. One electrical degree corresponds to $\beta/90 = 1.8/90 = 0.02^\circ$ mechanical, so the error is $30 \times 0.02 = 0.6^\circ$ mechanical.

TD 5.3 — Choosing an excitation mode

> An application needs 0.45° resolution from a 1.8° motor and smooth low-speed motion. Which mode suffices, and which is preferable?

$1.8/0.45 = 4$, so **quarter-step (1/4 microstepping)** meets the resolution. Because smooth low-speed motion and resonance suppression are wanted, microstepping is preferable to any full/half-step scheme even though half-step alone would not reach 0.45°.

5.10 Exercises

1. A VR stepper has stator and rotor teeth $N_s = 8$, $N_r = 6$. Compute its step angle from the multi-stack relation and its steps per revolution.
2. Plot the resultant MMF-vector angle versus micro-step index for a 1/8 scheme and comment on the linearity of position versus current ratio.
3. Derive the relation between holding torque and the peak phase current for a PM stepper and discuss thermal limits.
4. Explain why closed-loop (encoder) operation allows the current — and hence the heating — to be reduced under light load.
5. A stepper drives an inertial load through resonance at 250 steps/s. Propose two independent measures to traverse the band without step loss and justify each.

5.11 Stepper Drives in Depth

5.11.1 Operating principle of each type

- **Variable-reluctance (VR).** The toothed soft-iron rotor seeks the position of minimum reluctance for the energised phase. Torque is $T = \frac{1}{2} i^2 \, \mathrm{d}L/\mathrm{d}\theta$ — it depends on i^2, so it is independent of current *direction* (unipolar drive suffices) and there is **no detent torque** when unpowered.
- **Permanent-magnet (PM).** A magnetised rotor aligns with the stator field; torque is proportional to i and to the magnet flux, and the rotor holds a **detent** position when de-energised. Step angles are larger (7.5°–15°).
- **Hybrid (HB).** An axially-magnetised rotor with fine end-cap teeth combines PM torque with VR fine pitch, giving small steps (typically 1.8°) with high torque and accuracy — the industrial default.

5.11.2 Drive circuits: unipolar, bipolar and chopping

The winding current must be established and reversed quickly against the winding inductance L. Three circuit levels are used:

- **Unipolar** drive switches current in one direction through a centre-tapped winding — simple, but uses only half the copper.

- **Bipolar** drive uses an H-bridge per phase to reverse current, using the full winding; it delivers more torque for the same motor.
- **Chopper (constant-current) drive.** Because torque $\propto$ current and the winding time constant L/R is slow, high-performance drives apply a **high supply voltage** and *chop* it with current feedback, forcing current to its set-point far faster than L/R would allow. The current rise time improves roughly by the voltage-overdrive ratio V_{supply}/V_{rated}, which is how steppers reach useful speed before torque collapses.

5.11.3 Microstepping current control

Microstepping (§5.4) commands the two phase currents as quantised quadrature sinusoids $i_A = I\cos\theta_e$, $i_B = I\sin\theta_e$, advancing θ_e in small increments. The **incremental holding torque** at a microstep boundary falls as the step shrinks:

$$T_{hold,\,\mu} = T_h \sin\!\Big(\frac{\pi}{2N_\mu}\Big),$$

with N_μ microsteps per full step. For $N_\mu = 16$ the boundary torque is $T_h\sin(5.6^\circ) = 0.098\,T_h$ — small, so microstepping improves *smoothness and resolution* far more than *absolute accuracy*, which stays limited by detent torque and current-regulation precision.

5.11.4 Acceleration profiling and the mid-band instability

Open-loop steppers cannot start instantly at high rates (§5.7): the controller must **ramp** through the start/stop (pull-in) region into the slew region, and ramp down before stopping, or steps are lost. A separate hazard is **mid-band (mid-frequency) instability**, an oscillatory loss of synchronism around 500–1500 steps/s caused by the negative-damping interaction of the rotor with the drive; it is cured by mechanical damping, microstepping, or closed-loop control.

5.11.5 Closed-loop (servo) stepper control

Adding an encoder converts the stepper into a **two-phase PM servo** and removes its two fundamental weaknesses — lost steps and full-current-at-standstill. Two levels are common: **step-loss detection**, which monitors the following error and corrects or faults; and full **FOC of the stepper** (identical in principle to Chapter 3, with p equal to the rotor tooth number), which commutates current from measured position, scales current to actual load (cool, efficient), damps resonance actively, and roughly doubles the usable speed. The cost is the encoder and a current-controlled bridge — the stepper meets the servo drive.

5.12 Additional Solved Tutorials

TD 5.4 — Chopper overdrive and current rise

> A bipolar winding has $L = 3.2$ mH, $R = 1.4\ \Omega$, rated current 2 A. Compare the time to reach 2 A from a 2.8 V rated supply versus a 24 V chopper supply.

Rated supply: final current would be $V/R = 2.8/1.4 = 2$ A, time constant $\tau = L/R = 2.29$ ms; reaching 2 A (the asymptote) takes several τ — effectively > 7 ms to get near.

Chopper: the 24 V drives $\mathrm{d}i/\mathrm{d}t \approx (V - Ri)/L$. Initially $\mathrm{d}i/\mathrm{d}t \approx 24/0.0032 = 7500$ A/s, so 2 A is reached in $\approx 2/7500 = 0.27$ ms before the chopper begins regulating — a **~25× faster** current establishment, hence far more torque at speed.

TD 5.5 — Microstep resolution and boundary torque

> A 1.8° hybrid motor is driven at $N_\mu = 32$ microsteps/step. Give the microstep angle, steps/rev, and the incremental holding torque as a fraction of T_h.

Microstep angle $= 1.8/32 = 0.05625°$; steps/rev $= 200 \times 32 = 6400$. Incremental holding torque $= \sin(90°/32) = \sin(2.81°) = 0.049\,T_h$ — under 5 % of full holding torque at the finest boundary, illustrating the resolution-vs-torque trade.

TD 5.6 — Ramp time to avoid step loss

> Rotor+load inertia $J = 1.2 \times 10^{-4}$ kg·m², available pull-out torque 0.5 N·m, step angle 1.8°. Find the maximum step-rate slew reachable in a 0.15 s linear ramp from rest (steps/s²), and the final rate.

Angular acceleration $\alpha = T/J = 0.5/1.2 \times 10^{-4} = 4167$ rad/s². In steps/s²: $\alpha_{steps} = \alpha/\beta_{rad} = 4167/(1.8 \cdot \pi/180) = 4167/0.0314 = 1.33 \times 10^5$ steps/s². Over 0.15 s the reachable rate is $1.33 \times 10^5 \times 0.15 \approx 2.0 \times 10^4$ steps/s (100 rev/s), provided the pull-out torque curve still supports that rate.

5.13 Exercises (supplementary)

1. Derive the VR torque $T = \frac{1}{2} i^2\, \mathrm{d}L/\mathrm{d}\theta$ from co-energy and explain why VR steppers need no current reversal.
2. A hybrid motor has $N_r = 50$. Give the full-step angle and steps/rev for 2-phase excitation; repeat for half-stepping.
3. For $L = 2.5$ mH, $R = 1.2\,\Omega$, compare current rise times at 3 V and 30 V supplies; state the overdrive ratio.
4. Explain mid-band instability and give three practical cures.
5. Compare open-loop, step-loss-detecting, and full-FOC stepper control on cost, efficiency and maximum speed.
6. A microstepping drive at $N_\mu = 8$ shows torque ripple at each full-step boundary. Explain the mechanism and propose a mitigation.

6. Bibliography

Textbooks

[1] B. K. Bose, *Modern Power Electronics and AC Drives*. Upper Saddle River, NJ: Prentice Hall, 2002.

[2] R. Krishnan, *Electric Motor Drives: Modeling, Analysis, and Control*. Upper Saddle River, NJ: Prentice Hall, 2001.

[3] R. Krishnan, *Permanent Magnet Synchronous and Brushless DC Motor Drives*. Boca Raton, FL: CRC Press, 2010.

[4] W. Leonhard, *Control of Electrical Drives*, 3rd ed. Berlin: Springer, 2001.

[5] P. Vas, *Sensorless Vector and Direct Torque Control*. Oxford, U.K.: Oxford Univ. Press, 1998.

[6] N. Mohan, T. M. Undeland, and W. P. Robbins, *Power Electronics: Converters, Applications, and Design*, 3rd ed. Hoboken, NJ: Wiley, 2003.

[7] N. Mohan, *Advanced Electric Drives: Analysis, Control, and Modeling Using MATLAB/Simulink*. Hoboken, NJ: Wiley, 2014.

[8] D. G. Holmes and T. A. Lipo, *Pulse Width Modulation for Power Converters: Principles and Practice*. Piscataway, NJ: IEEE Press/Wiley, 2003.

[9] J. Chiasson, *Modeling and High-Performance Control of Electric Machines*. Hoboken, NJ: Wiley-IEEE Press, 2005.

[10] T. Kenjo and A. Sugawara, *Stepping Motors and Their Microprocessor Controls*, 2nd ed. Oxford, U.K.: Oxford Univ. Press, 1994.

[11] I. Boldea and S. A. Nasar, *Electric Drives*, 3rd ed. Boca Raton, FL: CRC Press, 2016.

Benchmark IEEE / archival papers

[12] F. Blaschke, “The principle of field orientation as applied to the new transvector closed-loop control system for rotating-field machines,” *Siemens Review*, vol. 34, pp. 217–220, 1972.

[13] I. Takahashi and T. Noguchi, “A new quick-response and high-efficiency control strategy of an induction motor,” *IEEE Trans. Ind. Appl.*, vol. IA-22, no. 5, pp. 820–827, 1986.

[14] M. Depenbrock, “Direct self-control (DSC) of inverter-fed induction machine,” *IEEE Trans. Power Electron.*, vol. 3, no. 4, pp. 420–429, 1988.

[15] H. W. van der Broeck, H.-C. Skudelny, and G. V. Stanke, “Analysis and realization of a pulsewidth modulator based on voltage space vectors,” *IEEE Trans. Ind. Appl.*, vol. 24, no. 1, pp. 142–150, 1988.

[16] G. S. Buja and M. P. Kazmierkowski, “Direct torque control of PWM inverter-fed AC motors — a survey,” *IEEE Trans. Ind. Electron.*, vol. 51, no. 4, pp. 744–757, 2004.

[17] D. Casadei, F. Profumo, G. Serra, and A. Tani, “FOC and DTC: two viable schemes for induction motors torque control,” *IEEE Trans. Power Electron.*, vol. 17, no. 5, pp. 779–787, 2002.

Reference manuals

[18] The MathWorks, *Simscape Electrical — Reference (Specialized Power Systems)*. Natick, MA, latest ed.

[19] Texas Instruments, *Field Orientated Control of 3-Phase AC-Motors*, Application Report BPRA073.

Appendix A — Coordinate-Transformation Reference

Clarke (abc → αβ), amplitude-invariant.

$$\begin{bmatrix} x_\alpha \\ x_\beta \\ x_0 \end{bmatrix} = \frac{2}{3} \begin{bmatrix} 1 & -\frac{1}{2} & -\frac{1}{2} \\ 0 & \frac{\sqrt{3}}{2} & -\frac{\sqrt{3}}{2} \\ \frac{1}{2} & \frac{1}{2} & \frac{1}{2} \end{bmatrix} \begin{bmatrix} x_a \\ x_b \\ x_c \end{bmatrix}$$

Inverse Clarke (αβ → abc).

$$\begin{bmatrix} x_a \\ x_b \\ x_c \end{bmatrix} = \begin{bmatrix} 1 & 0 \\ -\frac{1}{2} & \frac{\sqrt{3}}{2} \\ -\frac{1}{2} & -\frac{\sqrt{3}}{2} \end{bmatrix} \begin{bmatrix} x_\alpha \\ x_\beta \end{bmatrix}$$

Park (αβ → dq) and inverse.

$$\begin{bmatrix} x_d \\ x_q \end{bmatrix} = \begin{bmatrix} \cos\theta & \sin\theta \\ -\sin\theta & \cos\theta \end{bmatrix} \begin{bmatrix} x_\alpha \\ x_\beta \end{bmatrix}, \qquad \begin{bmatrix} x_\alpha \\ x_\beta \end{bmatrix} = \begin{bmatrix} \cos\theta & -\sin\theta \\ \sin\theta & \cos\theta \end{bmatrix} \begin{bmatrix} x_d \\ x_q \end{bmatrix}$$

The power-invariant variants multiply the Clarke matrix by $\sqrt{2/3}$ instead of $2/3$; be consistent, since the choice changes the torque-equation constant ($\frac{3}{2}p$ vs p).

Appendix B — The Per-Unit System

Drive equations are often normalised to per-unit (p.u.) using base quantities: base voltage V_b (rated peak phase voltage), base current I_b (rated peak phase current), base frequency ω_b (rated electrical). Derived bases follow: impedance $Z_b = V_b/I_b$, inductance $L_b = Z_b/\omega_b$, flux $\psi_b = V_b/\omega_b$, torque $T_b = \frac{3}{2} p\, \psi_b I_b$, power $P_b = \frac{3}{2} V_b I_b$. Per-unit modelling makes machines of different ratings directly comparable and keeps numerical values near unity, which improves the conditioning of simulations.

End of handout. © Dr. NOUR Mohamed — Centre Universitaire Nour El Bachir, El Bayadh.

Appendix C — MATLAB Reference Code

The listings below are self-contained and were written to accompany the corresponding chapters. They are deliberately compact so they can be typed into a live script; each can be pasted into a `.m` file and run in base MATLAB (no toolbox required except where noted).

C.1 Clarke and Park transformations (Chapter 3)

```
function [al,be] = clarke(a,b,c)
% Amplitude-invariant Clarke transform (abc -> alpha-beta)
    al = (2/3)*(a - 0.5*b - 0.5*c);
    be = (2/3)*((sqrt(3)/2)*(b - c));
end

function [d,q] = park(al,be,th)
% Park transform (alpha-beta -> dq), th = electrical angle [rad]
    d =  cos(th).*al + sin(th).*be;
    q = -sin(th).*al + cos(th).*be;
end

function [al,be] = ipark(d,q,th)
% Inverse Park (dq -> alpha-beta)
    al = cos(th).*d - sin(th).*q;
    be = sin(th).*d + cos(th).*q;
end
```

C.2 FOC of a surface PMSM — speed-step simulation (Chapter 3)

```
% Surface-PMSM FOC: cascaded PI (current + speed), forward Euler.
Rs=0.5; Ld=4e-3; Lq=4e-3; psi=0.15; p=4; J=1e-3; B=0;
Vdc=300; Vmax=Vdc/sqrt(3);
fsw=10e3; Ts=1/fsw; Tend=0.3; N=round(Tend/Ts);

% ---- controller tuning (IMC current loop, symmetric-optimum speed loop) ----
ac  = 2*pi*fsw/10;                % current-loop bandwidth [rad/s]
Kpc = ac*Ld;  Kic = ac*Rs;        % current PI
KT  = 1.5*p*psi;                  % torque constant
Teq = 1/ac;   a = 2;              % symmetry factor
Kps = J/(a*KT*Teq);  Kis = J/(a^3*KT*Teq^2);   % speed PI

% ---- states ----
```

```
id=0; iq=0; wm=0; th=0;
xi_d=0; xi_q=0; xi_w=0;            % integrators
wref=200; TL=2;                    % speed ref [rad/s], load torque [N.m]
log=zeros(N,4);

for k=1:N
    we = p*wm;
    % speed loop -> iq*
    ew = wref - wm; xi_w = xi_w + ew*Ts;
    iqref = Kps*ew + Kis*xi_w; iqref = max(min(iqref,15),-15);
    idref = 0;
    % current loops -> vd*, vq* (with decoupling)
    ed = idref-id; xi_d = xi_d + ed*Ts;
    eq = iqref-iq; xi_q = xi_q + eq*Ts;
    vd = Kpc*ed + Kic*xi_d - we*Lq*iq;
    vq = Kpc*eq + Kic*xi_q + we*(Ld*id + psi);
    % voltage saturation (circular limit)
    vm = hypot(vd,vq); if vm>Vmax, vd=vd*Vmax/vm; vq=vq*Vmax/vm; end
    % PMSM electrical dynamics (Euler)
    did = (vd - Rs*id + we*Lq*iq)/Ld;
    diq = (vq - Rs*iq - we*(Ld*id+psi))/Lq;
    id = id + did*Ts; iq = iq + diq*Ts;
    % torque + mechanics
    Te = 1.5*p*(psi*iq + (Ld-Lq)*id*iq);
    wm = wm + (Te - TL - B*wm)/J*Ts;
    th = mod(th + we*Ts, 2*pi);
    log(k,:) = [k*Ts, wm, iq, Te];
end
plot(log(:,1),log(:,2)); xlabel('t [s]'); ylabel('\omega_m [rad/s]');
title('FOC speed step'); grid on;
```

C.3 Space-Vector Modulation dwell times (Chapter 2)

```
function [Ta,Tb,T0,sector] = svm(Vref_mag, theta, Vdc, Ts)
% Symmetric SVM: returns active/zero dwell times and sector (1..6).
    theta  = mod(theta, 2*pi);
    sector = floor(theta/(pi/3)) + 1;
    thp    = theta - (sector-1)*(pi/3);          % in-sector angle
    K  = sqrt(3)*Vref_mag*Ts/Vdc;
    Ta = K*sin(pi/3 - thp);
    Tb = K*sin(thp);
    T0 = Ts - Ta - Tb;                           % split over V0,V7
end
```

C.4 DTC flux/torque estimator and switching table (Chapter 4)

```
function [Vidx] = dtc_step(valpha,vbeta,ialpha,ibeta,Rs,p,psi_ref,Te_ref,dpsi_band,dTe_band,state)
% One DTC decision step. 'state' carries integrator + previous outputs.
    % --- stator-flux estimator (voltage model with LPF-integrator) ---
    wc = 2*pi*5;                         % integrator cutoff [rad/s]
    state.pa = state.pa + (valpha - Rs*ialpha - wc*state.pa)*state.dt;
    state.pb = state.pb + (vbeta  - Rs*ibeta  - wc*state.pb)*state.dt;
    psi_mag = hypot(state.pa, state.pb);
    theta_s = atan2(state.pb, state.pa);
    Te = 1.5*p*(state.pa*ibeta - state.pb*ialpha);
    % --- hysteresis comparators ---
```

```
    dpsi = psi_mag <= (psi_ref - dpsi_band);       % 1 = increase flux
    if Te <= Te_ref - dTe_band, dTe = +1;
    elseif Te >= Te_ref + dTe_band, dTe = -1; else, dTe = 0; end
    % --- sector 1..6 ---
    k = mod(floor((theta_s+pi/6)/(pi/3)),6)+1;
    % --- Takahashi table (returns active vector index 1..6, or 0/7 zero) ---
    T = [ 2 3 4 5 6 1;   % dpsi=1, dTe=+1
          7 0 7 0 7 0;   % dpsi=1, dTe= 0
          6 1 2 3 4 5;   % dpsi=1, dTe=-1
          3 4 5 6 1 2;   % dpsi=0, dTe=+1
          0 7 0 7 0 7;   % dpsi=0, dTe= 0
          5 6 1 2 3 4 ]; % dpsi=0, dTe=-1
    row = (~dpsi)*3 + (2 - dTe);        % map (dpsi,dTe) -> row 1..6
    Vidx = T(row, k);
    state.psi_mag = psi_mag; state.Te = Te;
end
```

C.5 Microstepping current generation (Chapter 5)

```
function [iA,iB] = microstep(step_index, N_micro, Imax)
% Quadrature currents for a 2-phase stepper under microstepping.
% step_index increments by 1 per microstep; N_micro per full step.
    theta_e = (pi/2) * step_index / N_micro;   % 90 deg elec / full step
    iA = Imax*cos(theta_e);
    iB = Imax*sin(theta_e);
end

% Example: one electrical revolution (4 full steps) at 1/16 microstepping
N_micro = 16; Imax = 2;
idx = 0:(4*N_micro);
iA = Imax*cos((pi/2)*idx/N_micro);
iB = Imax*sin((pi/2)*idx/N_micro);
plot(idx,iA,idx,iB); grid on; xlabel('microstep'); ylabel('phase current [A]');
legend('i_A','i_B'); title('Microstepping quadrature currents');
```

C.6 V/f profile with boost and field weakening (Chapter 2)

```
function V = vf_profile(f, f_rated, V_rated, V_boost)
% Constant-V/f voltage command with low-speed boost and field weakening.
    if f <= f_rated
        V = V_boost + (V_rated - V_boost) * f / f_rated;   % constant flux
    else
        V = V_rated;                                       % field weakening
    end
end
```

These listings map one-to-one onto the block diagrams of their chapters: C.1–C.2 realise the FOC structure of Fig. 3 (complete FOC); C.3 the modulator of §2.4.2; C.4 the estimator-and-table loop of §4.4; C.5 the quadrature current generator of §5.4; and C.6 the profile of §2.2.

Appendix D — Formula and Design Summary

This appendix collects, in one place, every working equation of the course, grouped by theme, for use as a revision sheet and a design reference.

D.1 Mechanics of the drive

Quantity	Relation
Equation of motion	$T_{em} - T_L = J\dot{\Omega} + B\Omega$
Mechanical transfer function	$\dfrac{\Omega(s)}{T_{em}(s)} = \dfrac{1/B}{1 + s\tau_m}, \;\; \tau_m = J/B$
Referred inertia (ratio n)	$J = J_m + J_L/n^2$
Referred load torque	$T_{L,\text{ref}} = T'_L/n$
Optimal gear ratio (inertial)	$n_{opt} = \sqrt{J_L/J_m}$
RMS (thermal) torque	$T_{rms} = \sqrt{\frac{1}{T_{cyc}} \int T_{em}^2 \, \mathrm{d}t}$
Stability of an equilibrium	$\dfrac{dT_{em}}{d\Omega} < \dfrac{dT_L}{d\Omega}$
Two-mass resonance	$\omega_{res} = \sqrt{K_s(1/J_m + 1/J_L)}$
Two-mass anti-resonance	$\omega_{ar} = \sqrt{K_s/J_L}$

Load laws: constant $T_L = \text{const}$; fan/pump $T_L = k\Omega^2$; linear $T_L = k\Omega$; constant power $T_L = P/\Omega$.

D.2 Scalar control, inverter and PWM

Quantity	Relation
Synchronous speed	$n_s = 60f/p, \;\; \Omega_s = 2\pi f/p$
Air-gap flux	$\phi_m \propto E_s/f \approx V_s/f$
Constant-V/f law	$V_s/f = \text{const}$ (below base speed)
IM slip	$s = (\Omega_s - \Omega_r)/\Omega_s$
Active-vector magnitude	$\frac{2}{3}V_{dc}$

Quantity	Relation
SVM dwell (sector k, θ')	$T_a = \dfrac{\sqrt{3}\,\lvert\mathbf{V}_{ref}\rvert T_s}{V_{dc}} \sin(\frac{\pi}{3} - \theta')$ $T_b = \dfrac{\sqrt{3}\,\lvert\mathbf{V}_{ref}\rvert T_s}{V_{dc}} \sin\theta',\ \ T_0 = T_s - T_a - T_b$
SVM modulation index	$m = \lvert\mathbf{V}_{ref}\rvert / (V_{dc}/\sqrt{3})$, linear $0 \le m \le 1$
SVM vs SPWM ceiling	$2/\sqrt{3} = 1.155$ (15.5 % more)
Six-step peak fundamental	$\frac{2}{\pi} V_{dc}$
Dead-time voltage error	$\Delta V \approx t_d f_{sw} V_{dc}\,\mathrm{sgn}(i)$
Ripple current (worst)	$\Delta i_{pp} \approx V_{dc} T_s / (8L)$

D.3 PMSM model and FOC design

Quantity	Relation
d-axis voltage	$v_d = R_s i_d + L_d \dot{i}_d - \omega_e L_q i_q$
q-axis voltage	$v_q = R_s i_q + L_q \dot{i}_q + \omega_e (L_d i_d + \psi_f)$
Torque (general)	$T_{em} = \frac{3}{2} p [\psi_f i_q + (L_d - L_q) i_d i_q]$
Torque (surface)	$T_{em} = \frac{3}{2} p \psi_f i_q$
Current PI (IMC)	$K_p = \alpha_c L,\ \ K_i = \alpha_c R_s$
Current closed loop	$i/i^* = \alpha_c / (s + \alpha_c)$
Speed PI (sym. optimum)	$T_i = a^2 T_{eq},\ K_p = \dfrac{J}{a K_T T_{eq}},\ K_i = \dfrac{J}{a^3 K_T T_{eq}^2}$
Phase margin	$\varphi_m = \arctan\frac{a^2-1}{2a}$
Torque constant	$K_T = \frac{3}{2} p \psi_f$
Voltage limit	$\sqrt{v_d^2 + v_q^2} \le V_{dc}/\sqrt{3}$
MTPA (IPMSM)	$i_d = \dfrac{\psi_f - \sqrt{\psi_f^2 + 8(L_q - L_d)^2 i_q^2}}{4(L_q - L_d)}$

D.4 Direct torque control

Quantity	Relation
Stator flux	$\psi_s = \int (\mathbf{v}_s - R_s \mathbf{i}_s)\,\mathrm{d}t$

Quantity	Relation
Flux magnitude	$\lvert\psi_s\rvert = \sqrt{\psi_{s\alpha}^2 + \psi_{s\beta}^2}$
Torque (flux–current)	$T_{em} = \frac{3}{2}p(\psi_{s\alpha} i_{s\beta} - \psi_{s\beta} i_{s\alpha})$
Torque (load angle)	$T_{em} = \frac{3}{2}p\dfrac{L_m}{\sigma L_s L_r}\lvert\psi_s\rvert\lvert\psi_r\rvert \sin\delta$
Flux increment	$\Delta\psi_s \approx \mathbf{v}_s \Delta t$
Leakage factor	$\sigma = 1 - L_m^2/(L_s L_r)$
Switching-rate estimate	$f_{sw} \propto \lvert \mathrm{d}T/\mathrm{d}t\rvert/(2\Delta T)$
FCS-MPC cost	$g = \lvert T^* - \hat{T}\rvert + \lambda\big\lvert\lvert\psi_s^*\rvert - \lvert\hat{\psi}_s\rvert\big\rvert$

D.5 Stepper motors

Quantity	Relation
Full-step angle (2-phase HB)	$\beta = 360^\circ/(2mN_r)$
Steps per revolution	$S = 2mN_r$
Microstep angle	β/N_μ
Microstep currents	$i_A = I\cos\theta_e,\ i_B = I\sin\theta_e$
Boundary holding torque	$T_h \sin(\pi/2N_\mu)$
VR torque	$T = \frac{1}{2}i^2\,\mathrm{d}L/\mathrm{d}\theta$
Natural (resonant) frequency	$f_n \approx \frac{1}{2\pi}\sqrt{pN_r T_h/J}$

D.6 Design rules of thumb

- **Time-scale separation:** current-loop bandwidth $\alpha_c \approx 2\pi f_{sw}/10$; speed loop $\approx \alpha_c/10$.
- **Symmetry factor:** $a = 2$ fast (37° PM), $a = 3$–4 well damped (53–62° PM); always add the pre-filter.
- **Mechanical bandwidth:** keep the speed loop below $\frac{1}{3}\omega_{res}$ of any elastic coupling.
- **Reflected-inertia ratio:** keep $J_L/n^2 J_m \lesssim 5$–10 for good dynamics.
- **DTC bands:** narrow → low ripple, high f_{sw}; use DTC-SVM or FCS-MPC for a fixed frequency.
- **Stepper overdrive:** use a chopper supply several times the rated winding voltage to obtain torque at speed; ramp through pull-in and resonance.

Appendix E — Digital Implementation of Controllers

The controllers derived in Chapters 3–4 are continuous transfer functions, yet they run on a microcontroller or DSP that samples at a fixed rate $f_s = 1/T_s$ (usually equal to, or a multiple of, the PWM frequency). This appendix collects the practical rules that turn a continuous design into working firmware.

E.1 Why discretization is not optional

Sampling introduces three effects a continuous design ignores: a **zero-order hold** that keeps the command constant over T_s, a **computational delay** of up to one sample between measurement and actuation, and **aliasing** of high-frequency content above $f_s/2$. Together they erode phase margin. A robust rule of thumb is to keep the current-loop bandwidth below one-tenth of the sampling frequency,

$$\alpha_c \le \frac{2\pi f_s}{10},$$

so that the loop "sees" an almost-continuous plant and the discretization method chosen has little influence.

E.2 Discretization methods

Let $C(s)$ be the continuous controller and $C(z)$ its discrete equivalent. The three standard mappings substitute for s:

Method	Substitution	Character
Forward Euler	$s \leftarrow \dfrac{z-1}{T_s}$	simplest; can push stable poles outside the unit circle at large T_s
Backward Euler	$s \leftarrow \dfrac{z-1}{T_s\, z}$	always maps the left half-plane inside the unit circle (unconditionally stable)

Method	Substitution	Character
Tustin (bilinear)	$s \leftarrow \dfrac{2}{T_s}\dfrac{z-1}{z+1}$	best frequency match; warps frequencies near $f_s/2$

For controllers with a specific corner frequency ω_0 that must be preserved (e.g. a resonant or notch term), Tustin with **pre-warping** replaces $2/T_s$ by $\omega_0/\tan(\omega_0 T_s/2)$ so that ω_0 maps exactly.

E.3 The discrete PI controller

Applying backward Euler to $C(s) = K_p + K_i/s$ gives the recursive **position form**

$$u[k] = K_p\, e[k] + I[k], \qquad I[k] = I[k-1] + K_i T_s\, e[k],$$

where $e[k] = r[k] - y[k]$ is the error and $I[k]$ the integrator state. The equivalent **velocity (incremental) form**, convenient because it embeds anti-windup naturally, is

$$u[k] = u[k-1] + K_p(e[k] - e[k-1]) + K_i T_s\, e[k].$$

A minimal firmware kernel (per axis, per sample) reads:

```
e   = ref - meas;
I   = I + Ki*Ts*e;              // integrate
u   = Kp*e + I;                 // PI output
u_s = clamp(u, -Umax, +Umax);  // actuator limit
I   = I + Kaw*(u_s - u);        // back-calculation anti-windup
out = u_s;
```

E.4 Integrator wind-up and its cure

When the command saturates (large speed step, current limit), the error does not fall and the integrator keeps accumulating — **wind-up** — producing a long overshoot once the plant catches up. Two cures are standard: **clamping** (freeze I whenever the output is saturated and the error would push it further into saturation) and **back-calculation**, which feeds the difference $u_{sat} - u$ back into the integrator through a gain $K_{aw} \approx 1/(K_p T_t)$, with tracking time constant $T_t \approx \sqrt{T_i T_d}$ (for a PI, $T_t \approx T_i$). Figure E.1 shows the structure.

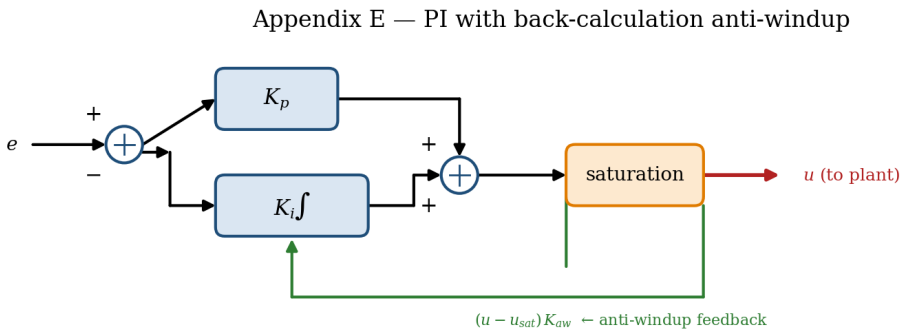


Figure 41: Figure E.1 — PI controller with back-calculation anti-windup: the saturated–unsaturated difference is fed back into the integrator so it never charges beyond the actuator limit.

E.5 Computational delay

Between sampling the currents and updating the duty cycles, the processor needs one execution cycle; the new duty cycle then takes effect at the next PWM reload. The net **actuation delay** is typically $1.5\,T_s$. Modelled as $e^{-1.5sT_s}$, it subtracts phase $1.5\,\omega T_s$ (radians) from the loop. It can be reduced by **current prediction** — extrapolating $i[k+1]$ from the model — or accounted for by de-rating the target bandwidth.

E.6 Choosing the sample time

Figure E.2 illustrates the trade-off: at $T_s = 20$ ms the discrete loop tracks the continuous design almost exactly, whereas at $T_s = 80$ ms the added phase lag produces visible overshoot and ringing. In a real drive T_s is tied to f_{sw} (often $T_s = 1/f_{sw}$ or $1/2f_{sw}$), so the modulator and the controller bandwidth are designed together.

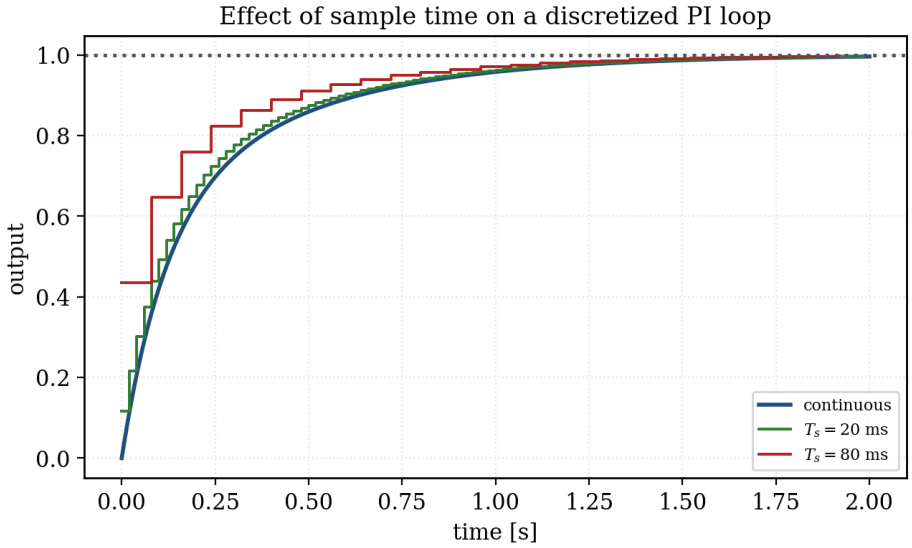


Figure 42: Figure E.2 — The same PI design discretized at two sample rates. Slower sampling adds phase lag and degrades the response.

Appendix F — Sensorless Position and Speed Estimation

FOC needs the electrical angle θ_e and DTC benefits from an accurate flux estimate; both traditionally require an encoder or resolver. **Sensorless** (self-sensing) control estimates these from the electrical terminals alone, removing the sensor's cost, cabling and failure modes. No single method spans the whole speed range, so practical drives blend two families.

F.1 Fundamental-excitation methods (medium and high speed)

These exploit the motional back-EMF, which is proportional to speed and therefore vanishes at standstill.

Voltage-model flux observer. Integrating the stator equation, as in DTC,

$$\psi_s = \int (\mathbf{v}_s - R_s \mathbf{i}_s)\,\mathrm{d}t, \qquad \hat{\theta}_e = \angle(\psi_s - L_s \mathbf{i}_s + \dots),$$

recovers the rotor-flux angle. It is simple but inherits the pure-integrator drift discussed in §4.6, so a low-pass replacement or a closed-loop correction is required.

Sliding-mode observer (SMO). A current observer is driven by a switching (sign) term whose equivalent value, once the estimated current slides onto the measured current, equals the back-EMF:

$$\frac{\mathrm{d}\hat{\mathbf{i}}_s}{\mathrm{d}t} = \frac{1}{L_s}(\mathbf{v}_s - R_s \hat{\mathbf{i}}_s - \hat{\mathbf{e}}) + \frac{K}{L_s}\,\mathrm{sgn}(\mathbf{i}_s - \hat{\mathbf{i}}_s), \qquad \hat{\mathbf{e}} = \big[K\,\mathrm{sgn}(\mathbf{i}_s - \hat{\mathbf{i}}_s)\big]_{\mathrm{LPF}}.$$

The estimated back-EMF $\hat{\mathbf{e}} = (\hat{e}_\alpha, \hat{e}_\beta)$ then yields the angle through $\hat{\theta}_e = \mathrm{atan2}(-\hat{e}_\alpha, \hat{e}_\beta)$. The SMO is prized for its robustness to parameter error at the cost of chattering, which a boundary layer or higher-order (super-twisting) design reduces.

Luenberger / extended-Kalman observers. A full state observer of the machine model, with a gain matrix placed for the desired estimation dynamics (Luenberger) or computed from noise statistics (EKF), estimates flux, back-EMF and speed simultaneously with good noise rejection.

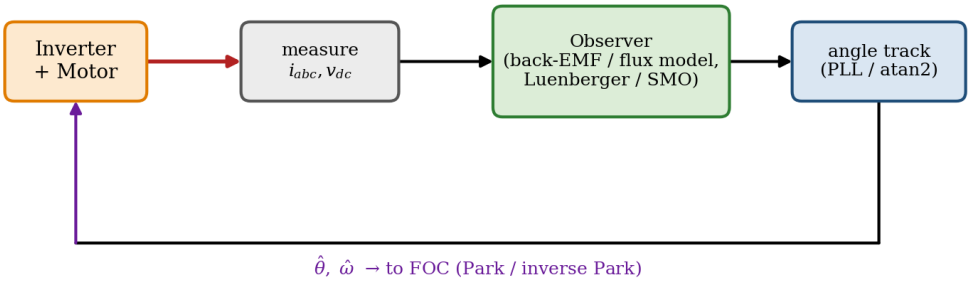


Figure 43: Figure F.1 — Sensorless estimation chain: measured currents and DC-bus voltage feed an observer whose back-EMF (or flux) output is converted to angle and speed for the FOC transforms.

F.2 Model-reference adaptive systems (MRAS)

An MRAS runs two flux (or back-EMF) estimators in parallel: a **reference model** independent of the unknown speed (the voltage model) and an **adjustable model** that depends on $\hat{\omega}$ (the current model). The cross-product of their outputs forms an error that a PI adaptation law drives to zero, whose output is the speed estimate:

$$\varepsilon = \psi_\alpha^{\text{ref}}\psi_\beta^{\text{adj}} - \psi_\beta^{\text{ref}}\psi_\alpha^{\text{adj}}, \qquad \hat{\omega} = \left(K_p + \frac{K_i}{s}\right)\varepsilon.$$

F.3 Saliency-tracking (high-frequency injection) at low and zero speed

Because back-EMF disappears at standstill, low-speed sensorless control instead exploits the machine's magnetic **saliency** ($L_d \neq L_q$). A high-frequency carrier voltage (typically 0.5–2 kHz) is injected; the resulting current carries a component modulated by $2\theta_e$, from which the angle is demodulated. This works down to zero speed and even supports initial-position and magnet-polarity detection, but requires saliency and adds acoustic noise. Surface PMSMs, having little saliency, need deliberate saturation-induced saliency for this to work.

F.4 Angle tracking

Any of the above yields a noisy raw angle; a **tracking observer / PLL** smooths it and produces a clean speed. The phase detector forms $\varepsilon = \sin(\hat{\theta} - \theta_{raw}) \approx \hat{\theta} - \theta_{raw}$, and a PI drives it to zero, its integral of the speed estimate giving $\hat{\theta}$. Figure F.2 shows estimated back-EMF components and the recovered angle.

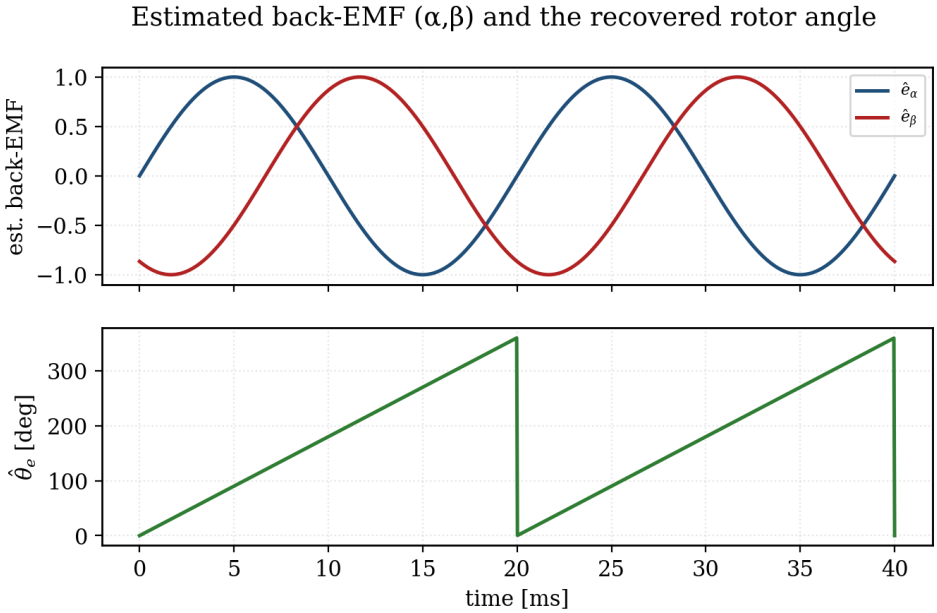


Figure 44: Figure F.2 — Estimated back-EMF in the stationary frame (top) and the rotor angle recovered from it (bottom).

F.5 Practical notes

Sensorless drives are near-universal in appliance, fan and pump applications where the low-speed start is undemanding, and increasingly used in traction with HFI hand-off. The two universal weaknesses are **parameter sensitivity** (especially R_s at low speed and temperature) and the **zero-speed observability gap** for non-salient machines; both are active research areas.

Appendix G — Extended Worked Problems

These self-contained problems integrate several chapters. Attempt each before reading the solution.

G.1 Thermal (RMS) sizing of a servo axis

Problem. A servo executes a repeating cycle: accelerate at 8 N·m for 0.2 s, run at 2 N·m for 0.5 s, decelerate at -8 N·m for 0.2 s, then dwell at 0 for 0.6 s. Find the RMS torque and check a motor rated 3 N·m continuous.

Solution. With $T_{rms} = \sqrt{\frac{1}{T_{cyc}} \sum T_i^2 t_i}$ and $T_{cyc} = 1.5$ s:

$$T_{rms} = \sqrt{\frac{8^2(0.2) + 2^2(0.5) + 8^2(0.2) + 0}{1.5}} = \sqrt{\frac{12.8 + 2.0 + 12.8}{1.5}} = \sqrt{18.4} = 4.29\,\text{N·m}.$$

Since $4.29 > 3$, the 3 N·m motor **overheats**; a motor of at least ~ 4.5 N·m continuous is required, even though the average torque is modest. RMS, not peak or mean, sets the thermal rating.

G.2 Inertia-matching gear ratio

Problem. A motor ($J_m = 0.4 \times 10^{-4}$ kg·m^2) drives a load ($J_L = 9 \times 10^{-4}$ kg·m^2) through a gearbox. Find the ratio $n = \Omega_m / \Omega_L$ that minimises the motor torque needed for a given load acceleration.

Solution. Reflected load inertia is J_L / n^2; the accelerating torque referred to the motor is proportional to $(J_m + J_L/n^2)\,\alpha_L \,/\, n$ balanced against gearing. Minimising gives the classic inertia-match

$$n_{opt} = \sqrt{J_L / J_m} = \sqrt{\frac{9 \times 10^{-4}}{0.4 \times 10^{-4}}} = \sqrt{22.5} = 4.74.$$

At this ratio the reflected load inertia equals the motor inertia, and the motor delivers acceleration most effectively.

G.3 V/f set-point with slip

Problem. A 4-pole IM (rated 400 V, 50 Hz) runs on constant V/f at a commanded 30 Hz and carries a load producing 3 % slip. Give the stator voltage, synchronous speed and shaft speed.

Solution. $V/f = 8$ V/Hz $\Rightarrow V_{30} = 240$ V. Synchronous speed $n_s = 120f/(2p) = 120(30)/4 = 900$ rpm. With $s = 0.03$, $n_r = (1-s)n_s = 0.97(900) = 873$ rpm.

G.4 Full SVM dwell times with overmodulation check

Problem. $V_{dc} = 540$ V, $T_s = 100$ μs. The reference is $|\mathbf{V}_{ref}| = 300$ V (peak phase) at $\theta = 100°$. Find the sector, dwell times and modulation index; is it in the linear range?

Solution. $100°$ falls in **Sector II** ($60°$–$120°$); the in-sector angle is $\theta' = 100 - 60 = 40°$.

$$K = \frac{\sqrt{3}\,|\mathbf{V}_{ref}|T_s}{V_{dc}} = \frac{\sqrt{3}(300)(100\times10^{-6})}{540} = 96.2\ \mu s.$$

$$T_a = K\sin(60-40)° = 96.2\sin 20° = 32.9\ \mu s, \quad T_b = K\sin 40° = 61.8\ \mu s,$$

$$T_0 = 100 - 32.9 - 61.8 = 5.3\ \mu s.$$

Modulation index $m = |\mathbf{V}_{ref}|/(V_{dc}/\sqrt{3}) = 300/311.8 = 0.962 < 1$, so operation is **just inside** the linear range (only 5.3 μs of zero-vector time remains — near the hexagon boundary).

G.5 Complete PMSM controller design

Problem. Surface PMSM: $R_s = 0.6\ \Omega$, $L = 5$ mH, $\psi_f = 0.12$ Wb, $p = 3$, $J = 0.8\times10^{-3}$ kg·m^2, $f_{sw} = 8$ kHz. Design both loops (current bandwidth $= f_{sw}/10$; speed loop by symmetrical optimum, $a = 3$).

Solution. Current loop: $\alpha_c = 2\pi(800) = 5027$ rad/s.

$$K_p = \alpha_c L = 25.1\ \text{V/A}, \qquad K_i = \alpha_c R_s = 3016\ \text{V/(A·s)}.$$

Torque constant $K_T = \frac{3}{2}p\psi_f = \frac{3}{2}(3)(0.12) = 0.54$ N·m/A. Equivalent current-loop lag $T_{eq} = 1/\alpha_c = 199$ μs. Speed loop, $a = 3$:

$$K_{p,\Omega} = \frac{J}{aK_T T_{eq}} = \frac{0.8\times10^{-3}}{3(0.54)(199\times10^{-6})} = 2.48\ \text{A·s/rad},$$

$$K_{i,\Omega} = \frac{J}{a^3 K_T T_{eq}^2} = \frac{0.8\times10^{-3}}{27(0.54)(199\times10^{-6})^2} = 1386\ \text{A/rad}.$$

Phase margin $\varphi_m = \arctan\frac{a^2-1}{2a} = \arctan\frac{8}{6} = 53°$ — comfortably damped.

G.6 Field-weakening operating point

Problem. For the machine of G.5 driven from $V_{dc} = 300$ V, find the base speed (at rated $i_q = 8$ A, $i_d = 0$) beyond which field weakening must begin.

Solution. Voltage limit $V_{max} = V_{dc}/\sqrt{3} = 173$ V. At base speed, ignoring R_s,

$$V_{max} = \sqrt{(\omega_e L i_q)^2 + (\omega_e \psi_f)^2} = \omega_e \sqrt{(L i_q)^2 + \psi_f^2}.$$

$(L i_q) = 0.005(8) = 0.04$; $\sqrt{0.04^2 + 0.12^2} = 0.1265$. Hence $\omega_e = 173/0.1265 = 1368$ elec rad/s, i.e. mechanical $\Omega = \omega_e/p = 456$ rad/s ≈ 4355 rpm. Above this, negative i_d is injected to hold $\sqrt{v_d^2 + v_q^2} \le V_{max}$.

G.7 DTC vector choice and flux ripple

Problem. In a DTC drive the flux is in Sector 3, and the comparators demand *decrease flux* ($d\psi = 0$) and *increase torque* ($dT = +1$). Which vector is applied? If $|\mathbf{V}| = \frac{2}{3} V_{dc}$ with $V_{dc} = 600$ V and it acts for 40 μs, estimate the flux increment magnitude.

Solution. From the switching table, $d\psi = 0, dT = +1$ in Sector k selects $\mathbf{V}_{k+2}$; for $k = 3$ that is $\mathbf{V}_5$. The flux increment $|\Delta\psi_s| \approx |\mathbf{V}|\Delta t = \frac{2}{3}(600)(40 \times 10^{-6}) = 0.016$ Wb per switching action — the granularity that sets the flux ripple band.

G.8 Stepper microstepping and resonance

Problem. A 1.8° hybrid stepper is driven at 1/8 microstepping. Give the microstep angle and steps/rev. If its holding torque is 0.9 N·m and total inertia 2×10^{-5} kg·m^2 ($N_r = 50$, $p = 1$), find the resonant frequency and the stepping rate to avoid.

Solution. Microstep angle $= 1.8/8 = 0.225^\circ$; steps/rev $= 200 \times 8 = 1600$.

$$f_n \approx \frac{1}{2\pi}\sqrt{\frac{p N_r T_h}{J}} = \frac{1}{2\pi}\sqrt{\frac{(1)(50)(0.9)}{2 \times 10^{-5}}} = \frac{1}{2\pi}\sqrt{2.25 \times 10^6} = 239 \text{ Hz}.$$

At full-step this is ≈ 239 steps/s; the drive should ramp quickly through this rate, and microstepping already softens the excitation that drives the resonance.

Appendix H — Mechanical Resonance and Two-Mass Systems

Chapter 1 modelled the drivetrain as a single rigid inertia. Real couplings — long shafts, belts, gearboxes — have finite stiffness, so the motor and load form a **two-mass** system whose resonance limits the achievable speed-loop bandwidth.

H.1 The two-mass model

Motor inertia J_m and load inertia J_L are joined by a shaft of stiffness K_s (and small damping d). The torsion torque is $T_s = K_s \int (\Omega_m - \Omega_L)\,\mathrm{d}t$, giving

$$J_m \dot{\Omega}_m = T_{em} - T_s, \qquad J_L \dot{\Omega}_L = T_s - T_L.$$

H.2 Resonance and anti-resonance

The transfer function Ω_m / T_{em} has a resonant pole pair and, because the load is measured through the shaft, an **anti-resonant** zero pair:

$$\omega_{res} = \sqrt{K_s \left(\frac{1}{J_m} + \frac{1}{J_L} \right)}, \qquad \omega_{ar} = \sqrt{\frac{K_s}{J_L}}.$$

The anti-resonance always lies below the resonance ($\omega_{ar} < \omega_{res}$). Figure H.1 shows the characteristic dip-then-peak in the frequency response.

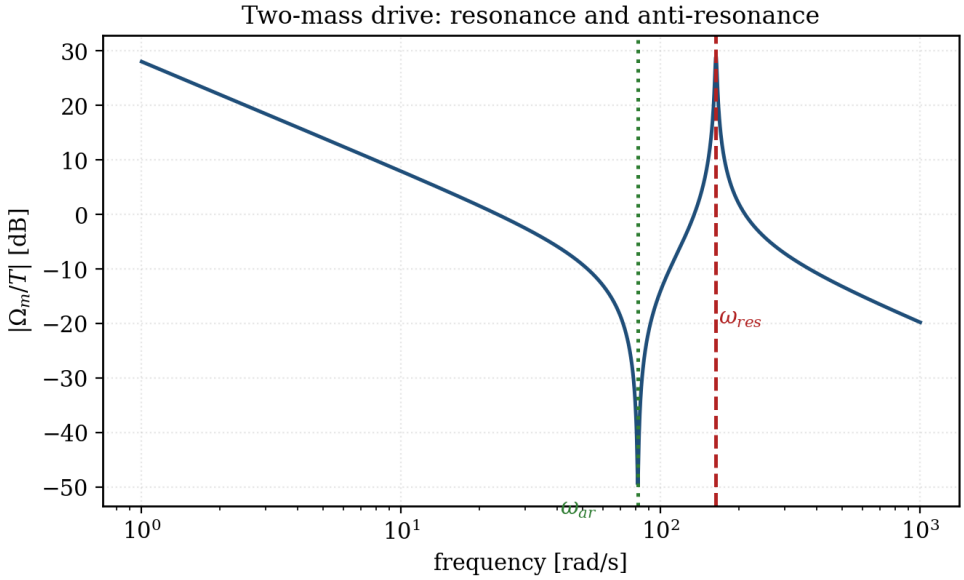


Figure 45: Figure H.1 — Frequency response of a two-mass drive, showing the anti-resonant notch ω_{ar} below the resonant peak ω_{res}.

H.3 Consequences for control and mitigation

If the speed-loop bandwidth approaches ω_{res}, the loop excites the resonance and the shaft torque oscillates, causing audible noise, fatigue and even instability. Standard mitigations are: limit the speed-loop bandwidth to well below ω_{res} (typically $\leq \omega_{ar}/2$); insert a **notch filter** at ω_{res} in the speed controller; add mechanical or active damping; or, in demanding servos, use **state-feedback** with an observer that estimates and actively damps the shaft torsion. The inertia ratio $R = J_L/J_m$ governs the difficulty — a large mismatch pushes ω_{ar} and ω_{res} apart and makes the resonance more prominent, which is a further reason the inertia-matching of G.2 is desirable.

G.9 Clarke and Park with numbers

Problem. Balanced currents $i_a = 10$ A, $i_b = -6$ A, $i_c = -4$ A are measured at a rotor electrical angle $\theta_e = 30^\circ$. Find i_α, i_β and then i_d, i_q.

Solution. Amplitude-invariant Clarke:

$$i_\alpha = \tfrac{2}{3}\big(i_a - \tfrac{1}{2}i_b - \tfrac{1}{2}i_c\big) = \tfrac{2}{3}\big(10 + 3 + 2\big) = 10.0 \text{ A},$$

$$i_\beta = \tfrac{2}{3}\cdot\tfrac{\sqrt{3}}{2}\big(i_b - i_c\big) = \tfrac{1}{\sqrt{3}}\big(-6 + 4\big) = -1.155 \text{ A}.$$

Park at $\theta_e = 30^\circ$ ($\cos = 0.866,\ \sin = 0.5$):

$$i_d = i_\alpha \cos\theta_e + i_\beta \sin\theta_e = 10(0.866) + (-1.155)(0.5) = 8.08 \text{ A},$$

$$i_q = -i_\alpha \sin\theta_e + i_\beta \cos\theta_e = -10(0.5) + (-1.155)(0.866) = -6.00 \text{ A}.$$

The current vector has magnitude $\sqrt{8.08^2 + 6.0^2} = 10.06$ A, matching $\sqrt{i_\alpha^2 + i_\beta^2}$ as the transform is rotation-preserving.

G.10 Verifying the symmetrical-optimum margin

Problem. For the speed design of G.5 ($a = 3$, $T_{eq} = 199$ μs), confirm the crossover frequency and phase margin.

Solution. The symmetrical optimum places the gain crossover at the geometric mean of the two corner frequencies $1/T_i$ and $1/T_{eq}$, i.e. $\omega_c = 1/(aT_{eq}) = 1/(3{\cdot}199{\times}10^{-6}) = 1675$ rad/s. The phase margin is $\varphi_m = \arctan\frac{a^2-1}{2a} = \arctan\frac{8}{6} = 53.1^\circ$. Both are consistent with a well-damped speed loop about one decade below the current-loop bandwidth ($\alpha_c = 5027$ rad/s).

G.11 Flux-estimator drift

Problem. A DTC voltage-model integrator has a stator-current sensor with a 1 % DC offset on a 10 A signal; $R_s = 0.5\ \Omega$. Estimate the resulting rate of flux drift, and the flux error after 0.1 s.

Solution. The offset current is 0.1 A, producing a spurious voltage $R_s\Delta i = 0.05$ V that the pure integrator accumulates: $\dot{\psi}_{err} = 0.05$ Wb/s. After 0.1 s the flux error is 0.005 Wb — already several percent of a typical 0.1 Wb set-point, illustrating why the pure integrator must be replaced by a low-pass or closed-loop estimator (§4.6).

G.12 Stepper pull-in versus pull-out

Problem. A stepper's pull-out torque at 500 steps/s is 0.6 N·m and its pull-in torque there is 0.35 N·m. A load needs 0.45 N·m at that rate. Can the motor (a) start directly into the load at 500 steps/s, and (b) run it at 500 steps/s after ramping?

Solution. (a) Direct start requires the load torque to be below the **pull-in** curve: $0.45 > 0.35$, so the motor **cannot start** directly at 500 steps/s and would lose steps. (b) Running after a ramp requires the load below the **pull-out** curve: $0.45 < 0.60$, so once accelerated gradually from a lower rate, the motor **can sustain** 500 steps/s. The lesson: always ramp into high step rates.

Appendix I — Control-Strategy Selection Guide

This appendix condenses the whole course into a practical chooser: given an application, which machine, converter and control law fit best.

I.1 Method comparison matrix

Criterion	Scalar V/f	FOC	DTC	Stepper (open-loop)
Dynamic torque response	slow	fast	fastest	n/a (position)
Torque/speed ripple	moderate	low	higher	cogging at steps
Needs rotor position	no	yes (or estimate)	no	no
Switching frequency	fixed	fixed	variable	fixed (chopper)
Computational load	low	high	medium	low
Parameter sensitivity	low	medium (L_d, L_q, ψ)	low (mainly R_s)	low
Low-speed behaviour	poor	excellent	fair	excellent (holding)
Typical use	fans, pumps	servo, traction, EV	traction, high-dynamic	positioning, printers

I.2 Application-to-method mapping

- **Fans, pumps, blowers, HVAC:** scalar V/f (often sensorless), quadratic load, energy savings from speed control dominate; dynamic performance is unimportant.
- **Machine-tool spindles and feed axes, robotics:** FOC of PMSM with encoder, for smooth low-ripple torque and precise position/speed.

- **Electric-vehicle and rail traction:** FOC or DTC of PMSM/IM with field weakening for the wide constant-power range; regeneration mandatory (four-quadrant, active front end).
- **Incremental positioning (printers, small CNC, valves, cameras):** hybrid stepper, microstepped, open-loop where torque margin allows, closed-loop ("smart stepper") where lost steps are unacceptable.
- **High-dynamic torque control (rolling mills, cranes):** DTC or FOC with fast inner loops and four-quadrant converters.

I.3 Converter and modulator selection

- **Two-level VSI + SVM** is the default for the entire low-voltage range; use SVM over SPWM for the 15.5 % higher bus utilisation and lower harmonics.
- Add a **braking chopper** for occasional regeneration into a resistor, or an **active front end** where energy is returned to the grid or the duty cycle is regenerative (hoists, traction).
- **Dead-time compensation** and adequate f_{sw} (to keep current ripple and audible noise acceptable) are needed once the drive runs closed-loop current control.
- For very high dynamic torque with a fixed switching frequency, consider **DTC-SVM** or **finite-control-set model-predictive control (FCS-MPC)**, which unify the fast response of DTC with the spectral cleanliness of SVM.

I.4 Study questions

The following consolidate the course's key ideas; they are suitable for revision or oral examination.

1. Explain physically why a fan load stabilises a drive operating point while a constant-torque load does not.
2. Derive the constant-V/f law from the stator EMF equation and state where and why it breaks down.
3. Why does SVM reach a higher fundamental voltage than SPWM from the same DC bus? Quantify the margin.
4. In FOC, what is decoupled from what, and which feed-forward terms achieve the decoupling?
5. Contrast the variables controlled by FOC and DTC and relate each to its dynamic-response and ripple behaviour.
6. Explain the pure-integrator drift in DTC flux estimation and two remedies.
7. State the role of the $i_d < 0$ current in field weakening and the voltage constraint it satisfies.
8. Why must a stepper be ramped into high step rates rather than started directly, and how does microstepping help with resonance?
9. Describe how a sliding-mode observer recovers the rotor angle, and why it fails at zero speed.
10. Given a new application, walk through the selection of machine, converter, modulator and control law using Appendix I.

Appendix J — Typical Machine and Drive Parameters

Realistic starting values help when building the Simulink models of the course before real nameplate data are available. The tables below give representative ranges for low-voltage machines in the sub-10 kW class; always replace them with measured or datasheet values for quantitative work.

J.1 Induction motors (star-connected, 50 Hz)

Parameter	0.75 kW	4 kW	7.5 kW
Rated voltage (line)	400 V	400 V	400 V
Pole pairs p	2	2	2
Stator resistance R_s	6.0 Ω	1.1 Ω	0.5 Ω
Rotor resistance R'_r	4.5 Ω	0.9 Ω	0.4 Ω
Stator/rotor leakage L_{ls}, L'_{lr}	22 mH	6 mH	3 mH
Magnetising inductance L_m	0.45 H	0.16 H	0.09 H
Inertia J	2×10^{-3}	1.2×10^{-2}	3×10^{-2} kg·m²

J.2 Permanent-magnet synchronous motors

Parameter	Surface (SPMSM)	Interior (IPMSM)
Pole pairs p	3–5	3–4
R_s	0.3–1.0 Ω	0.2–0.8 Ω
L_d	3–8 mH	4–8 mH
L_q	$= L_d$	$1.5–3 \times L_d$ (salient)
Magnet flux ψ_f	0.08–0.2 Wb	0.08–0.2 Wb

Parameter	Surface (SPMSM)	Interior (IPMSM)
Saliency ratio L_q/L_d	≈1	1.5–3
Torque terms used	magnet only	magnet + reluctance

The saliency of the IPMSM both enables reluctance torque (via MTPA, Appendix D.3) and makes low-speed sensorless control by high-frequency injection (Appendix F.3) practical.

J.3 Hybrid stepper motors (NEMA sizes)

Parameter	NEMA 17	NEMA 23
Full-step angle	1.8° (200/rev)	1.8° (200/rev)
Rotor teeth N_r	50	50
Holding torque	0.3–0.6 N·m	1.0–2.5 N·m
Phase current	1.2–2.0 A	2.8–4.2 A
Phase inductance	2–5 mH	2–8 mH
Rotor inertia	4×10^{-5}	2.8×10^{-4} kg·m²

J.4 Typical control settings

Setting	Typical value
PWM / sampling frequency f_{sw}	5–20 kHz (LV drives)
Current-loop bandwidth α_c	$2\pi f_{sw}/10$
Speed-loop bandwidth	$\alpha_c/10$ to $\alpha_c/5$
Symmetrical-optimum factor a	2–4
Dead time t_d	0.5–3 µs
DC-bus voltage (400 V drive)	540–650 V

J.5 Further reading

Beyond the numbered bibliography, the following are useful primary sources and standards for deeper study: manufacturer application notes on FOC and sensorless control (Texas Instruments InstaSPIN, STMicroelectronics MC-SDK), the IEC 60034 series on rotating machinery ratings, and survey papers on model-predictive control of drives (e.g. Rodríguez and Cortés). The MathWorks Motor Control Blockset documentation gives a modern, worked Simulink treatment aligned with Chapters 3–4.

This concludes the handout. The five chapters, worked tutorials, exercises and appendices together form a self-contained one-semester treatment of the control of electrical machines, from the mechanics of the drive through scalar, vector and direct-torque control to stepper drives, digital implementation and sensorless operation.